THE ARF-GEFS GEA1 AND GEA2 INTEGRATE SIGNALS TO COORDINATE VESICLE TRAFFICKING AT THE GOLGI COMPLEX

A Dissertation
presented to the Faculty of the Graduate School
of Cornell University
in Partial Fulfillment of the Requirements for the Degree of
Doctor of Philosophy

by

Margaret Ann Gustafson

August 2017

- ABSTRACT -

THE ARF-GEFS GEA1 AND GEA2 INTEGRATE SIGNALS TO COORDINATE VESICLE TRAFFICKING AT THE GOLGI COMPLEX

Margaret Ann Gustafson, Ph.D.
Cornell University 2017

At the Golgi complex, the biosynthetic sorting center of the cell, the Arf GTPases are responsible for coordinating vesicle formation. The Arf-GEFs activate Arf GTPases and are therefore the key molecular decision-makers for both anterograde and retrograde trafficking out of the Golgi. In *Saccharomyces cerevisiae*, three conserved Arf-GEFs function at the Golgi: Sec7, Gea1, and Gea2. Our group has described the regulation of Sec7, the *trans*-Golgi Arf-GEF, through autoinhibition, positive feedback, dimerization, and interactions with a suite of small GTPases. However, we lack a clear understanding of the regulation of the early Golgi Arf-GEFs Gea1 and Gea2. Here, I present insights into this regulation.

I demonstrate that Gea1 and Gea2 prefer neutral over anionic membrane surfaces *in vitro*, consistent with their localization to the early Golgi, and that Gea1, Gea2, and Sec7 each localize to different Golgi compartments. I also show that a critical mass of either Gea1 or Gea2 is required for the essential role which Gea plays *in vivo*.

Using *in vitro* membrane binding and catalytic activity assays, I show that the C-terminal domains of Gea1 and Gea2 toggle roles in the cytosol and at the membrane surface, preventing

membrane binding by Gea in the absence of a recruiting interaction but promoting maximum catalytic activity once recruited. *In vivo* assays highlight the importance of these domains in recruitment of Gea to Golgi compartments and cell viability.

I have identified the small GTPase Ypt1 as a recruiter for Gea1 and Gea2 *in vitro*, and I demonstrate that this interaction is dependent upon the C-terminus of Gea. I have also uncovered an additional interaction between Gea2 and the Golgi SNARE Gos1 which may provide the specific interaction required to target Gea1 and Gea2 to different compartments. I describe additional preliminary results and propose future experiments that will advance this line of research.

This evidence evokes a model for intricate regulation of function and localization for Gea1 and Gea2 and raises interesting questions about the roles Gea1 and Gea2 play in Golgi trafficking. My findings not only illuminate core regulatory mechanisms unique to the early Golgi Arf-GEFs, but also pave the way for a clearer understanding of the coordination of Golgi membrane trafficking across transport events controlled by small GTPases, their regulators, and their effectors working in concert.

- BIOGRAPHICAL SKETCH -

Maggie Gustafson was born and raised in Vienna, Virginia, before moving to Pennington, NJ, when she was twelve. She graduated from Hopewell Valley Central High School in 2005.

Maggie graduated with honors from the University of Richmond in 2009, earning a B.S. in Biochemistry and Molecular Biology and B.A in Latin American and Iberian Studies. Her research with Dr. Michelle Hamm focused on the molecular mechanism of mutagenesis during DNA synthesis after oxidative DNA damage. This work was published in 2011.

In 2009, Maggie joined the lab of Dr. Joel Meyer in the Nicholas School of the Environment at Duke University, where she worked as a lab manager and research technician. While there, she studied the effects of mitochondrial DNA damage at the molecular, cellular, and whole animal level in *C. elegans*. This work culminated in two publications in 2012.

Maggie enrolled in the graduate field of Biochemistry, Molecular and Cell Biology at Cornell University in 2011. She joined Dr. Chris Fromme's lab in May 2012, where she studied the mechanisms of regulation of Golgi membrane trafficking using protein biochemistry, yeast cell biology and microscopy, and x-ray crystallography. This work culminated in two publications, one in 2016 and one in 2017 (in review).

DEDICATION

To my mother and father,
Lynn and Peter,
who fostered in me the inquisitiveness, creativity, and passion that make me who I am.

ACKNOWLEDGMENTS

I am grateful to my advisor, Chris Fromme, for his stalwart support, brilliant guidance, and infinite patience.

I would like to thank my committee members, Eric Alani and Bill Brown, for their helpful feedback on my work, thoughtful mentorship, and training in and out of the classroom.

I am so fortunate to have had wonderful mentors at every stage of my education: Karen Lucci at HVCHS, Michelle Hamm and Rob Miller at the University of Richmond, and Joel Meyer at Duke University.

Thanks are due to Caitlin McDonold and Brian Richardson for laying the groundwork for my project and providing training and helpful discussions, and especially to my baymate Brian for moral support during difficult experiments.

I am thankful for the opportunity to mentor two undergraduate researchers, Joe Manzi and Yi Fan Chen, who have worked diligently on Gea projects, as well as two rotation students, Jon Wasilko and Abigail Miller, who contributed experiments to this study.

I appreciate the help and useful discussions provided by other members of the Fromme lab: Laura Thomas, Carolyn Diefenderfer, Steve Halaby, Aaron Joiner, Jon Paczkowski, and Amanda Weiskoff. It's been wonderful working with such bright, interesting, and fun labmates.

I have benefited a great deal from the collaborative nature of Cornell, the Weill Institute, and the department of Molecular Biology and Genetics, in particular from reagents, equipment, and advice provided by the following groups: S. Emr lab, T. Bretscher lab, H. Sondermann lab, M. Smolka lab, F. Hu lab, Y. Mao lab, the Macromolecular Diffraction Facility at the Cornell High Energy Synchrotron source (MacCHESS), and the Cornell Institute of Biotechnology.

I am thankful for Mary Godec, Sarah Griffin, and Nadia Nikulin, who have kept the Institute running and made my research indescribably easier over the years, and for the WICMB administrative staff and BMCB GFAs.

This work was funded by NIH grant R01GM098621, NIH training grant T32GM007273, and the Harry and Samuel Mann Outstanding Graduate Student Award.

I am so grateful for the wonderful friends I have made during my time in Ithaca – I couldn't have done this without them.

Thanks to my sister, Sarah, for always having my back.

The encouragement and support of my parents, Lynn and Peter, made all of this possible.

And thanks to Ian Hensley, for his love and support in everything that I do.

- TABLE OF CONTENTS -

- CHAPTER 1 -

INTRODUCTION

Organization of eukaryotic cells

Both eukaryotic and prokaryotic cells are complex and intricately organized. Across the spectrum of cells, we find single-celled organisms as small as 1 μm in diameter, specialized mammalian cells as large as 100 μm in diameter, and even unusually large cells with diameters measured in millimeters and lengths in feet. Yet all of these cells face similar challenges. Within these varying confines and with varying degrees of complexity, the same fundamental functions which permit cell survival and growth must be carried out: maintenance, replication, and transcription of DNA, translation, editing, and transport of RNA, modification, transport, and regulation of proteins, biogenesis and transport of sugars, lipids, and the building blocks of macromolecules, production of ATP which drives essential, energetically unfavorable reactions throughout the cell. All of this must occur while maintaining the integrity of the cell in its environment and yet also allowing for exchange with the outside of the cell: sensing environmental changes, cell-cell communication, and uptake of extracellular molecules. The plasma membrane and its supporting structures therefore represent critical and necessarily dynamic structures for all cells.

In eukaryotic cells, the separation of functions is largely achieved through elaborate intracellular compartmentalization: eukaryotic cells contain numerous distinct organelles in which specific cellular functions are carried out. And while each of these organelles must maintain its own identity, defined by its characteristic complement of macromolecules, there is

a great deal of communication and exchange among organelles. For example, functions achieved in the nucleus are intrinsically linked to and regulated by events and molecules in the cytosol. Many transcription factors remain in a cytosolic pool until signals for gene regulation send them into the nucleus through nuclear pores, where RNA is transcribed and must leave the nucleus through these same pores for editing and translation in the cytosol and at the endoplasmic reticulum (ER) (Whiteside and Goodbourn 1993; Köhler and Hurt 2007; Nyathi, Wilkinson, and Pool 2013).

Most exchange between organelles, however, occurs through regulated fission and fusion of membranes (Figure 1.1 A). The mitochondrial morphology is closely tied to, among other factors, the cell's metabolic state, and mitochondria divide and fuse to maintain energetic homeostasis, protect themselves from autophagy, and preserve mitochondrial DNA integrity (Wai and Langer 2016). Many other organelles in the cell participate in a complex membrane trafficking network, through which membrane-bound packets, called vesicles, bud from donor compartments and fuse with target compartments to deliver proteins and lipids. In particular, newly synthesized transmembrane proteins and proteins destined for secretion rely on this membrane trafficking system for delivery to the plasma membrane (Palade 1975). Along the way, each cargo protein must be modified and appropriately sorted multiple times, and specific and highly orchestrated sets of machinery have evolved to ensure that each delivery and receipt of cargo occurs at the correct time and place within the cell.

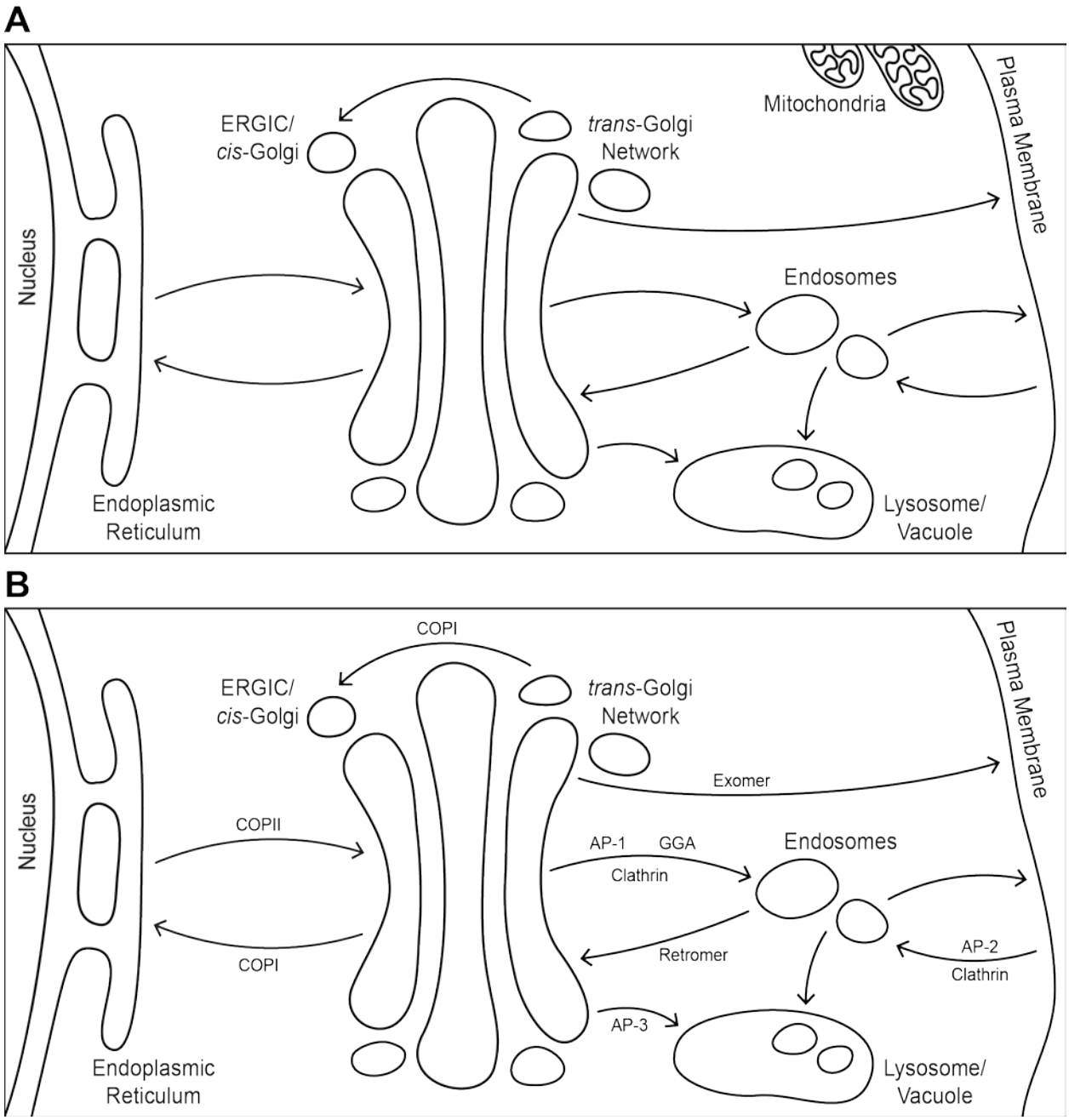

Figure 1.1. The endomembrane system and vesicle coat complexes. (A) Cartoon of the endomembrane system showing membrane trafficking pathways. Lysosome, human; vacuole, yeast. (B) Cartoon of the coat protein complexes which facilitate vesicle transport in various trafficking pathways. Note that mammals do not have an exomer homolog. AP-4 and AP-5 adaptor complexes not shown.

Perturbations in these pathways result in a broad array of human diseases (Howell et al. 2006). Mutations which disrupt ER exit are implicated in cancer and liver, kidney, cardiac, and vascular disease, among others. Those which compromise the formation of clathrin-coated vesicles are associated with leukemia and autoimmune diseases. Many others are associated with neurodevelopmental or neurodegenerative diseases, such as Alzheimer's and Parkinson's diseases, which highlights the particular demands on membrane trafficking in human neurons. Accurate and timely trafficking between intracellular compartments and the plasma membrane is essential for eukaryotic cells from yeast through humans, and as our fundamental understanding of these processes grows more complete, so will our understanding of the human diseases caused by mutations which disrupt these processes.

Trafficking within the endomembrane system

The proteins and mechanisms which regulate membrane trafficking in eukaryotes are highly conserved (Schlacht et al. 2014). Cells move newly synthesized proteins from the ER to the plasma membrane through a system called the secretory pathway. This pathway, first described through electron microscopy of mammalian cells, was meticulously dissected in the relatively simple model organism *Saccharomyces cerevisiae* using temperature sensitive mutants to disrupt different trafficking steps and also characterized using isolated Golgi cisternae from mammalian cells (Palade 1975; P. J. Novick and Schekman 1979; P. Novick, Field, and Schekman 1980; P. Novick, Ferro, and Schekman 1981; Balch, Glick, and Rothman 1984; Balch et al. 1984). Proteins are shuttled in vesicles or membrane-bound tubules from ER exit sites through the ER-

Golgi intermediate compartment (ERGIC) to the *cis*-Golgi. They then move through the Golgi, where some are modified by Golgi-resident enzymes, before repackaging into vesicles at the *trans*-Golgi network (TGN) and shipment to endosomes, the lysosome (vacuole in yeast) and the plasma membrane.

This flow of anterograde traffic, carrying cargos destined for secretion or incorporation into the plasma membrane, is complemented by a retrograde trafficking pathways. Endocytosis recycles plasma membrane proteins through endosomes back into the secretory pathway or to the lysosome (vacuole in yeast) for degradation. Retrograde traffic from the Golgi to the ER facilitates the retrieval of ER resident proteins, vesicle fusion machinery, and misfolded secretory proteins to the ER.

Retrograde traffic is also required among Golgi cisternae. While the Golgi forms distinct perinuclear stacks in mammalian cells, yeast Golgi are spread through the cell as individual cisternae (Franzusoff et al. 1991; Preuss et al. 1992; Wooding and Pelham 1998). This feature allowed the visualization and validation of a model of Golgi transport in which cisternae mature individually and retain their cargo, rather than remaining constant while secretory cargo are transferred forward between cisternae in vesicles (Losev et al. 2006; Matsuura-Tokita et al. 2006). As each cisternae matures, resident Golgi proteins, such as glycosylation enzymes, must be recycled to new early compartments through vesicle transport. It should be noted that there are arguments for a hybrid system, in which cisternal maturation is complemented by

anterograde vesicle and tubule trafficking of cargo within the Golgi (Martínez-Menárguez 2013; Morriswood and Warren 2013).

Membrane tubules have also be shown to play a role in many of the trafficking events in the endomembrane system (Bonifacino and Lippincott-Schwartz 2003; De Matteis and Luini 2008; Bard and Malhotra 2006; Tomás et al. 2010; Heffernan and Simpson 2014; de Figueiredo et al. 1998). It has been proposed that these tubules are used for specific cargos or when trafficking demand is high, but a full picture of how vesicles and tubules cooperate to accomplish membrane trafficking is still emerging.

Regulation and specificity in vesicle trafficking

The general life cycle of a transport vesicle is common across trafficking events in the endomembrane system (Figure 1.2) (Bonifacino 2014). An activated small guanosine triphosphatase (GTPase) binds to the donor membrane, where it recruits coat proteins. The coat proteins interact with cargos and cargo adapters before the membrane deforms and eventually buds off. As the vesicle travels to the target membrane – either by diffusion or through interactions with motor proteins which traverse the cytoskeletal network – it also loses its protein coat (Santiago-Tirado and Bretscher 2011; Kyoung and Sheets 2008; Trahey and Hay 2010; Cai, Reinisch, and Ferro-Novick 2007). At the target membrane, the vesicle is tethered, and then SNAP (soluble NSF attachment protein) receptor (SNARE) complex formation drives

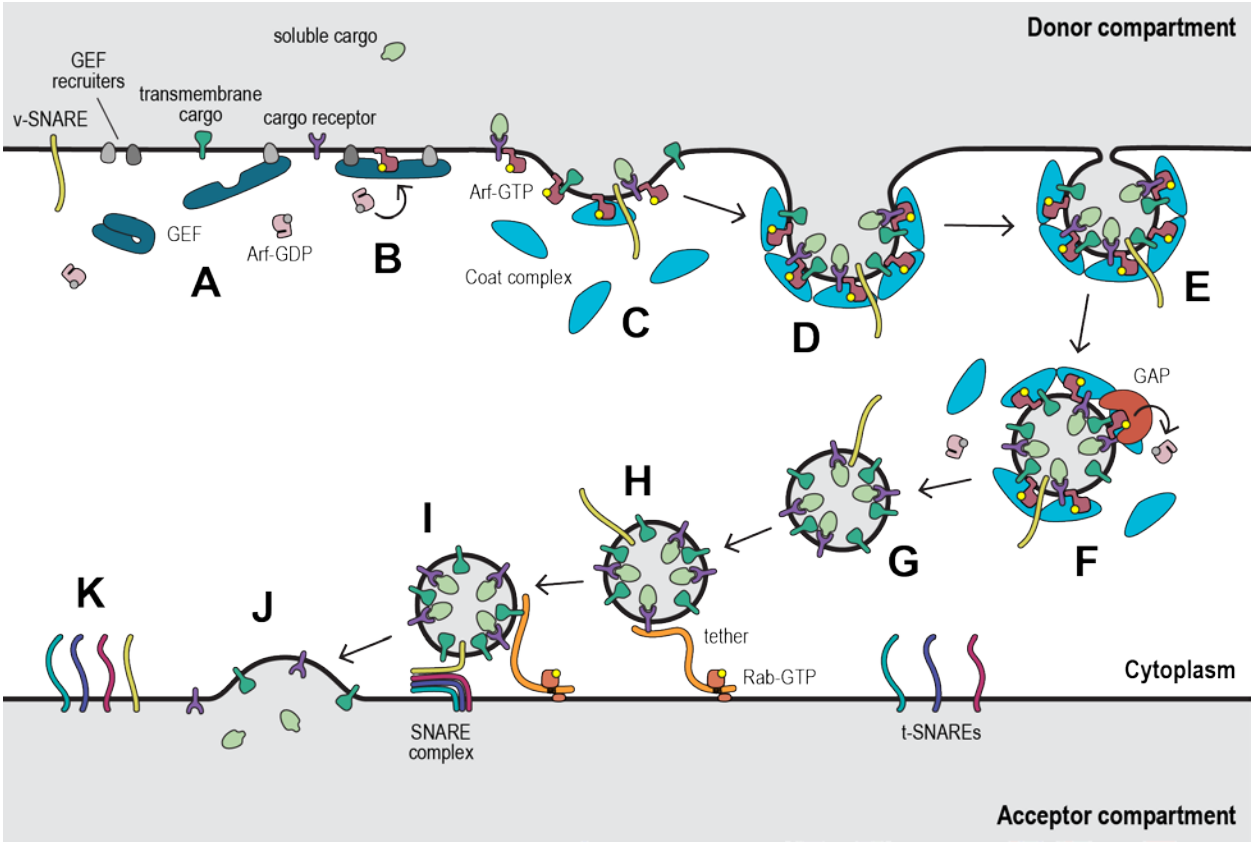

Figure 1.2. The life cycle of a coated vesicle. (A) Recruitment of GEF to membrane surface. (B) Nucleotide exchange and membrane insertion of Arf GTPase. (C) Recruitment of coat proteins, cargos, and v-SNARE. (D) Membrane deformation. (E) Budding. (F) GTP hydrolysis by Arf catalyzed by GAP drives vesicle uncoating. (G) Transport to target membrane, either by diffusion or along cytoskeleton filaments. (H) Vesicle tethering facilitated by Rab GTPase. (I) Docking and fusion coupled to SNARE complex assembly. (J) Release of soluble cargo and diffusion of transmembrane cargo and SNARE complexes. (K) SNARE complex disassembly and SNARE recycling. Note that not all coated vesicle trafficking involves Arf and Rab GTPases. SNARE disassembly is an active process carried out by SNARE regulator proteins.

Used as references: (Alberts et al. 2007; Bonifacino 2014)

membrane fusion (Rothman 1994; Mcnew et al. 2000; Pelham 2001; Malsam and Söllner 2011; Whyte and Munro 2002; Yu and Hughson 2010).

Vesicle trafficking is tightly controlled so that cargos are appropriately packaged and delivered from one specific membrane to another. The specificity of these events is determined by the machinery – GTPases, protein coats and adaptors, tethers, SNAREs – employed at each compartment and the interactions between each set of machinery and the cargos it is designated to transport.

Vesicle coat complexes

Most trafficking events involve specific vesicle coats: protein complex oligomers which form a cage around each vesicle and aide in cargo recruitment, membrane deformation, and fission (Figure 1.2 C) (Kirchhausen 2000; Paczkowski, Richardson, and Fromme 2015; Cai, Reinisch, and Ferro-Novick 2007; Bonifacino and Lippincott-Schwartz 2003). Different coats are employed in different trafficking steps (Figure 1.1 B). The first coat discovered, clathrin, is found on vesicles trafficked from the TGN and the plasma membrane, with specific adaptor proteins working at different donor membranes and for different cargos and destinations (Kirchhausen 2000; De Matteis and Luini 2008). The adaptor protein 1 (AP-1) and Golgi-localized, gamma-ear containing, ARF-binding (GGA) complexes function with clathrin in vesicle trafficking between the TGN and endosomes (De Matteis and Luini 2008). AP-3 functions in TGN-to-lysosome/vacuole transport, but interaction with clathrin is not essential for its function (Peden et al. 2002). Two other adapter protein complexes, AP-4 and AP-5, have

more recently been described (Hirst, Irving, and Borner 2013). AP-4 is believed to be required only for specific cargos trafficked from the TGN and functions independently from clathrin, while AP-5, despite clues that it functions as an adapter complex, remains largely uncharacterized (Hirst, Irving, and Borner 2013).

AP-2 interacts with clathrin at the plasma membrane to coat endocytic vesicles for retrograde traffic from the plasma membrane (Kirchhausen 2000). Retrograde traffic from endosomes to the TGN, an important pathway for recycling transmembrane protein receptors, utilizes the highly divergent retromer complex (Seaman 2005; Hierro et al. 2007).

Anterograde traffic from the ER to the Golgi is largely mediated by coatomer protein complex II (COPII) coated vesicles (Barlowe and Schekman 1993). COPII, while functionally similar to other protein coats, is structurally unrelated to clathrin and its adaptors (Bonifacino and Lippincott-Schwartz 2003). Retrograde vesicle traffic within Golgi compartments and from the Golgi to the ER relies on coatomer protein complex I (COPI), the membrane-proximal subunits of which share structural similarity with clathrin adaptor proteins (Waters, Serafini, and Rothman 1991; Bonifacino and Lippincott-Schwartz 2003).

Some steps of trafficking remain unresolved. A small percent of direct traffic between the TGN and the plasma membrane is mediated by the exomer complex in yeast, but no homologous complex has been identified for polarized transport in mammalian cells (Mellman and Nelson 2008; Payne and Schekman 1985; Folsch 2008). Exomer, a cargo adapter, also fails to interact

with any of the canonical protein coats, leaving open the question of how exomer-sorted vesicles undergo fission (Barfield, Fromme, and Schekman 2009; Wang et al. 2006).

The recruitment of the correct vesicle coat to collect specific cargo is inextricable from the appropriate transport and targeting of vesicles to the correct acceptor compartments, not least because the coats ensure packaging of the appropriate SNAREs into vesicles. To achieve this specificity, coat proteins rely on the coincidence of multiple interactions.

Sorting signals in vesicle trafficking

Sorting signals on the cytoplasmic domains of cargo proteins present one source of these specific interactions. Clathrin and its AP-1, AP-2, AP-3, and AP-4 adaptors recognize YXXØ motifs in cargo proteins (where Ø may be leucine, isoleucine, phenylalanine, methionine or valine and X represents any amino acid) (Bonifacino and Lippincott-Schwartz 2003; Cocucci et al. 2012). The GGA clathrin adaptor recognizes cargos with acidic dileucine (DXXLL) sorting signals as well as ubiquitinated cargos at the TGN (Takatsu et al. 2001; Puertollano et al. 2003; Bonifacino 2004). The interaction between clathrin, its adaptors, and its cargo is intrinsic to its role in vesicle formation: upon recruitment to membranes displaying clathrin cargo, clathrin changes conformation, and the oligomerization of the clathrin cage drives membrane deformation and vesicle budding (B. T. Kelly et al. 2014).

COPI binds canonical dilysine motifs, as well as arginine- and tryptophan-based signals, to recycle cargos within the Golgi and from the Golgi to the ER (Gomez-Navarro and Miller 2016;

L. P. Jackson et al. 2012). The COPII subunit Sec24 serves as a binding scaffold for a variety of cargo sorting motifs – diacidic, dihydrophobic, and tyrosine-containing motifs, as well as sequences specific to SNAREs – permitting efficient sorting of diverse cargos for ER export (Sato and Nakano 2007). Neither COPI nor COPII display the direct link between oligomerization and membrane deformation observed with clathrin, leading to the hypothesis that additional proteins recruited to the nascent vesicle contribute to vesicle budding (Gomez-Navarro and Miller 2016).

Vesicle targeting and fusion

After vesicles bud, they shed their coats, a process dependent either on GTP hydrolysis by the GTPases associated with COPI, COPII, and some clathrin vesicles or on hydrolysis of the phosphoinositide $PI(4,5)P_2$ in the case of endocytic clathrin vesicles (Figure 1.2 F) (Trahey and Hay 2010; Cai, Reinisch, and Ferro-Novick 2007; Cremona et al. 1999). The remaining proteins on each vesicle coordinate transport to, recognition of, and fusion with specific target membranes. At the receiving end of vesicle transport, vesicle proteins interact with target-specific tethers, which lends specificity to vesicle targeting (Figure 1.2 H) (Whyte and Munro 2002; K.-Y. Chen et al. 2010). Vesicle tethering facilitates vesicle docking, in which vesicle-borne v-SNAREs form a complex with target membrane t-SNAREs (Rothman 1994). The zippering of the SNARE domains of each set of four SNARE proteins is very energetically favorable, and therefore the formation of SNARE complexes between the vesicle and target membranes is the driving force behind vesicle fusion (Figure 1.2 1-J) (Y. A. Chen and Scheller 2001). Different sets of SNAREs are specific to each trafficking pathway, imparting further specificity to vesicle

targeting (Mcnew et al. 2000; Pelham 2001; Malsam and Söllner 2011). The SNAREs, most of which are tethered by transmembrane proteins, must be unzipped by the action of NSF/α-SNAP and recycled between compartments for reincorporation into new vesicles, and therefore also serve as cargos in retrograde trafficking steps (Figure 1.2 K) (Baker and Hughson 2016).

Vesicle formation at donor membranes and fusion at target membranes relies on coincidence detection of multiple signals at the same place and time to ensure accuracy in membrane trafficking. In addition to the specificity of membrane coats, sorting signals, tethering proteins, and SNARE complexes, the localization and timing of vesicle trafficking is tightly regulated through binary molecular switches: the small GTPases of the Arf and Rab families.

The Ras superfamily of small GTPases

The Arf and Rab families of GTPases belong to the Ras superfamily. This superfamily is generally divided into five subfamilies based on similarities in sequence and function (Rojas et al. 2012). The founding Ras sarcoma (Ras) and Ras homologous (Rho) families act in pathways which respond to extracellular stimuli, including regulation of the cytoskeleton, cell cycle progression, and control of gene expression (Wennerberg, Rossman, and Der 2005). The Ras-like nuclear (Ran) family is largely involved in the transport of RNA and proteins between the nucleus and cytoplasm, while the Ras-like proteins in brain (Rab) and ADP ribosylation factor (Arf) families feature widely in the organization of endomembrane trafficking (Wennerberg, Rossman, and Der 2005).

Despite the breadth of cellular roles filled by its members, the superfamily is unified by several key features. All members of the Ras superfamily, and some GTPases beyond it, share a highly conserved GDP/GTP binding motif called a G-domain (Wennerberg, Rossman, and Der 2005; Rojas et al. 2012). Ras superfamily GTPases have high affinity for both GDP and GTP and low intrinsic rates of exchange for GTP and hydrolysis of GTP to GDP, so activation and inactivation of these GTPases present excellent opportunities for regulation (Luo et al. 2007; Mizuno-Yamasaki, Rivera-Molina, and Novick 2012). GTP exchange is facilitated by guanine nucleotide exchange factors (GEFs), while GTP hydrolysis is stimulated by GTPase-activating proteins (GAPs) (Figure 1.3) (Cherfils and Zeghouf 2011; Gillingham and Munro 2007b). Members of the superfamily undergo conserved, nucleotide-dependent conformational changes: two switch regions, Switch 1 and Switch 2, rearrange upon GTP binding (Cherfils and Zeghouf 2011). These conformational changes facilitate binding to effectors of the activated GTPases.

Many Ras subfamilies, including the Arf and Rab families, rely on lipid modifications for membrane targeting (Wennerberg, Rossman, and Der 2005). Arf family GTPases employ a myristoylated amphipathic helix which inserts into the membrane upon GTP binding (B Antonny et al. 1997). The hydrophobic residues of this amphipathic helix are buried in the core of the protein when GDP-bound. Members of the Rab family, on the other hand, sport a longer tail capped with two prenylated cysteines; these prenyl groups insert into the target membrane (E. E. Kelly et al. 2012). Rab GTPases cannot pack away their lipid modifications, but rather rely on partners to remain soluble when inactive. After translation, Rabs are bound by a Rab escort

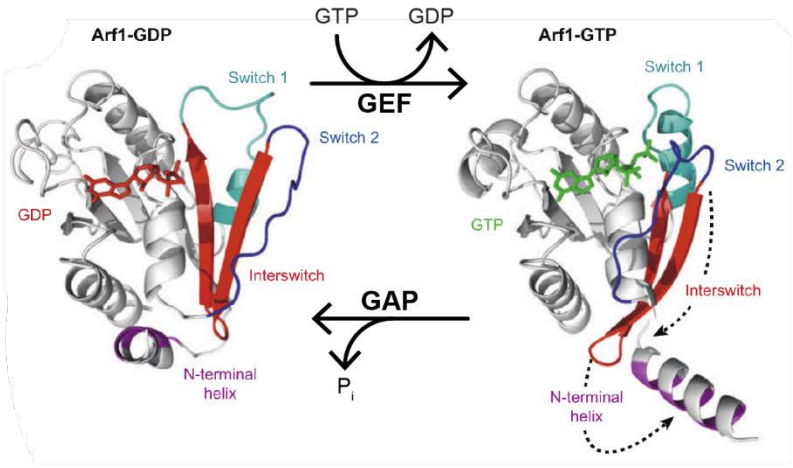

Figure 1.3. Arf1 GTPase cycle. A GEF catalyzes the exchange of GDP for GTP on Arf1, inducing conformational changes in the Switch 1 and 2 regions and exposing the N-terminal amphipathic helix, which will insert into the membrane. In this GTP-bound conformation, Arf1 is active and can interact with effectors. A GAP stimulates GTP hydrolysis by Arf1, releasing inorganic phosphate and returning Arf1 to its cytosolic, inactive state.

Adapted from: (Gillingham and Munro 2007)

protein (REP) which allows lipid modification of the tail by a geranylgeranyl transferase (GGTase) (Alexandrov et al. 1994). The REP facilitates the first membrane insertion of the Rab upon GTP exchange by its GEF. When the Rab is inactivated by GTP hydrolysis, paired with its GAP, the Rab is bound by a GDP dissociation inhibitor (GDI), which shields the prenyl groups while the Rab remains in the cytosol (E. E. Kelly et al. 2012; Cherfils and Zeghouf 2013).

Arf and Rab GTPases are involved in all stages of membrane trafficking. Arf GTPases recruit protein coats to the site of vesicle formation and interact with cargos. Arfs also count various lipid-metabolizing enzymes among their effectors, such as phospholipase D and PI kinases, coupling vesicle formation to changes in the donor membrane composition (Brown et al. 1993; De Matteis and Godi 2004). Both Arfs and Rabs function in membrane deformation, fission, and uncoating of vesicles, while vesicle transport, target membrane recognition, and fusion are largely the domain of Rabs (E. E. Kelly et al. 2012; Goud and Gleeson 2010; Barr 2009).

There is considerable overlap and cooperation between Arf and Rab GTPases in the secretory pathway. Rab GTPases are well-documented to hand off cargos to one another in Rab cascades, where the GEF of the next Rab in line is an effector for the previous Rab and/or the GAP of the previous Rab is recruited by the next (Pfeffer 2012; Suda et al. 2013; P. Novick 2016). Several Arf GTPases have shown to be regulated by positive feedback loops and interactions with other Arfs (Richardson, McDonold, and Fromme 2012; Stalder and Antonny 2013; McDonold and Fromme 2014). There is also a great deal of cross talk between Arfs and Rabs, leading to recruitment of Arf-GEFs by Rabs and of Rab-GEFs by Arfs (Mizuno-Yamasaki, Rivera-Molina,

and Novick 2012; Cherfils and Zeghouf 2013; Stalder and Antonny 2013; Thomas and Fromme 2016; McDonold and Fromme 2014). This elaborate network of interactions serves to coordinate the multitude membrane trafficking events in the endomembrane system, and at the Golgi in particular.

Roles and Regulation of Golgi Rab GTPases

Rab GTPases are essential for the maintenance of the Golgi as a dynamic organelle (Kim et al. 2016). Two main sets of Rabs function at opposite ends of the Golgi: yeast Ypt1 (matched by several isoforms of Rab1 in humans) and the homologous pair Ypt31/32 (Rab11) (Figure 1.4 A) (Barr 2009). An additional Rab, Ypt6 (Rab6), coordinates vesicle traffic from the endosome to the TGN (S. Siniossoglou and Pelham 2001; Symeon Siniossoglou, Peak-Chew, and Pelham 2000; Bensen, Yeung, and Payne 2001; Suda et al. 2013). After vesicles leave the Golgi complex, the Rab GTPase Sec4 (Rab8A/8B/10/1) is responsible for shuttling them to the plasma membrane (Ortiz et al. 2002; Mizuno-Yamasaki, Rivera-Molina, and Novick 2012). A number of human diseases have been linked Golgi Rabs and their regulators and effectors, including neurological disorders, cancer, and infectious diseases, highlighting the critical role that these GTPases play (E. E. Kelly et al. 2012).

Ypt1 is most well-known for its role in targeting COPII vesicles to the *cis*-Golgi, where it interacts with the tether Uso1 (Figure 1.4 A) (Jedd et al. 1995; Bacon et al. 1989; Segev, Mulholland, and Botstein 1988). However, it has been implicated in many trafficking steps, including endocytic recycling, recruitment of Arf-GEFs to the Golgi, intra-Golgi trafficking

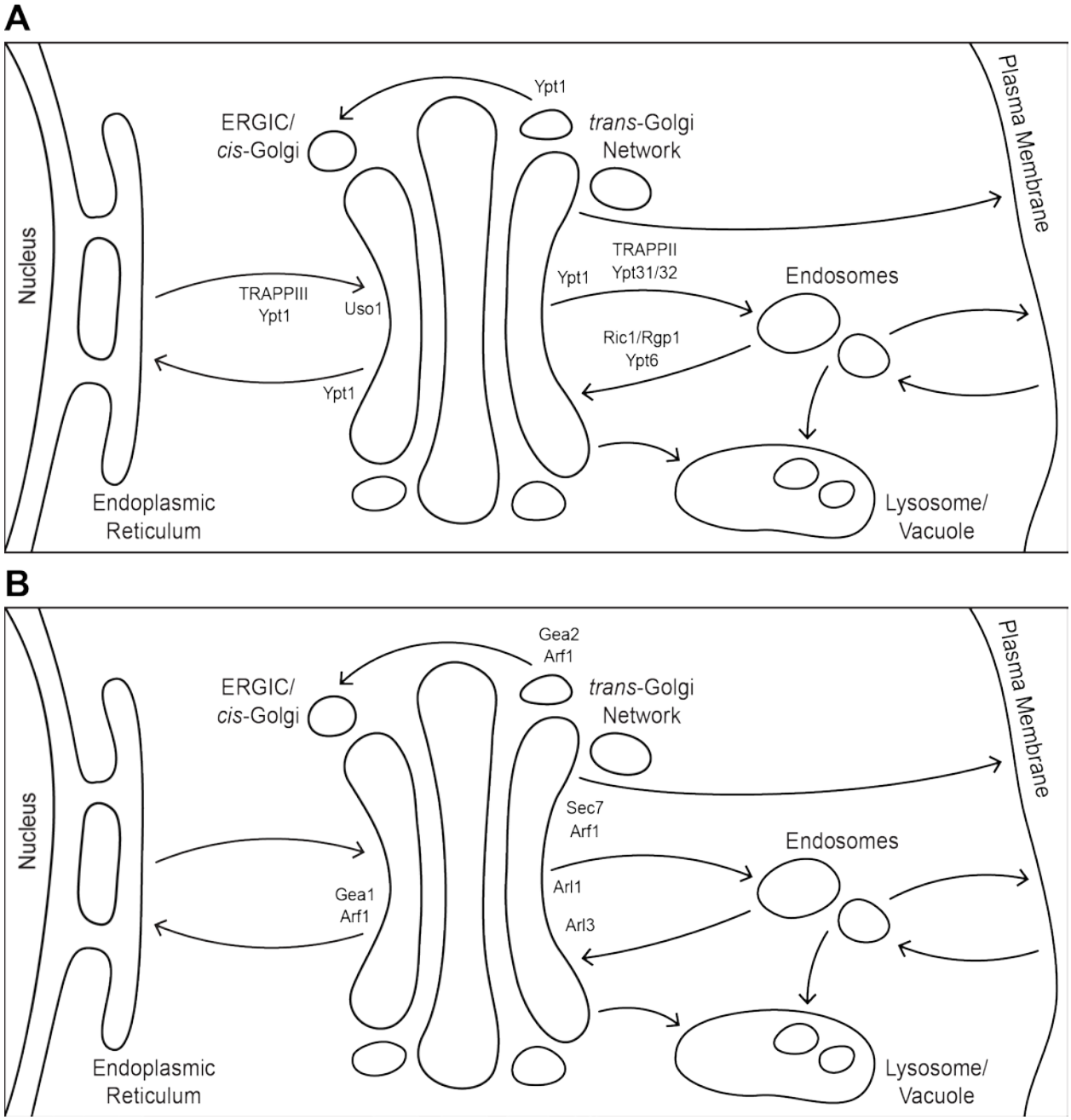

Figure 1.4. Rab and Arf GTPases in Golgi membrane trafficking. (A) Rab GTPases and Rab-GEFs at the Golgi complex. (B) Arf family GTPases and the large Golgi Arf-GEFs. Yeast proteins are labeled. Arf1 represents yeast Arf1 and Arf2. Human homologs: Ypt1, Rab1; Ypt31/32, Rab11, Ypt6, Rab6; Arl3, ARFRP1; Gea1/2, GBF1; Sec7, BIG1/2/3.

(through interactions with the conserved oligomeric Golgi [COG] complex), and autophagosome formation (Figure 1.4 A) (Sclafani et al. 2010; McDonold and Fromme 2014; Lynch-Day et al. 2010; Cai, Reinisch, and Ferro-Novick 2007; Smith and Lupashin 2008).

Nucleotide exchange on Ypt1 is catalyzed by the Rab-GEF complex transport protein particle III (TRAPPIII) at both the Golgi and in its role at autophagosomes (article in progress, Fromme lab). GTP hydrolysis is stimulated by the Rab-GAP GAP for Ypt1 (Gyp1) (Du and Novick 2001).

Ypt31/32 represent a genetically redundant pair in yeast and localize mainly to the TGN (Figure 1.4 A), whereas their human homolog, Rab11, localizes to recycling endosomes, which have not been found in yeast (Benli et al. 1996; Ullrich et al. 1996). Ypt31/32 stimulate nucleotide exchange activity of the Arf-GEF Sec7 and also participate in TGN to plasma membrane traffic by recruiting the Sec4 GEF, Sec2, to secretory vesicles (McDonold and Fromme 2014; Ortiz et al. 2002). Ypt31/32 are activated by the Rab-GEF complex TRAPPII, which shares its core subunits with TRAPPIII but is distinguished by several unique subunits (Thomas and Fromme 2016). Gyp2 has been proposed as a Rab-GAP for Ypt31/32 based on genetic interactions (Sciorra et al. 2005). Ypt31/32 have also been implicated in a Rab-GAP cascade, recruiting Gyp1 to inactive Ypt1 at the late Golgi (Rivera-Molina and Novick 2009). In this way, Ypt1 and Ypt31/32 define and differentiate Golgi compartments across their overlapping territories (Kim et al. 2016).

Arf GTPases in Membrane Trafficking

The Arf family of GTPases includes both true Arfs and Sar1, which is included in the family due to structural (myristoylated amphipathic helix) and functional (coat protein recruitment) similarities (Gillingham and Munro 2007b). The Arf GTPases are grouped into three classes based on closest sequence homology. Class I Arfs (Arf1/2 in yeast, Arf1-3 in humans) are found throughout eukaryotes and function in membrane trafficking (Figure 1.4 B). Class II Arfs (Arf4/5 in humans) are found only in higher eukaryotes, where they a proposed to play specialized roles in Golgi trafficking. Class III Arfs (Arf3 in yeast, Arf6 in humans) localize to the plasma membrane and to endosomes, where they function in endocytic trafficking and cytoskeleton remodeling (D'Souza-Schorey and Chavrier 2006; Donaldson and Jackson 2011; Gillingham and Munro 2007b).

Other members of the Arf family include a host of Arf-related proteins (Arls), which are structural similar to Arf but lack ADP-ribosylation activity (Gillingham and Munro 2007b). Yeast claim three Arl GTPases: Arl1, Arl3, and Cin4 (human Arl2). Cin4 plays a non-essential role in β-tubulin folding, while Arl1 and Arl3 are involved in membrane trafficking at the TGN (Bhamidipati, Lewis, and Cowan 2000). Arl3 (human ARFRP1) regulates the pathway leading to activation of Arl1, which in turn interacts with golgin-97, RabBP2α, Imh1p, and p230 (GRIP) domain golgin protein Imh1 and the Golgi-associated retrograde protein (GARP) complex to tether endosomal vesicles at the TGN (Figure 1.4 B) (Panic, Whyte, and Munro 2003; Setty et al. 2003). Arl1 also interacts with Golgi Arf-GEFs (Figure 1.4 B) (McDonold and Fromme 2014; Tsai et al. 2013).

The true Arf GTPases are activated by the Sec7 family of GEFs, which share a highly conserved catalytic GEF domain (originally termed the Sec7 domain, after its discovery in the first identified member of the family). The Sec7 family GEF domain consists of 10 alpha helices and induces a conformational change on Arf which forces GDP release (Goldberg 1998). The GEF for Sar1, Sec12, has no Sec7 domain (Gillingham and Munro 2007b). Yeast possess three members of the BIG/GBF subfamily (Gea1/2 and Sec7), one member of the PH and Sec7 domain (PSD)/EFA6 subfamily (Yel1), and one member of the brefeldin A-resistant Arf-GEFs (BRAG)/IQSEC7 subfamily (Syt1), but lack members of the cytohesin and FBXO8 subfamilies (Gillingham and Munro 2007b; Casanova 2007; Donaldson and Jackson 2011). Yel1 catalyzes nucleotide exchange on Arf3 at the plasma membrane, while Syt1 activates Arl1 at the TGN (K.-Y. Chen et al. 2010; Donaldson and Jackson 2011).

Sec7 family Arf-GEFs diverge widely in their regulatory domains (Figure 1.5) (Casanova 2007). The EFA6, cytohesin, and BRAG subfamilies all contain domains with homology to domains of known function, including coiled coil (CC) domains and membrane-targeting pleckstrin homology (PH) domains (C. L. Jackson and Casanova 2000). Even an uncharacterized subfamily, FBXO8, contains a conserved F-box domain, known to mediate interactions with ubiquitin ligases in other proteins. Only the Golgi Arf-GEFs, Sec7/BIG and Gea/GBF1, lack domains homologous to any outside their own subfamily, suggesting specialized regulation at the Golgi complex (Casanova 2007; Anders and Jürgens 2008).

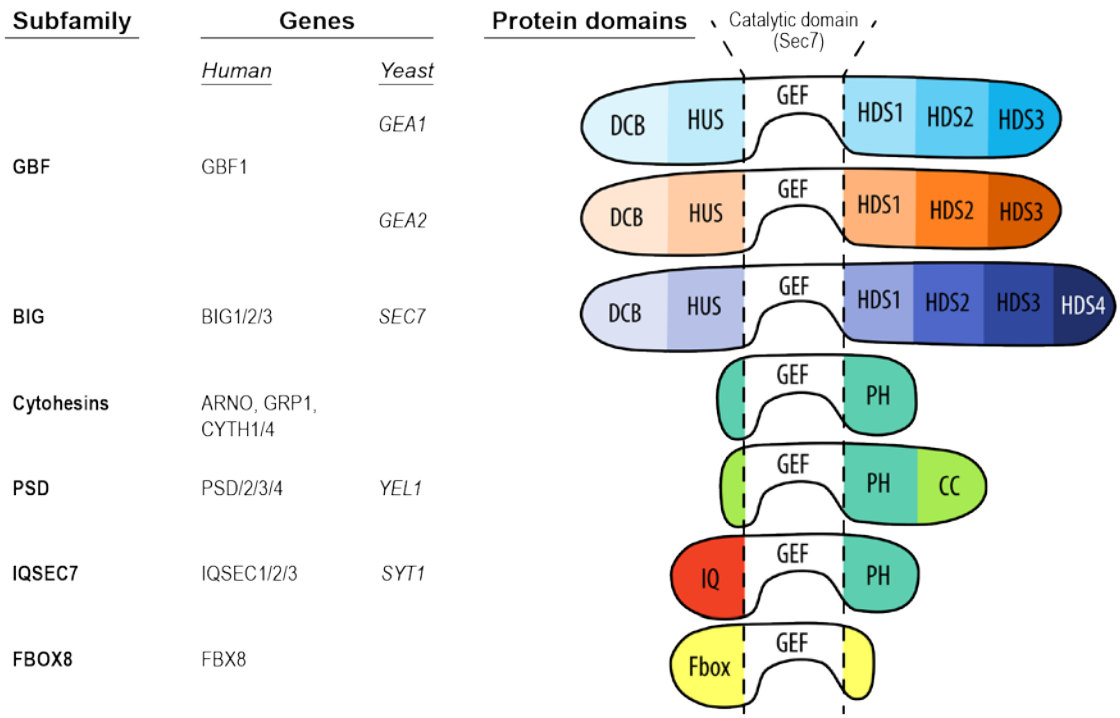

Figure 1.5. Comparison of the domains of Sec7 family Arf-GEFs. Domain diagram comparing the domains of Sec7 family GEFs found in humans and yeast.

There are 10 families of Arf-GAPs, though most are not represented in yeast (Kahn et al. 2008). Arf-GAP function is achieved through a conserved GAP domain including a catalytically-required zinc finger motif containing four cysteines and an arginine residue (Kahn et al. 2008). The Arf-GAPs identified in yeast thus far are Age1, Age2, Gcs1, Glo3, and Gts1. Many of the yeast Arf-GAPs seem to play overlapping roles: no single yeast Arf-GAP is essential, although simultaneous deletion of Gcs1 and Age2 is lethal (Poon et al. 2001). Gcs1, Glo3, Age1, and Age2 are all able to stimulate GTPase activity of Arf1 (Poon et al. 1999; Poon et al. 1996; Poon et al. 2001; Zhang et al. 2003). Gcs1 can also act on Arl1, while Gts1 displays activity on Arf3 at the plasma membrane (Smaczynska-de Rooij, Costa, and Ayscough 2008; Liu et al. 2005). Glo3, the yeast ortholog of human ArfGAP2/3, has been shown to participate in retrograde trafficking by COPI vesicles from the Golgi to the ER; it has been identified on COPI vesicles (Lewis et al. 2004; Poon et al. 1999). GTP hydrolysis by Arf1 has been shown to be required for uncoating of COPI vesicles (Tanigawa et al. 1993).

The Arf GTPases may have less diverse roles than Rabs in the secretory pathway, but they are central regulators of essential events: coat recruitment and membrane deformation. Upon activation by its GEF, Sec12, Sar1 interacts directly with Sec23 to recruit the Sec23/24 cargo adaptor and initiate COPII vesicle coat oligomerization (Barlowe et al. 1994; Bi, Corpina, and Goldberg 2002). Effectors of the redundant pair Arf1 and Arf2 at the Golgi include COPI, AP-1, GGA, and exomer, identifying Arf1/2 as a lynchpin regulator in both anterograde and retrograde Golgi trafficking (Paczkowski et al. 2012; Donaldson and Jackson 2011; Dell'Angelica et al. 2000; S. Y. Park and Guo 2014). Arf1, Arf3 (Arf6 in humans), and Sar1 have all been

implicated in the induction of membrane curvature (Krauss et al. 2008; Lee and Pohajdak 2000; Lundmark et al. 2008). As they hold the keys to vesicle coating and budding, Arf GTPases represent regulatory focal points for the secretory pathway. The GEFs which activate Arf GTPases are therefore crucial decision-makers in membrane trafficking, particularly at the Golgi complex.

Regulation of the Golgi Arf-GEFs

The Sec7/BIG and Gea/GBF1 Arf-GEFs are considerably larger than the rest of their family members, between 160-200 kD. The BIG subfamily includes yeast Sec7, the founding member of the Sec7 family, and BIG1/2/3 in humans, although BIG3 is thought to lack catalytic GEF activity (Casanova 2007). The Gea/GBF1 subfamily includes Gea1 and Gea2 in yeast and GBF1 in humans (Bui, Golinelli-Cohen, and Jackson 2009). Unlike other members of the Sec7 family, the Golgi Arf-GEFs are sensitive to the drug brefeldin A (BFA), which locks the GEF-Arf complex in the GDP-bound state and causes gross disruption of Golgi morphology (Wood, Park, and Brown 1991; Lippincott-Schwartz et al. 1991; Sata et al. 1998; Peyroche et al. 1999). The importance of the roles the Golgi Arf-GEFs play is highlighted by mutation in BIG2 which have been linked to neurological disorders (Sheen et al. 2004; De Wit et al. 2009).

Both Sec7/BIG and Gea/GBF1 subfamilies contain six predicted conserved domains, with an additional domain found in the Sec7/BIG subfamily (Figure 1.5) (Bui, Golinelli-Cohen, and Jackson 2009). The N-terminal dimerization and cyclophilin binding (DCB) domain was

described in the plant Gea/GBF1 Arf-GEF, GNOM, as facilitating dimerization and binding to cyclophilin 5 (Grebe et al. 2000), although the functional importance of dimerization and conservation of the cyclophilin 5 interaction have not been reported. Immediately C-terminal to the DCB domain is the homology upstream of Sec7 (HUS) domain, which our group recently showed to fold as a single domain with the DCB domain in *Thielavia terrestris* Sec7 (DCB/HUS) (Richardson et al. 2016). In addition, we showed that this joint DCB/HUS domain in Sec7 facilitates membrane insertion of the Arf1 amphipathic helix upon nucleotide exchange.

The catalytic GEF domain follows the DCB/HUS domain and is in turn followed by three more, the homology downstream of Sec7 (HDS1, HDS2, and HDS3) domains. It should be noted that these domains show no homology to one another, but rather each domain is conserved across species. Comprehensive roles for these domains remain unclear, despite recent advances. Our group showed that the C-terminal domains of Sec7 regulate catalytic function through autoinhibition and that HDS1 domain interacts with Arf1-GTP in a positive feedback loop (Richardson, McDonold, and Fromme 2012). The HDS1 domain of GBF1 has been implicated in targeting to lipid droplets and the Golgi membrane (Bouvet et al. 2013), but this role has not been tested for conservation in yeast. Finally, the Sec7/BIG Arf-GEFs have an additional domain, HDS4, which is not conserved among Gea/GBF1 Arf-GEFs. We recently described a novel role for this domain in dimerization of yeast Sec7 (Richardson et al. 2016).

Sec7/BIG function at the trans-Golgi network to facilitate anterograde traffic, while Gea/GBF1 function in intra-Golgi and Golgi-ER retrograde traffic. Therefore, understanding the

mechanisms which regulate localization of these Arf-GEFs to distinct parts of the Golgi is essential to understanding overall regulation of Arf1-initiated vesicle trafficking. Our group demonstrated that several small GTPases, Arf1, Ypt1, Arl1, and Ypt31/32, cooperate to recruit Sec7 to Golgi membranes and stimulate its activity (McDonold and Fromme 2014). Other Arf-GEFs are regulated by equally complex interaction networks (Stalder and Antonny 2013). While a similarly fine-tuned coordination of signals is likely to recruit Gea1 and Gea2 to early and medial Golgi membranes, recruiting interactions have remained elusive.

A direct interaction between the N-terminus of GBF1 and the human Ypt1 homolog, Rab1b, has been reported, but no functional significance for this interaction has previously been described (Monetta et al. 2007). The trans-Golgi lipid flippase Drs2 and the small GTPase Arl1 have been identified as Gea interactors, although the reason for these interactions is unresolved (Chantalat et al. 2004; Tsai et al. 2013). Similarly, no mechanistic explanation has been uncovered for the interaction between Gea2 and Gmh1, a Golgi protein of unknown function (Chantalat et al. 2003), and the reported interaction between Gea/GBF1 and the COPI coat seems likely to occur downstream of Gea/GBF1 membrane recruitment (Deng et al. 2009). In addition, many of these studies rely on yeast two-hybrid experiments with truncated proteins, which may be prone to artefacts, and none report *in vitro* mechanistic studies with completely purified full length Gea/GBF1.

Summary of presented work

Here I will present my contributions to our understanding of the regulation of Gea1 and Gea2. First, I will share a completed story which describes the different membrane preferences of Gea1/2 and Sec7, the role of the HDS1-3 domains, and Gea recruitment by Ypt1 in a C-terminal dependent manner. I will then outline my efforts to crystallize and solve the structure of Gea. Next, I will share further evidence of the roles of the domains of Gea1 and Gea2, as well as demonstrate that Gea1 and Gea2 occupy distinct Golgi compartments. I will also describe my strategies for uncovering Gea interactors, culminating in the discovery of a potential new recruiting partner. Finally, I will summarize future directions for this line of inquiry. Throughout, I will make the case that understanding the regulation of Gea1 and Gea2 will provide insight into the essential role that these proteins play and may offer evidence of conserved mechanisms for the regulation of membrane trafficking.

- CHAPTER 2 -

REGULATION OF ARF ACTIVATION OCCURS VIA DISTINCT MECHANISMS AT EARLY AND LATE GOLGI COMPARTMENTS

Introduction

Intracellular membrane trafficking is an essential and intricately coordinated process in eukaryotes. Membrane-bound vesicles transport synthesized proteins and lipids to compartments where modifications occur, deliver them to their final destinations, and shuttle them between organelles and the plasma membrane as needed. The Golgi complex is the central sorting compartment for intracellular membrane trafficking, and vesicular traffic out of the Golgi is both tightly regulated and highly conserved to ensure that cargo only leaves the Golgi at the appropriate place and time.

A key regulator of vesicle formation throughout the Golgi is the small GTPase Arf1 and its paralogs (Stearns et al. 1990; Donaldson and Honda 2005). As with other small GTPases, Arf1 functions as a molecular switch. When GDP-bound, it is inactive and cytoplasmic. Upon GTP binding, Arf1 inserts its myristoylated N-terminal amphipathic helix into the membrane and changes conformation to recruit cargos, cargo adapters, and coat proteins to generate a vesicle (Bruno Antonny et al. 1997; Goldberg 1998). Thus, the decision to switch Arf1 "on" through nucleotide exchange is a pivotal regulatory event in Golgi membrane trafficking.

Nucleotide exchange on Arf1 is carried out by the Sec7 family of guanine nucleotide exchange factors (Arf-GEFs) (C. L. Jackson and Casanova 2000; Gillingham and Munro 2007a; Casanova

2007). Two highly conserved subfamilies of Arf-GEFs function at the Golgi complex: Gea/GBF and Sec7/BIG, in *Saccharomyces cerevisiae*/humans, respectively (Achstetter et al. 1988; Peyroche, Paris, and Jackson 1996). Outside of the highly-conserved catalytic GEF domain, these Golgi Arf-GEFs differ greatly from the rest of the Sec7 family to which they belong (Mouratou et al. 2005; Bui, Golinelli-Cohen, and Jackson 2009). They are considerably larger and share no sequence homology with any known domains in other proteins, including canonical membrane-targeting domains, outside of the GEF domain. Yet understanding how these Golgi Arf-GEFs are regulated and recruited to the correct membrane surface is essential to understanding the regulation of Arf1 activation and subsequent vesicle formation.

The Sec7/BIG subfamily of Golgi Arf-GEFs functions at the TGN, activating Arf1 to form secretory vesicles and vesicles that traffic to endosomes and lysosomes. Our group has shown that Sec7 is regulated through strong autoinhibition, a positive feedback loop with Arf1, interactions with several other small GTPases, and dimerization through its C-terminal HDS4 domain (Richardson, McDonold, and Fromme 2012; Richardson et al. 2016; McDonold and Fromme 2014). Sec7, Gea1, and Gea2 share predicted domain architecture (Bui, Golinelli-Cohen, and Jackson 2009), which suggests shared regulation. However, Gea1 and Gea2, which function in intra-Golgi and Golgi-ER retrograde traffic, lack similar positive feedback and dimerization regulatory mechanisms (Richardson, McDonold, and Fromme 2012). Evidence of protein interactors has been presented by other groups (Jones et al. 1999; Chantalat et al. 2003; Chantalat et al. 2004; Monetta et al. 2007; Deng et al. 2009; Christis and Munro 2012; Tsai et al. 2013), but to date no clear picture of the regulation of Gea/GBF has been established.

Here, we present evidence for a model in which the C-terminal domains of Gea1 and Gea2 serve both inhibitory and stimulatory functions in regulation. We also show that the nature of the membrane surface is important for function of Gea1 and Gea2 and that the Rab GTPase Ypt1 recruits Gea1 and Gea2 to membranes in a manner dependent on the C-terminus of Gea2. Our findings define several important mechanistic differences between the Sec7/BIG and Gea/GBF1 families and indicate that Arf1-dependent trafficking can be regulated independently at early versus late Golgi compartments.

Results

Gea1 and Gea2 localize differently relative to early and late Golgi markers.

Sec7 is well-established as localizing to the TGN, where it activates Arf1 to initiate formation of secretory vesicles and vesicles that traffic to endosomes and the lysosome/vacuole. In contrast, Gea1 and Gea2 have been shown to function in COPI vesicle-mediated intra-Golgi and Golgi-ER traffic and to fractionate with early Golgi markers (Spang et al. 2001; Deng et al. 2009). To confirm the distribution of large Arf-GEFs at the Golgi in live cells, we generated strains that co-expressed endogenously-tagged Gea1 or Gea2 with either the early Golgi marker Vrg4 or with Sec7 as a marker for the TGN (Losev et al. 2006; Matsuura-Tokita et al. 2006). Gea1 shows greater colocalization with Vrg4-labeled Golgi compartments (Figure 2.1 A) than with Sec7 compartments (Figure 2.1, B & E), while Gea2 colocalizes more with Sec7 (Figure 2.1 C) than Vrg4 (Figure 2. 1, D & F). Neither Gea1 nor Gea2 shows perfect colocalization or anti-

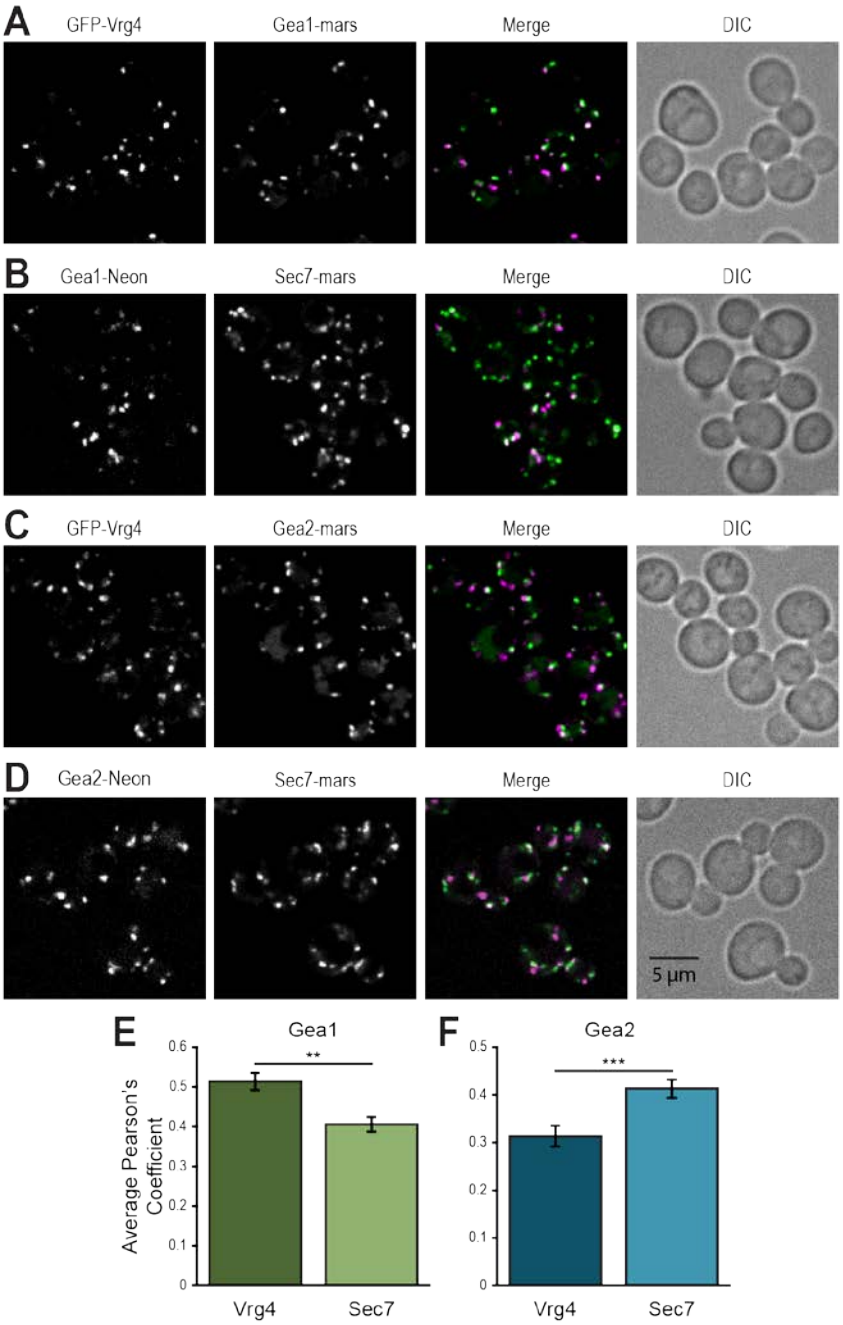

Figure 2.1. Gea1 and Gea2 localize differently relative to early and late Golgi markers. (A) Subcellular localization of GFP-Vrg4, an early Golgi marker, and Gea1-3xmRFPmars and (B) of Gea1-mNeonGreen and mRFPmars-Sec7, a late Golgi marker. (C) Subcellular localization of GFP-Vrg4 and Gea2-3xmRFPmars and (D) of Gea2-mNeonGreen and mRFPmars-Sec7. Quantification of colocalization of Gea1 (E) or Gea2 (F) with Vrg4 or Sec7 at puncta. Error bars represent 95% CIs for n = 76 (Gea1 v. Vrg4), n = 84 (Gea1 v. Sec7) cells, n = 59 (Gea2 v. Vrg4), or n = 58 (Gea2 v. Sec7) cells. In all Merge panels, the GFP channel is shown in green, the RFP channel in magenta, and areas of overlap in white. Differential interference contrast (DIC) panels show cells in the field. **, $P < 0.01$; ***, $P < 0.0001$.

correlation with either marker, suggesting that the Gea Arf-GEFs occupy intermediate or hybrid compartments and reflecting the dynamic nature of the Golgi. These data indicate that Gea1 occupies earlier Golgi compartments than Gea2 (Figure 2.2A), hinting at differences in their roles and regulatory mechanisms.

The in vitro *membrane preferences of Gea1, Gea2, and Sec7 correspond to their sub-Golgi localization* in vivo.

One feature that distinguishes the early Golgi from the TGN is the net charge of the cytosolic membrane surface. There is a well-established gradient of anionic phosphatidylserine (PS) across the secretory pathway, with very little PS exposed to the cytosol at the ER and as much as 10% or more PS in the cytosolic lipid content of the PM (Figure 2.2A) (van Meer, Voelker, and Feigenson 2008; Leventis and Grinstein 2010; Bigay and Antonny 2012). This gradient is achieved by lipid flippases including Drs2, which flips PS from the lumen to the cytosol at the TGN (Natarajan et al. 2004). Additionally, the phosphatidylinositol 4-kinase Pik1 phosphorylates phosphatidylinositol (PI) to PI4P at the TGN (Walch-Solimena and Novick 1999; Strahl et al. 2005). Both PI4P and PS lend negative charges to the membrane surface of the TGN which are absent at earlier Golgi compartments. I hypothesized that the nature of the lipid environment in which each of the Golgi Arf-GEFs functions would impact their regulation, so I tested the membrane preferences of each Arf-GEF using *in vitro* catalytic assays.

To measure the catalytic activity of Arf-GEFs, I employed a well-established assay which measures native tryptophan fluorescence of Arf1 to monitor GEF-catalyzed nucleotide exchange

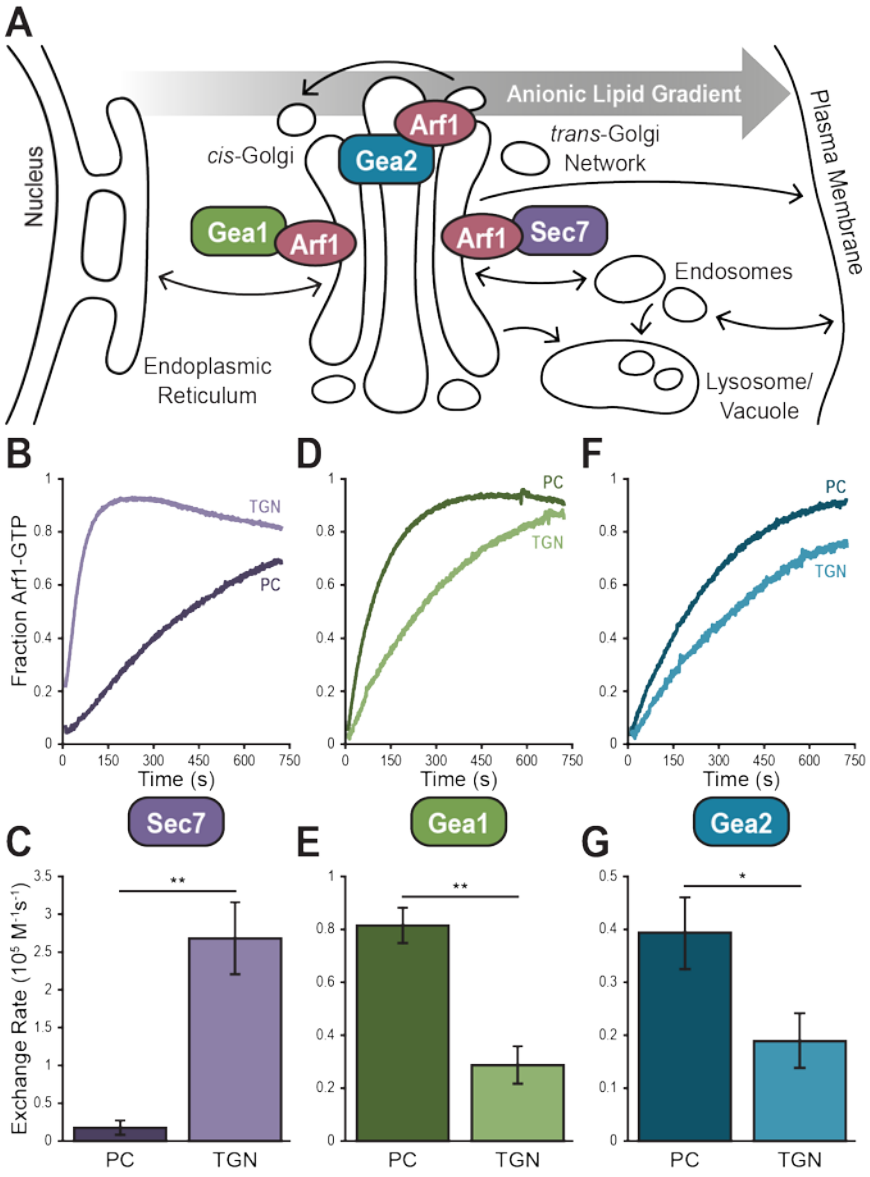

Figure 2.2. The *in vitro* membrane preferences of Gea1, Gea2, and Sec7 correspond to their sub-Golgi localization *in vivo*. (A) Cartoon of the secretory pathway, showing relative sub-Golgi localization of Gea1, Gea2, and Sec7 as well as the gradient of anionic lipids on the cytosolic membrane surface from the ER to the plasma membrane. Representative normalized traces showing activation of Arf1 by Sec7$_f$ (B), Gea1 (D), and Gea2 (F) on synthetic PC and TGN liposomes. Rates of Arf1 activation determined from full sets of traces for Sec7$_f$ (C), Gea1 (E), and Gea2 (G). Error bars represent 95% CIs for n = 3 reactions. *, $P < 0.05$; **, $P < 0.01$.

in real time (Higashijima et al. 1987; Richardson and Fromme 2015). These experiments were performed at approximate physiological concentrations of GEF (100 nM) and Arf1 (600 nM) (Ghaemmaghami et al. 2003) in the presence of artificial liposomes.

As we reported previously, our group has purified a functional recombinant construct of Sec7 ($Sec7_t$) for use in *in vitro* studies (Richardson, McDonold, and Fromme 2012; McDonold and Fromme 2014). Similar biochemical studies of Gea1 and Gea2 have been precluded by the difficulty in purifying stable Arf-GEFs in sufficient quantities for study. Therefore, we established protocols for purifying full length recombinant Gea1 and Gea2, allowing us to make biochemical inquiries into the mechanisms of Gea1 and Gea2 regulation (Figure 2.3 A).

We benefit from a detailed model for TGN lipid composition (Klemm et al. 2009; Richardson, McDonold, and Fromme 2012), which we used to generate liposomes that mimic the TGN's lipid environment. We lack similar data describing the precise lipid composition of the earlier Golgi compartments, so we used a simplistic model of neutral phosphotidylcholine (PC) to simulate the lipid environment of the early Golgi.

When we measured catalysis of Arf1 activation by Sec7, we observed a 10-fold higher rate on TGN than on PC liposomes (Figure 2.2, B & C). This parallels the inherent preference of Arf1 for TGN liposomes when intrinsic exchange was stimulated by incubation with EDTA (Figure 2.4) and matches the known localization of Sec7 to the anionic TGN. Notably, Gea1 and Gea2 both display the opposite preference: Gea1 demonstrated a 3-fold and Gea2 a 2-fold higher rate

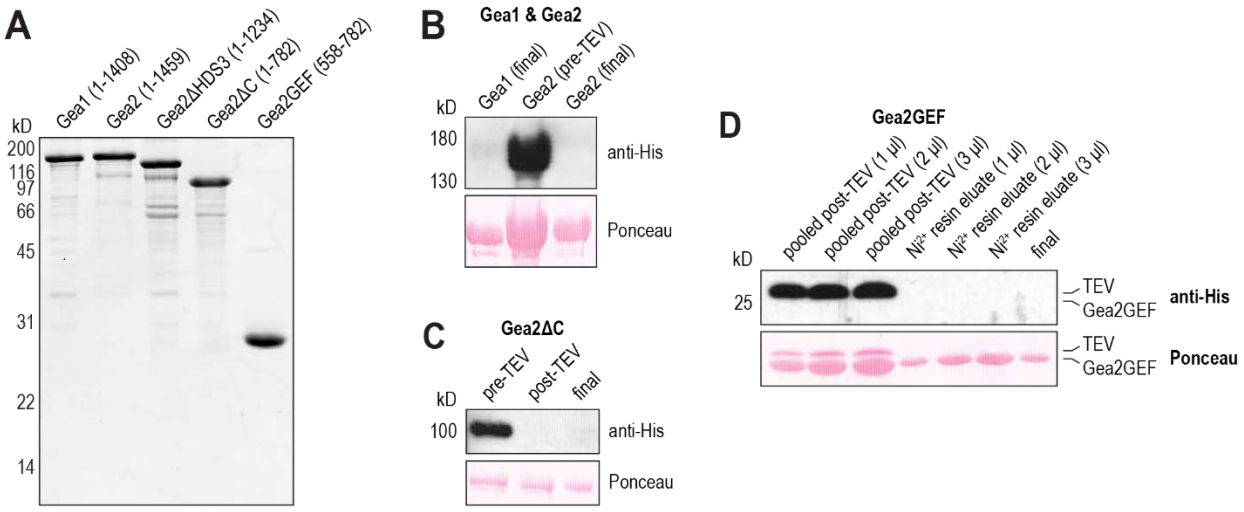

Figure 2.3. GEF constructs used for biochemistry are pure and His_6 tags were successfully cleaved. (A) After purification from *Escherichia coli*, equal masses of full length Gea1 and Gea2, Gea2ΔHDS3, Gea2ΔC, and Gea2GEF were separated on an 8% polyacrylamide gel and visualized by Coomassie staining. Western blots with anti-His antibody against (B) Gea2 before TEV cleavage of the His_6 tag and final reagent samples of Gea1 and Gea2, (C) Gea2ΔC before and after TEV cleavage of the His_6 tag, as well as the final Gea2ΔC reagent, and (D) dilutions of fractions of Gea2GEF pooled after TEV cleavage, after incubation with and elution from Ni-NTA resin, and the final Gea2GEF reagent. For all western blots, Ponceau stains reveal protein on the membrane. Note that TEV protease is His_6-tagged.

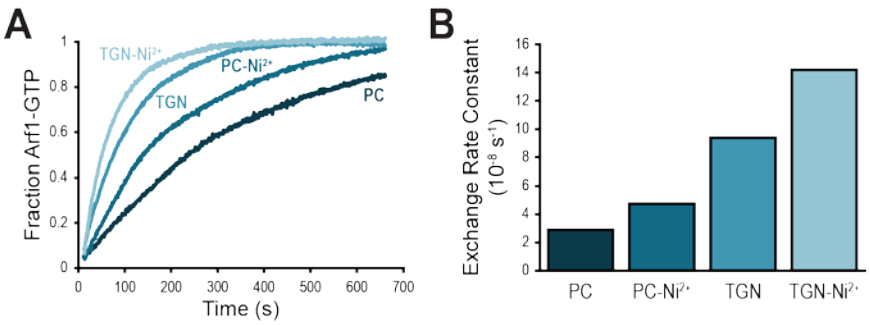

Figure 2.4. EDTA-induced Arf1 nucleotide exchange favors TGN over PC liposomes *in vitro*. (A) Normalized traces showing EDTA exchange of Arf1 on PC, PC-Ni^{2+}, TGN, and TGN-Ni^{2+} liposomes. (B) Rates of Arf1 exchange determined from traces in (A).

of Arf1 exchange on PC over TGN liposomes (Figure 2.2, D-G). This is contrary to the intrinsic preference of Arf1, indicating that the Gea GEFs themselves prefer PC over TGN lipids. This finding is consistent with the localization of Gea1 and Gea2 to earlier Golgi compartments, which lack exposed anionic lipids such as PS and PI4P.

Cells require a critical mass of either Gea1 or Gea2 for growth.

Gea1 and Gea2 are genetically redundant under normal growth conditions (Peyroche, Paris, and Jackson 1996). However, although an *arf1Δgea1Δ* mutant (sustained by wild type Arf2, which is expressed at 10-fold lower cellular concentrations than Arf1 (Stearns et al. 1990)) is viable, an *arf1Δgea2Δ* is not (Spang et al. 2001). One possible explanation for this phenotype is some separation of function between Gea1 and Gea2, with Gea2 serving a function that is essential under stress conditions. Another possibility is a simple difference in expression levels: Gea2 is expressed at approximately 5-fold higher levels than Gea1 (Ghaemmaghami et al. 2003). In light of our observation that Gea1 and Gea2 show different localization patterns, we tested the simpler of these two possibilities by creating promoter swaps to invert expression levels of the two Arf-GEFs.

Using a plasmid shuffling strain (*gea1Δgea2Δ*) maintained by *GEA2* on a *URA3* plasmid, we compared *LEU2* plasmids harboring GFP-tagged wild type *GEA1* or *GEA2* to the promoter swaps P_{GEA2}-*GEA1* and P_{GEA1}-*GEA2*. Western blotting of GFP-immunoprecipitation samples confirmed that the promoter swap had the expected effect, significantly reducing cellular expression levels of Gea2 (Figure 2.5 A).

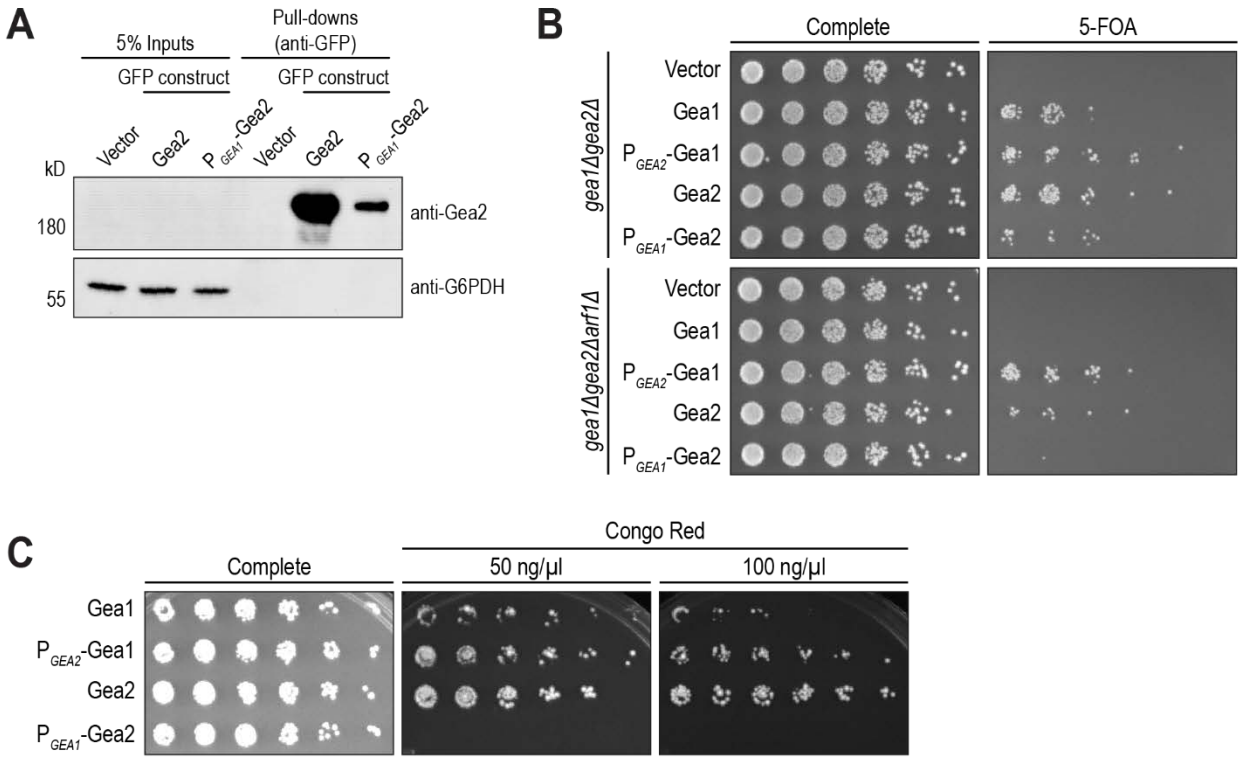

Figure 2.5. Cells require a critical mass of either Gea1 or Gea2 for growth. (A) Protein expression levels of Gea2 expressed through its endogenous promoter (Gea2) and through Gea1's promoter (P_{GEA1}-Gea2) were visualized by Western blot after GFP pull-downs. G6PDH serves as a loading control. (B) Gea1 and Gea2, expressed through their endogenous promoters or with swapped promoters, were expressed on *CEN* plasmids in *gea1Δgea2Δ* and *gea1Δgea2Δ*arf*1Δ* cells and selected for with 5-FOA. Relative growth of colonies on 5-FOA media reflects sufficiency of each construct to support growth as the sole early Arf-GEF in the cell. (C) Cells from the top right panel of B were cultured and plated onto media containing 50 ng/µl and 100 ng/µl Congo Red to test for sensitivity to this compound. Data shown represent ≥3 independent experiments.

We observed that yeast growth was impaired in cells harboring only wild type Gea1, compared to only wild type Gea2 (Figure 2.5 B). Yeast harboring the promoter-swapped P_{GEA2}-Gea1 grew as well as those with wild type Gea2, while promoter swapped P_{GEA1}-Gea2 yielded growth impairment similar to wild type Gea1 (Figure 2.5 B). Furthermore, in a shuffling strain stressed by reduced levels of Arf at the Golgi (*gea1Δgea2Δarf1Δ*), the phenotype was more stark: cells harboring Gea1 or Gea2 expressed via the *GEA2* promoter grew, while cells with the *GEA1* promoter-driven Gea1 or Gea2 constructs failed to grow.

Another previously observed difference between Gea1 and Gea2 is the sensitivity of *gea2Δ* cells to Congo Red, a dye which interferes with cell wall integrity by binding nascent β-glucan chains. *gea2Δ* cells, but not *gea1Δ* cells, are hypersensitive to Congo Red (Tsai et al. 2013), again suggesting some function of Gea2 that Gea1 cannot complement. However, when we tested the promoter swap constructs, the Congo Red phenotype was revealed to also depend on expression levels (Figure 2.5 C). Cells with only wild type Gea1 were more sensitive to Congo Red than cells with only wild type Gea2. Cells harboring P_{GEA2}-Gea1, on the other hand, grew as well as cells with wild type Gea2, while cells with P_{GEA1}-Gea2 did not grow.

These results demonstrate that the sensitivity of *gea2Δ* and survival of *gea1Δ* cells under stress conditions can be attributed to differential expression levels of Gea1 and Gea2, rather than to an essential function specific to Gea2. It also highlights the requirement for a critical mass of either Gea1 or Gea2 under stress conditions.

The HDS1 and HDS2 domains of Gea1 and Gea2 are required for localization and essential in vivo, *while the HDS3 domain is dispensable.*

Studies of human GBF1 have revealed roles for its N-terminal domains in homodimerization and for its HDS1 domain in membrane targeting (Ramaen et al. 2007; Bhatt et al. 2016; Bouvet et al. 2013). The roles of the HDS2 and HDS3 domains remain unresolved, and Gea1 and Gea2 may have evolved separate regulatory mechanisms from GBF1 after the whole genome duplication event in yeast. Therefore, we pursued more information regarding the roles of the C-terminal domains of Gea1 and Gea2.

In addition to full length (FL) Gea1 (1-1408) and Gea2 (1-1459), we generated C-terminal truncations of Gea1 and Gea2 harboring C-terminal mNeonGreen tags: Gea1ΔHDS3 (1-1225), Gea1ΔC (1-774), Gea2ΔHDS3 (1-1234), and Gea2ΔC (1-782) (Figure 2.6 A). We found that constructs lacking both the HDS2 and HDS3 domains were unstable. The stable constructs were introduced into wild type yeast and expressed under the native *GEA1* and *GEA2* promoters. We verified by Western blotting that the truncations do not dramatically diminish expression levels under these conditions (Figure 2.6 B).

Fluorescence microscopy revealed that, for both Gea1 and Gea2, the FL and ΔHDS3 constructs localized normally to Golgi puncta (Figure 2.6 C). The ΔHDS3 signal was weaker than the FL, likely reflecting the slight reduction in expression shown in Figure 2.6 B. Strikingly, Gea1ΔC

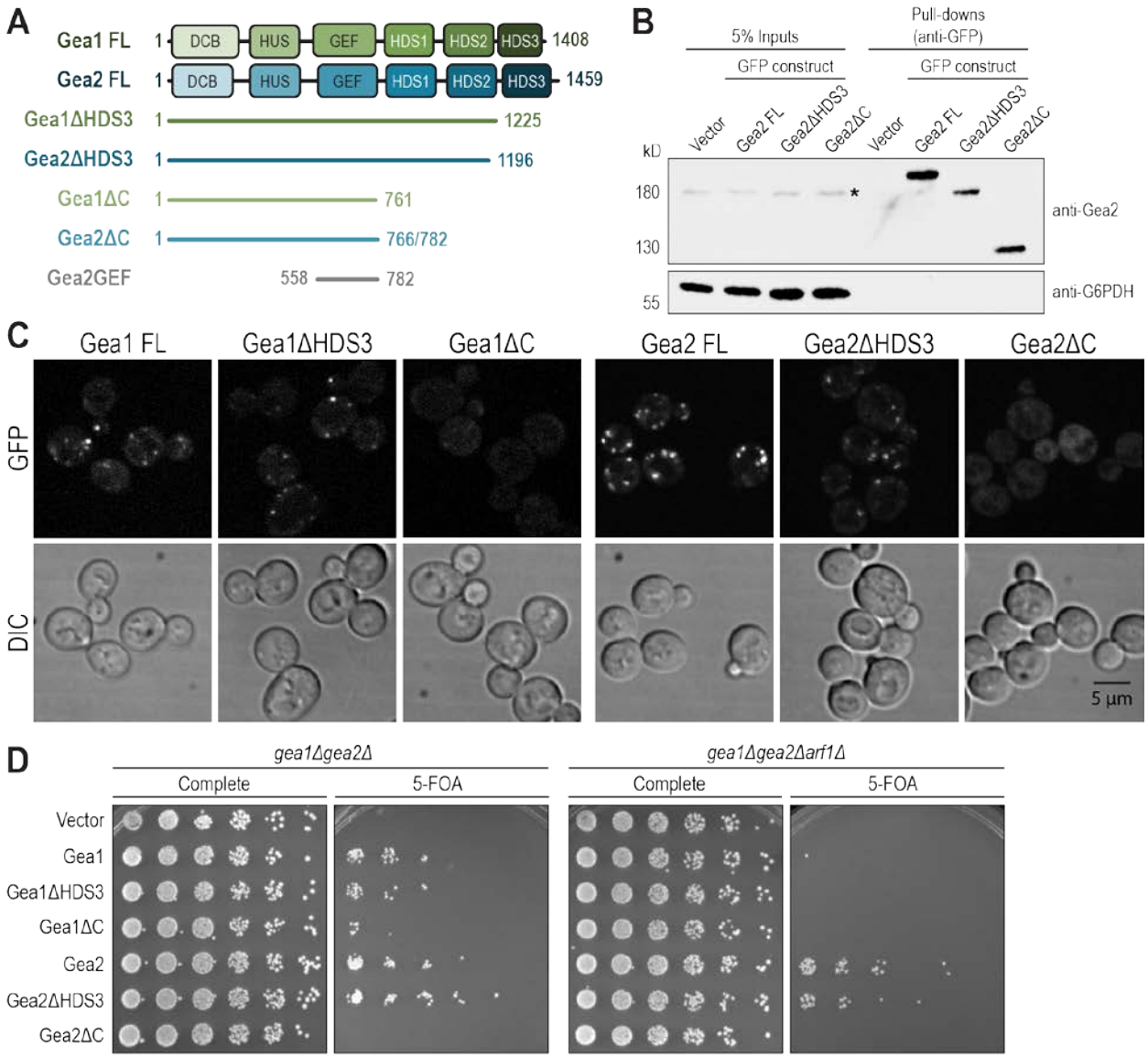

Figure 2.6. The HDS1 and HDS2 domains of Gea1 and Gea2 are required for localization and essential *in vivo*, while the HDS3 domain is dispensable. (A) Diagram of full length and truncated constructs of Gea1 and Gea2 employed in this study. DCB, dimerization and cyclophilin binding; HUS, homology upstream of Sec7; GEF, guanine nucleotide exchange factor (catalytic, aka "Sec7" domain); HDS, homology downstream of Sec7. Note that the HDS1, 2, and 3 domains are not homologous to one another. (B) Full length Gea2 (Gea2 FL), Gea2 lacking the HDS3 domain (Gea2ΔHDS3), and Gea2 lacking all domains downstream of the GEF domain (Gea2ΔC) were expressed with GFP tags through Gea2's endogenous promoter on *CEN* plasmids in wild type cells. After pull-down with GFP, expression levels of each construct were assessed through Western blot. *, signal from endogenous Gea2 in the whole cell extract before pull-downs. G6PDH serves as a loading control. (C) Gea1 and Gea2 constructs (FL, ΔHDS3, and ΔC) were tagged with 3xGFP and visualized in wild type cells. DIC panels show cells in the field. (D) The same constructs of Gea1 and Gea2 were expressed in *gea1Δgea2Δ* and *gea1Δgea2Δ*arf*1Δ* cells as in Figure 3B. Data shown represent ≥3 independent experiments.

and Gea2ΔC were completely mislocalized to the cytoplasm, showing no punctate signal despite expression comparable to that of the ΔHDS3 construct.

We next tested the ability of these C-terminal truncations to provide essential Gea function and observed that for both Gea1 and Gea2, the FL and ΔHDS3 constructs supported growth in the *gea1Δgea2Δ* strain (Figure 2.6 D). The growth of cells harboring only Gea1ΔC is considerably impaired, while cells harboring only Gea2ΔC do not grow at all. As expected, none of the Gea1 constructs supported growth in *gea1Δgea2Δarf1Δ* strain, while the relative growth of cells harboring the Gea2 truncation constructs remained the same.

Together, these results indicate that the HDS3 domains of Gea1 and Gea2 are dispensable for subcellular localization and essential function. In contrast the HDS1 and HDS2 domains are required for localization to Golgi cisternae and for cell survival.

The C-terminus of Gea2 both inhibits membrane binding in vitro *and contributes to Arf1 nucleotide exchange.*

To try to understand the reason for mislocalization of Gea1ΔC and Gea2ΔC, we purified recombinant Gea2ΔC as well as a construct comprising the GEF domain of Gea2 (558-782) (Figure 2.6 A). We then tested membrane binding of each construct in membrane pelleting assays (Paczkowski and Fromme 2016). As PC liposomes do not pellet efficiently in this assay, we incubated each construct with TGN liposomes. After subjecting each binding reaction to ultracentrifugation, we isolated the membrane pellet, including any membrane-associated

proteins, and quantified the amount of each Gea2 construct in the pellet and the supernatant by measuring band intensity after SDS PAGE. We controlled for background pelleting of Gea2 by carrying out parallel experiments in the absence of liposomes (Figure 2.7 A). After normalizing for background pelleting, we found about 15% of Gea2 FL bound to membranes (Figure 2.7 B). Unexpectedly, considering the *in vivo* results, Gea2ΔC showed higher affinity for membranes, with approximately 30% of that construct pelleting. Finally, the Gea2GEF construct showed no affinity for membranes above background.

As the C-terminal domains of Gea2 are essential *in vivo* but not required for membrane binding *in vitro*, we tested whether the C-terminus might play a role in the nucleotide exchange function of Gea2. First, we tested Arf1 nucleotide exchange by Gea2 FL, Gea2ΔC, and Gea2GEF in the presence of PC liposomes. Gea2FL and Gea2ΔC showed no significant difference in exchange rates on these liposomes, while the GEF domain displayed no measurable exchange activity (Figure 2.7 C).

Considering the very slow rates of Arf1 activation observed on PC liposomes, we hoped to tease out subtle differences in activity by observing reactions under different conditions. We have observed that Gea1 and Gea2 show a significant preference for liposomes containing the artificial lipid Ni^{2+}-DOGS, used in assaying potential recruiting interactions with poly-histidine-anchored proteins. Despite lacking histidine tags (Figure 2.3, B-D), full length Gea1 and Gea2 display higher reaction rates on PC-Ni^{2+} liposomes than on PC liposomes, and Arf1 itself shows a subtle preference for PC-Ni^{2+} over PC liposomes when activated by EDTA (Figure 2.4). A

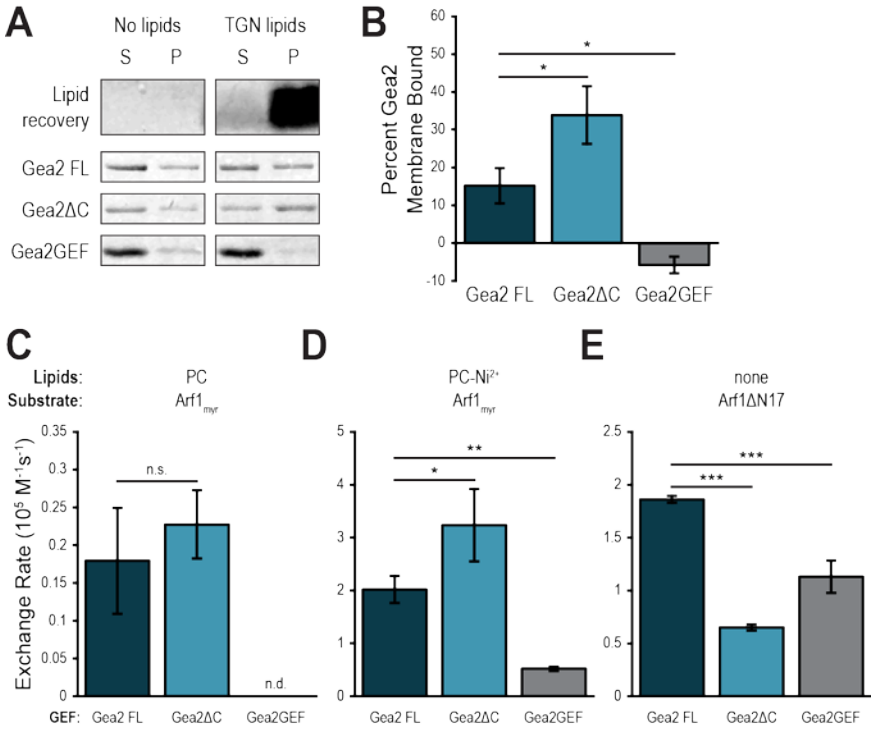

Figure 2.7. The C-terminus of Gea2 both inhibits membrane binding and contributes to Arf1 nucleotide exchange. (A) Purified full length Gea2 (Gea2 FL), Gea2 lacking its C-terminal domains (Gea2ΔC), and the isolated catalytic domain (Gea2GEF) were incubated with or without TGN liposomes before ultracentrifugation. Supernatant (S) and pellet (P) were separated and lipids and proteins in each fraction were visualized by SDS PAGE. (B) Quantification of band intensity represented as percent Gea2 in pellet after subtracting background, for n = 3 (Gea2FL and Gea2ΔC) and n = 2 (Gea2GEF) independent assays. Rates of Arf1 activation by Gea2 FL, Gea2ΔC, and Gea2GEF on PC (C) or PC-Ni^{2+} (D) liposomes or in the absence of liposomes using the soluble mutant Arf1ΔN17 (E). n = 3. n.d., not detectable (the Arf1 was not activated by the GEF, and exponential functions could not be fit to experimental curves); n.s., not significant; *, $P < 0.05$; **, $P < 0.01$; ***, $P < 0.001$.

similar affinity for Ni^{2+}-DOGS lipids has been observed previously for other GEFs (Thomas and Fromme 2016). While we lack a physiological explanation for the phenomenon, we reasoned that faster rates overall would amplify differences in catalytic rates. Therefore, we tested the catalytic activity of Gea2ΔC and Gea2GEF on PC-Ni^{2+} liposomes.

Interestingly, Gea2ΔC catalyzed exchange on Arf1 at a higher rate than Gea2 FL on PC-Ni^{2+} liposomes (Figure 2.7 D). The GEF domain remained inefficient at catalysis in the absence of Gea2's other domains, but catalyzed low level, measurable exchange on PC-Ni^{2+} liposomes. These relative exchange reaction rates correlated with the relative membrane affinities of these constructs (Figure 2.7, A and B).

To examine how the C-terminus contributes to catalysis without the confounding factor of membrane interaction, we employed the mutant Arf1ΔN17, which is missing its amphipathic membrane-inserting helix and can therefore be activated in solution. Based on the results in Figures 5, C and D, we expected one of two outcomes when testing Arf1 exchange by Gea2 constructs in solution. If the difference in rates observed on membranes was due to an allosteric effect of removing the HDS domains, the activity of Gea2ΔC would be higher than the activity of Gea2 FL in solution. If the increased catalytic activity of Gea2ΔC was due to its increased membrane binding, and therefore higher likelihood of successful catalytic events, then Gea2ΔC and Gea2 FL would activate Arf1 at similar rates in solution. Surprisingly, a third possibility proved true for this experiment: in these soluble exchange reactions, Gea2 FL showed the

highest catalytic rate on Arf1ΔN17, followed by Gea2GEF (Figure 2.7 E). Gea2ΔC showed the slowest catalytic rate on Arf1ΔN17 in the absence of liposomes.

Taken together, the results of these membrane binding and catalytic assays suggest a complex role for the C-terminus of Gea2 in regulating activation of Arf1, but show a clear role for the N-terminus in membrane binding.

Gea1 and Gea2 are recruited to membranes by the small GTPase Ypt1.

As shown in Figure 2.7 A, approximately 15% of Gea2 FL is membrane bound *in vitro* in the absence of other factors. Furthermore, *in vivo*, both N-terminal and C-terminal domains of Gea1 and Gea2 are needed for Golgi localization. This suggests that the intrinsic membrane affinity of Gea1 and Gea2 is likely not the only factor regulating their recruitment to Golgi membranes. Sec7 has been shown to be recruited to membranes and is regulated by interactions with several GTPases, so an analogous mechanism may regulate Gea1 and Gea2. Although Gea1 lacks the positive feedback interaction observed between Sec7 and Arf1 (Richardson, McDonold, and Fromme 2012), the Arf-like GTPase Arl1 interacts with Gea2 (Tsai et al. 2013) and human Rab1b (yeast Ypt1) GTPase interacts with the N-terminus of human GBF1 (yeast Gea1/Gea2) (Monetta et al. 2007).

To explore physical regulatory interactions between Golgi GTPases and Gea1/2, we carried out Gea1 and Gea2 membrane binding assays on PC-Ni^{2+} liposomes preloaded with activated (GTP-bound) myristoylated Arf1, myristoylated Arl1, Ypt1-His_7, or the Rab GTPase Ypt6-His_7. These

assays confirmed that Arf1 does not recruit either Gea1 or Gea2 to membranes (Figure 2.8, A and B). Furthermore, neither Arl1 nor Ypt6 increased membrane binding of Gea1 or Gea2 (Figure 2.9). The only Golgi small GTPase that increased membrane binding was Ypt1.

We hypothesized that this recruitment of Gea1 and Gea2 to membranes by Ypt1 would increase their catalytic rates on Arf1 by concentrating the GEFs at the membrane surface where activation of Arf1 must occur. To test this hypothesis, we performed catalytic assays using liposomes alone, liposomes preloaded with activated Arf1, and liposomes preloaded with activated Ypt1-His_7. As expected from the membrane binding results, Arf1 conferred no improvement of catalytic activity for Gea1 or Gea2 (Figure 2.8, C & D). Surprisingly, recruitment by Ypt1 under these conditions yielded only a subtle increase in catalytic rate for Gea1 and a statistically insignificant increase for Gea2. To dissect this apparent discrepancy between our expectations and results, we halved the concentration of liposomes in the catalytic assays. If recruitment is important for activity, increasing the scarcity of membranes in the reaction should resolve a difference between intrinsic, weak membrane binding of Gea1 or Gea2 and active recruitment by Ypt1. Indeed, in catalytic assays with reduced liposome concentrations, both Gea1 and Gea2 showed higher catalytic rates on Ypt1-preloaded liposomes compared to liposomes alone (Figure 2.8, E & F).

These results indicate that Ypt1 increases Gea1 and Gea2 GEF activity by increasing membrane recruitment of the GEF, thereby increasing the likelihood of productive catalytic interactions between the GEF and Arf1 at the membrane surface.

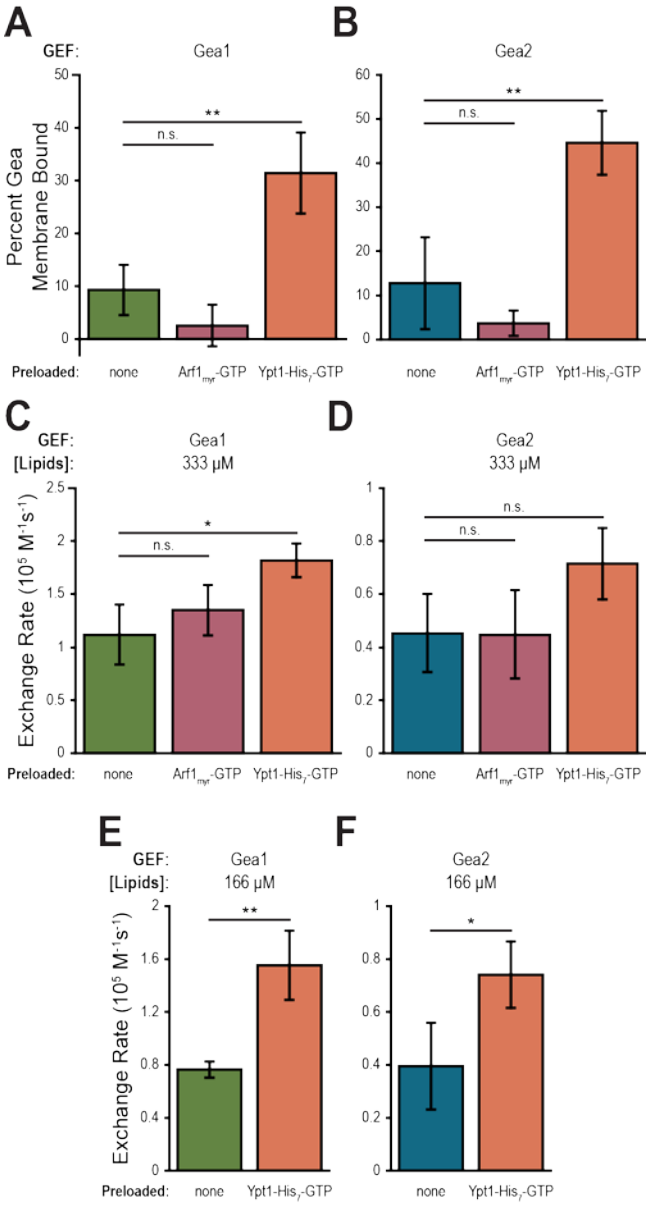

Figure 2.8. Gea1 and Gea2 are recruited to membranes by the small GTPase Ypt1. Membrane pelleting assays as in Figure 5 including preloaded small GTPases. Graphs show percent of Gea1 (A) or Gea2 (B) bound to membranes after incubation with PC-Ni^{2+} liposomes alone, preloaded with Arf1-GTP, or preloaded with Ypt1-His_7-GTP. n = 3. Rates of Arf1 activation by Gea1 (C) and Gea2 (D) on 333 µM PC-Ni^{2+} liposomes alone, preloaded with Arf1-GTP, or preloaded with Ypt1-His_7-GTP. n = 3. Rates of Arf1 activation by Gea1 (E) and Gea2 (F) with 166 µM PC-Ni^{2+} liposomes alone or preloaded with Ypt1-His_7-GTP. n = 3. n.s., not significant; *, $P < 0.05$; **, $P < 0.01$.

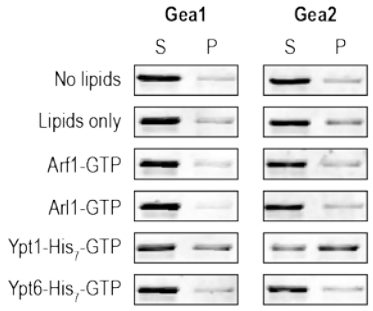

Figure 2.9. Neither Arl1 nor Ypt6 recruits Gea1 or Gea2 to membranes. Purified Gea1 and Gea2 were incubated with or without PC-Ni^{2+} liposomes and with no recruiter or GTP-bound Arf1, Arl1, Ypt1-His_7, or Ypt6-His_7 before ultracentrifugation. Supernatant (S) and pellet (P) were separated and proteins in each fraction were visualized by SDS PAGE.

The C-terminus of Gea2 is required for recruitment by Ypt1.

Finally, we set out to understand how regulation by the domains of Gea2 is coordinated with regulation through recruitment by Ypt1. To add a further degree of biological relevance, we carried out these assays using recombinant prenylated Ypt1 (prenyl-Ypt1). We used a protocol for purifying and modifying Ypt1 *in vitro*, yielding a complex of prenyl-Ypt1 and its stabilizing protein, GDP Dissociation Inhibitor (GDI) (Thomas and Fromme 2016). Using prenyl-Ypt1 enabled us to test Gea2 membrane binding and catalytic activity on membranes without any confounding effect from Ni^{2+}-DOGS.

First, we observed that prenyl-Ypt1 can recruit Gea2 FL to TGN liposomes (Figure 2.10 A). While the increase in membrane binding was more subtle with prenyl-Ypt1 and TGN liposomes than with Ypt1-His_7 and PC-Ni^{2+} liposomes, the trend endured under the more physiological conditions. Despite the documented interaction between Rab1b and GBF1's N-terminus (Monetta et al. 2007), prenyl-Ypt1 did not increase membrane binding of Gea2ΔC on TGN liposomes (Figure 2.10 B). The observed slight reduction in membrane binding of Gea2ΔC may reflect crowding of the membrane surface by prenyl-Ypt1 that cannot effectively recruit the truncated GEF. This result indicates that the C-terminal domains of Gea2 are required to stabilize the Ypt1-Gea2 interaction on membranes.

We next tested whether the failure of prenyl-Ypt1 to recruit Gea2ΔC to membranes coincided with an inability to improve catalytic activity. Gea2 FL showed an approximately 2-fold

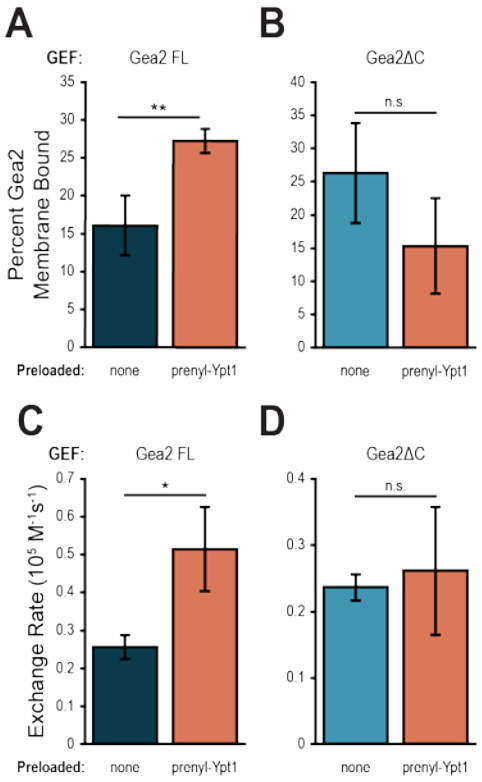

Figure 2.10. The C-terminus of Gea2 is required for recruitment by Ypt1. Percent of Gea2 FL (A) or Gea2ΔC (B) in membrane pellet after incubation with either TGN liposomes alone or with prenylated Ypt1-GTP (prenyl-Ypt1). $n \geq 3$. Rates of Arf1 activation by Gea2 FL (C) or Gea2ΔC (D) on PC liposomes alone or preloaded with prenylated Ypt1-GTP. $n = 3$. n.s., not significant; *, $P < 0.05$; **, $P < 0.01$.

increase in catalytic rate on PC liposomes preloaded with prenyl-Ypt1 (Figure 2.10 C), similar to that observed on PC-Ni^{2+} liposomes preloaded with Ypt1-His_7 (Figure 2.8 F). However, Gea2ΔC catalyzed Arf1 exchange at nearly the same rate on PC liposomes alone as on PC liposomes preloaded with prenyl-Ypt1 (Figure 2.10 D), indicating that the C-terminus of Gea2 is required for effective membrane recruitment by Ypt1, as well as for the positive effect on catalysis conferred by Ypt1 recruitment.

Discussion

Arf1 and its homologs are the central coordinators for Golgi vesicle formation in eukaryotic cells, where cargos are sorted for transport to the plasma membrane, the lysosome, and the endosome, as well as for retrograde traffic within the Golgi and to the ER. Thus, the activation of Arf GTPases at the Golgi represents a critical and conserved point for regulation of Golgi membrane trafficking. In yeast, the activation of Arf1/2 is carried out at the late Golgi by Sec7 and at earlier Golgi compartments by Gea1 and Gea2, implicating these Arf-GEFs as the key decision-makers in initiation of vesicle formation at the Golgi. Despite the essential role of Gea1 and Gea2 in retrograde transport, the mechanisms that govern regulation of these Arf-GEFs have remained elusive.

We have relatively little structural information about these large proteins, beyond structures of the GEF domain (Renault et al. 2002) and of a portion of the N-terminus of *Thielavia terrestris* Sec7 (Richardson et al. 2016), leaving any structure/function clues in the C-terminus obscured.

Temperature sensitive mutants have proven useful in describing whole-Golgi or whole cell phenotypes for Gea1 and Gea2 mutations (Spang et al. 2001; S.-K. Park, Hartnell, and Jackson 2005), but the precise reasons for these phenotypes are difficult to infer. Descriptions of genetic and physical interactions with Ypt1/Rab1b, COPI coat proteins, Drs2, Arl1, and Gmh1 allude to the complex environment in which Gea/GBF function (Jones et al. 1999; Chantalat et al. 2003; Chantalat et al. 2004; Monetta et al. 2007; Deng et al. 2009; Christis and Munro 2012; Tsai et al. 2013), but fail to separate recruiting from effector interactions, leaving the order of events of these interactions and the identity of recruiting partners unknown. The question of how these interactions fit into the overall tasks of Golgi membrane trafficking is unclear, and an exact picture of detailed regulatory mechanisms for Gea/GBF recruitment and function has yet to emerge.

In this study, we demonstrate that Gea1 and Gea2 share their essential function and several regulatory features (Figure 2.11 A). We show that while the HDS3 domain of Gea1 and Gea2 is dispensable for both localization and function *in vivo*, the HDS1 and HDS2 domains are required for localization. Our findings also reveal that the C-terminus of Gea2 is required for the interaction between Gea2 and Ypt1, which recruits Gea2 to membranes *in vitro*. Together with a previously reported role for the GBF1 HDS1 domain in targeting to lipid droplets (Bouvet et al. 2013), our results indicate a general role of the C-terminal domains in organelle targeting.

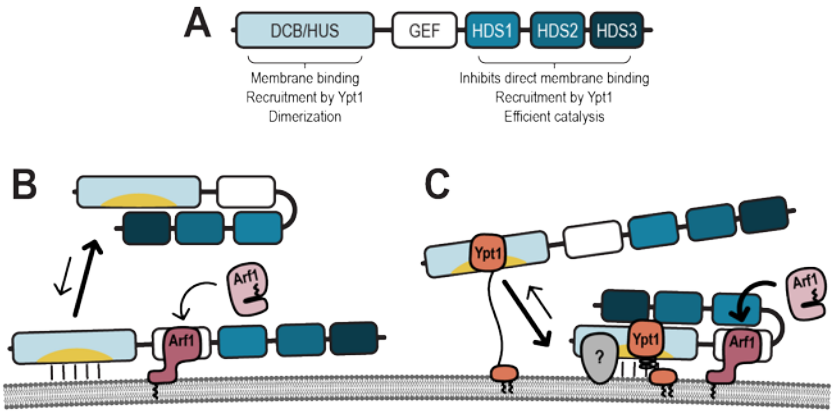

Figure 2.11. Model of Gea regulation. (A) Assignment of functions and interactions to domains of Gea1/Gea2. Membrane binding and the behavior of the C-terminus of Gea1/Gea2 in the absence (B) and presence (C) of active recruiting interactions. Note that the membrane diagramed represents a neutral membrane, lacking anionic lipids. Grey (?) represents a potential interactor which confers specificity of localization to Gea1 and Gea2.

Our colocalization studies show Gea1 and Gea2 to have different colocalization patterns relative to the early and late Golgi markers Vrg4 and Sec7. This is consistent with a model in which Gea1 and Gea2 occupy intermediate compartments within the Golgi, overlapping at *cis* and *trans* compartments with Vrg4 and Sec7. This model posits a continuum of Arf-GEFs across the Golgi (Figure 2A) and is consistent with evidence that GBF1 (Gea1/Gea2) provides the seed Arf-GTP to recruit BIG1/BIG2 (Sec7) to the TGN (Richardson, McDonold, and Fromme 2012; Lowery et al. 2013). In addition, Gea1 occupies earlier Golgi compartments than Gea2, which must require distinct recruitment mechanisms and implies different roles for the two GEFs. Further study is needed to understand how and why Gea1 and Gea2 show different colocalization patterns.

It appears that any specialized roles for Gea1 or Gea2 are not essential, however, as we show here that Gea1 and Gea2 are equally functional in stressed cells when expressed with the higher copy *GEA2* promoter. This confirms a redundant essential function and highlights the requirement for a critical cellular concentration of Gea under stress conditions.

We observed that Gea1 and Gea2 display a preference for neutral over anionic membranes in catalytic assays. Sec7, on the other hand, prefers anionic membranes. These preferences correlate with the localization patterns of the GEFs, with Gea1 and Gea2 occupying earlier Golgi compartments than Sec7, which functions at the late Golgi. Intriguingly, a recent study showed that recruitment of *Caenorhabditis elegans* GBF1 to membranes was reduced in an siRNA knockdown of the rate-limiting enzyme for PC synthesis (Smulan et al. 2016), suggesting a

physiological role for Golgi lipid composition in recruitment of GBF1/Gea family Arf-GEFs. Together with our previous observation that another late Golgi GEF, TRAPPII, prefers anionic membranes (Thomas and Fromme 2016), these results suggest a general mechanism for regulating the membrane specificity of Golgi GEFs. As these GEFs lack traditional membrane binding domains, the increasing negative charge of the late Golgi and TGN may help exclude early Golgi GEFs and recruit late Golgi GEFs to the TGN.

We found that the HDS3 domain of Gea1 and Gea2 is dispensable for *in vivo* localization to the Golgi and for the essential function of Gea. In biochemical studies (not shown), we found that Gea2ΔHDS3 showed a milder version of each phenotype observed for Gea2ΔC. Future investigations may reveal whether this conserved domain plays a regulatory role separate from the HDS1 and HDS2 domains.

Unlike Sec7, whose C-terminal domains function in both strong catalytic autoinhibition and the protein interactions which relieve that autoinhibition, Gea1 and Gea2 are not catalytically autoinhibited. Instead, we show here that the C-terminus of Gea2 inhibits membrane binding, perhaps by masking the intrinsic affinity of the Gea2 N-terminus for membranes. Removal of the C-terminal domains of Gea2 increased both membrane binding and the rate of Arf1 exchange on membranes, yet the C-terminus of Gea2 was required for Golgi localization and full exchange function in the absence of membranes.

Our results combine to evoke a model for carefully calibrated regulation of Gea2 by its C-terminal domains: in the absence of active recruitment to membranes, the C-terminus functions to keep Gea2 in the cytosol (Figure 2.11 B). Once this membrane-binding inhibition is relieved by active recruitment, the C-terminus switches functions to promote efficient catalysis of Arf1 exchange (Figure 2.11 C).

We have identified Ypt1 as one of the active recruiters for Gea1 and Gea2. The functional importance of this interaction is underscored by the suppression of the *gea1-6* temperature sensitive mutation by overexpression of Ypt1 (Jones et al. 1999). Ypt1 recruits Gea1 and Gea2 to membranes *in vitro*, and this recruiting interaction requires the C-terminal domains, despite previous evidence of a direct interaction between the N-terminus of GBF1 and Rab1b (Figure 2.11 C) (Monetta et al. 2007). It is possible that the C-terminus stabilizes the interaction with Ypt1, or that intrinsic membrane binding in the HDS1 domain of Gea1 and Gea2 complements the Ypt1 recruitment. As both the Ypt1 interaction and intrinsic membrane binding seem weak or transient, it is likely that concomitant interactions cooperate to fully recruit Gea1 and Gea2 to the membrane surface (Figure 2.11 C).

Our results clearly distinguish the regulation of Gea1 and Gea2 from that of Sec7. Gea1 and Gea2 do not participate in a positive feedback loop with Arf1 (Richardson, McDonold, and Fromme 2012); Arf1 cannot recruit either Gea1 or Gea2 to membranes and it does not stimulate GEF activity *in vitro*. This characteristic represents an important regulatory divergence from Sec7, as does the absence of apparent catalytic autoinhibition and the failure of Arl1 to have a

recruiting or stimulating effect on Gea1 or Gea2, and the lack of autoinhibition resembles more distant members of the Sec7 family of Arf-GEFs, such as BRAG, which functions in endocytosis (Aizel et al. 2013). Additionally, Gea1 and Gea2 lack a fourth C-terminal domain, HDS4, which is conserved within the Sec7/BIG subfamily. We recently described the role of this domain in homodimerization of Sec7 (Richardson et al. 2016). However, Gea2 is dimeric in the absence of the HDS4 domain, reinforcing previous observations that the N-terminal domains of Gea/GBF1 are responsible for dimerization (Grebe et al. 2000; Ramaen et al. 2007; Bhatt et al. 2016) and further differentiating regulation of the early Golgi Arf-GEFs from that of the late.

One regulatory feature that Gea1 and Gea2 share with Sec7 is the interaction with Ypt1. Ypt1 may serve as a general Golgi recruiter for Arf-GEFs. However, the specific sub-Golgi localization of Gea1, Gea2, and Sec7 must require additional specific recruiting interactions for each Gea1 and Gea2, either with proteins or with the membrane surface (Figure 2.11 C). Our results imply that membrane lipid character likely plays an important role in Golgi Arf-GEF targeting and GEF activity. The comprehensive identification and characterization of protein-protein and protein-membrane interactions will be crucial to a full understanding of how vesicular membrane trafficking at the Golgi is coordinated.

- CHAPTER 3 -

IN PURSUIT OF A CRYSTAL STRUCTURE OF GEA

Introduction

As mentioned in Chapter 2, structural information about the large Golgi Arf-GEFs is relatively limited. While we have crystal structures of the catalytic GEF domain of several family members and part of the N-terminus of Sec7 (Renault et al. 2002; Qiu et al. 2014; Richardson et al. 2016), how those domains relate to one another remains obscure, and we have no structure of the C-terminus nor an overall structure of these GEFs. Such a structure would shed light on how the domains of the Golgi Arf-GEFs might interact to form tertiary or quaternary structures and could also reveal protein- or membrane-binding surfaces as targets for further study. As it stands now, comprehensive scanning mutagenesis is challenging in such large proteins (160-200 kD), so without a structure, we have been limited to studying the effects of a few temperature sensitive mutants and of large truncations. With this in mind, I aimed to purify full length Gea1 or Gea2. After exhausting a number of approaches, the best crystals I grew yielded only low resolution diffraction data, but hint at an attainable structure for Gea1.

Results

Before my work, crystallization of Gea1 and Gea2 had been prohibited by the inability to produce sufficiently pure Gea. While the *E. coli* purification protocol that we have established yields modest amounts of recombinant Gea1 and Gea2, they are sufficient, and more importantly, sufficiently pure, for crystallography. I also applied our protocol to the

purification of shorter constructs that might illuminate relationships between domains (Table 3.1).

In light of the anticipated difficulty in crystallizing these proteins, I also identified and cloned homologs from additional yeast species, including thermophiles (Table 3.1). The testing of homologous proteins for crystallography is a well-established approach for improving the likelihood of finding ideal conditions, and the thermophilic homologs in particular were chosen because they should be more stable and therefore more likely to form ordered crystals.

Of all constructs tested, only Gea1 formed potentially useful crystals (Table 3.2). Two constructs of Gea1, one full length with its histidine-tag cleaved and one lacking the first 14 residues, formed crystals with rhomboid prism morphology under a number of conditions, all containing an acidic carbohydrate sodium salt (either trisodium citrate or sodium malonate). Full length Gea2 produced spherulites which failed to resolve into useful crystals through optimization, and the two thermophilic Geas tested for crystallization, from *M. thermophila* (Mt Gea) and *C. thermophilum* (Ct Gea), yielded no hits.

I tested numerous cryoprotectant strategies to optimize diffraction (Table 3.3). In addition to the gradual transfer of crystals into cryoprotectant solutions, I grew crystals in buffer containing cryoprotectant levels of DMSO before harvesting. I also attempted growth in buffer containing cryoprotectant glycerol, which failed to produce crystals. We collaborated with Q. Huang to

Table 3.1. Constructs cloned and purified for crystallography.

Construct	Species	Residues	Notes
Gea1ΔHis-tag	*S. cerevisiae*	1-1408	expresses worse than Gea2 (0.5-1 mg/8 L TB)
Gea2	*S. cerevisiae*	1-1459	expresses well (1-2 mg/8 L TB)
Gea1ΔHDS3	*S. cerevisiae*	1-1225	expresses poorly (0.5 mg/8 L TB)
Gea2ΔHDS3	*S. cerevisiae*	1-1196	expresses worse than Gea2 (0.5-1 mg/8 L TB)
Gea1ΔC+24	*S. cerevisiae*	1-777	failed to express stably
Gea2ΔC+24	*S. cerevisiae*	1-782	expresses worse than Gea2 (0.5-1 mg/8 L TB)
Gea2GEF	*S. cerevisiae*	558-782	expresses very well; note that TEV cleaves well despite mis-cloned cleavage site
Gea1ΔN14	*S. cerevisiae*	15-1408	expresses well (1-1.5 mg/8 L TB)
Gea2ΔC50	*S. cerevisiae*	1-1409	expresses well (1 mg/8 L TB)
Gea	*C. thermophilum*	1-1643	expresses well (1 mg/8 L TB)
Gea	*K. lactis*	1-1397	expresses poorly (200 μg/8 L TB)
Gea	*K. thermotolerans*	1-1399	expresses poorly (200 μg/8 L TB)
Gea	*M. thermophila*	1-1400	expresses well (1-2 mg/8 L TB)
Gea	*Z. rouxii*	1-1526	failed to express stably

Table 3.2. Crystallization screens and optimization conditions. S, small; M, medium; L, large; v., very

Construct	[Protein] (mg/ml)	Drop size (µl)	Kit screen or followup	Temp.	Hit conditions
Gea2	15	0.2 + 0.2	JCSG+	RT	A7 (spherulites, 0.1 M CHES pH 9.5, 20% (w/v) PEG 8000)
			ComPAS		A12 (spherulites, 0.1 M CHES pH 9.5, 20% (w/v) PEG 8000)
			50% Classics		---
			50% JCSG+		
	30	1 + 1	24-well hanging drop: 100 mM CHES pH 9.5, 8-23% (w/v) PEG 8000		
			100 mM Bicine pH 9.0, 8-23% (w/v) PEG 8000		
			100 mM Tris pH 8.5, 8-23% (w/v) PEG 8000		
			100 mM Tris pH 8.0, 8-23% (w/v) PEG 8000		
			24-well hanging drop: 100 mM CHES pH 9.5, 8-13% (w/v) PEG 8000, 30 mg/ml Gea2		
			100 mM CHES pH 9.5, 8-13% (w/v) PEG 8000, 15 mg/ml Gea2		
			24-well hanging drop: 100 mM CHES pH 9.5, 15% (w/v) PEG 8000, 3.75-15 mg/ml Gea2		
			100 mM CHES pH 9.5, 20% (w/v) PEG 8000, 3.75-15 mg/ml Gea2		
		0.2+0.2	96-well robot: 100 mM CHES pH 9.5, 0-24% (w/v) PEG 8000		
			100 mM Tris pH 8.5, 0-24% (w/v) PEG 8000		
			50% JCSG+		
	10		50% JCSG+		A10 (spherulites, 0.1 M Potassium formate, 10% (w/v) PEG 3350) G4 (spherulites, 0.1 M Trimethylamine N-oxide, 0.05 M Tris pH 8.5, 10% (w/v) PEG MME 2000)
			ComPAS		B6 (spherulites, 0.1 M Tris pH 8.5, 16% (w/v) PEG 10000)
			50% JCSG+	4°C	---
		0.5 + 0.5	24-well hanging drop: 0-150 mM Potassium formate, 2.5-15% (w/v) PEG 3350		
		0.2 + 0.2	96-well robot: 0-0.2 M Potassium formate, 0-22% (w/v) PEG 3350		
			0.1 M Tris pH 8.0/Tris pH 8.5/Bicine pH 9, 10-20% (w/v) PEG 8000		
			0.1 M Tris pH 8.5, 13-23% (w/v) PEG 3350		
			0-0.2 M Trimethylamine N-oxide, 0.05 M Tris pH 8.5, 4-14% (w/v) PEG MME 2000		

Table 3.2. (continued)

Construct	[Protein] (mg/ml)	Drop size (µl)	Kit screen or followup	Temp.	Hit conditions
Mt Gea	10	0.2 + 0.2	50% JCSG+	RT	---
			ComPAS		
			50% JCSG+	4°C	
			ComPAS		
			25% ComPAS	RT	
			25% JCSG+		
			25% ComPAS	4°C	
			25% JCSG+		
Ct Gea			50% ComPAS		
			50% JCSG+	RT	
			50% ComPAS		
Gea1ΔHis-tag		1 + 1	24-well hanging drop: 600-800 mM Trisodium citrate, 0.1 M HEPES pH 7.4	4°C	A1 drops (600 mM Trisodium citrate) show film of tiny rhomboid crystals
		0.2 + 0.2	50% JCSG+		E9 (needles + spherulites, 0.8 M Magnesium sulfate, 0.05 M MES pH 6.5) F10 (needles, 0.55 M Sodium malonate, 0.05 M HEPES pH 7.0, 0.25% (v/v) Jeffamine ED-2001)
			50% ComPAS		---
		1 + 1	24-well hanging drop: 400-600 mM Trisodium citrate, 0.1 mM HEPES pH 7.4		B3 (rhomboid prisms, 500 mM Trisodium citrate)
			0.5-1 M Magnesium sulfate, 50 mM MES pH 6.5		---
			24-well hanging drop: 465-540 mM Trisodium citrate, 0.1 M HEPES pH 7.4		A3 (3-4 L crystals, ~10 M, many S, 540 mM Trisodium citrate) -> warm to RT before harvesting crystals
			24-well hanging drop: 450-550 mM Trisodium citrate,		A6 (10 L crystals, 30 M, some S, 525 mM Trisodium citrate)
			450-700 mM Sodium malonate, 0.05 M HEPES pH 7.4, 0.25% (v/v) Jeffamine ED-2000		B1 (15 M crystals, many S, 540 mM Trisodium citrate)
			450-700 mM Sodium malonate, 0.05 M HEPES pH 7.4		B2 (20 M crystals, many S, 550 mM Trisodium citrate) C4 (one M, 600 mM Sodium malonate, 0.25% (v/v) Jeffamine ED-2000) C5,6 (rods, 650-700 mM Sodium malonate, 0.25% (v/v) Jeffamine ED-2000) D6 (rods, 700 mM Sodium malonate)
		0.2 + 0.2	50% JCSG+	RT	---
			50% ComPAS		
			50% JCSG+		
			50% ComPAS		
			50% JCSG+	4°C	
			50% ComPAS		
		1 + 1	24-well hanging drop: 0.5-1 M Magnesium sulfate, 0.05 M MES pH 6.5		
Gea1ΔN14			24-well hanging drop: 400-600 mM Trisodium citrate, 0.1 M HEPES pH 7.4		A4 (rhomboid prisms, many S, 550 mM Trisodium citrate) A5 (sheet of v. S crystals, 600 mM Trisodium citrate)

Table 3.2. (continued)

Construct	[Protein] (mg/ml)	Drop size (µl)	Kit screen or followup	Temp.	Hit conditions
Gea1ΔN14	10	0.2 + 0.2	50% ComPAS	RT	---
			50% JCSG+		
			50% ComPAS	4°C	G2 (rhomboid prisms, 0.05 M HEPES pH 7.5, 0.35 M Sodium citrate) G12 (sheet of v. S crystals, 0.05 M Tris pH 8.5, 0.75 M Lithium sulfate)
			50% JCSG+		F10 (needles + S crystals, 0.55 M Sodium malonate, 0.05 M HEPES pH 7.0, 0.25% (v/v) Jeffamine ED-2001)
		1 + 1	24-well hanging drop: 490-560 mM Trisodium citrate, 0.1 M HEPES pH 7.4		B2 (few S, one L, 500 mM Trisodium citrate)
			1.2-1.45 M Lithium sulfate, 0.1 M Tris pH 8.5		B4 (many M, 520 mM Trisodium citrate) B5 (few S to L, 530 mM Trisodium citrate) B6 (few M to L 540 mM Trisodium citrate)
			24-well hanging drop: 510-560 mM Trisodium citrate, 0.1 M HEPES pH 7.4		A5 (few S, 550 mM Trisodium citrate) A6 (many S to M, 560 mM Trisodium citrate) B5 (few, v. S, 550 mM Trisodium citrate) B6 (v. S to S, 560 mM Trisodium citrate) C5 (few, S to M, 550 mM Trisodium citrate) C6 (many S to L, 560 mM Trisodium citrate) D5 (few, S to M, 550 mM Trisodium citrate) D6 (many v. S to S, 560 mM Trisodium citrate)
			24-well hanging drop: 510-560 mM Trisodium citrate, 0.1 M HEPES pH 7.4		A5 (many S to L, 550 mM Trisodium citrate)
			400-650 mM Trisodium citrate, 0.1 M HEPES pH 7.4, 10% (v/v) DMSO		A6 (v. many S to M, 560 mM Trisodium citrate)
			400-650 mM Trisodium citrate, 0.1 M HEPES pH 7.4, 10% (v/v) Glycerol		B3 (one M, many S, 500 mM Trisodium citrate, 10% (v/v) DMSO)
			300-550 mM Trisodium citrate, 0.1 M HEPES pH 7.4, 10% (w/v) PEG400		B4 (many v. S, 550 mM Trisodium citrate, 10% (v/v) DMSO) B5 (many vv. S, 600 mM Trisodium citrate, 10% (v/v) DMSO) B6 (inf. tiny, 650 mM Trisodium citrate,10% (v/v) DMSO) C3 (many v. S, 500 mM Trisodium citrate, 10% (v/v) Glycerol) C4-6 (inf. tiny, 550-650 mM Trisodium citrate, 10% (v/v) Glycerol) D6 (one v. S, 550 mM Trisodium citrate, 10% (w/v) PEG400)
			24-well hanging drop: 400-550 mM Trisodium citrate, 0.1 M HEPES pH 7.4, 10% (v/v) DMSO		A5 (one S, 480 mM Trisodium citrate, 10% (v/v) DMSO)

Table 3.2. (continued)

Construct	[Protein] (mg/ml)	Drop size (µl)	Kit screen or followup	Temp.	Hit conditions
Gea1ΔN14	10	1 + 1	100-600 mM Trisodium citrate, 0.1 M HEPES pH 7.4, 20% (v/v) DMSO	4°C	A6 (many S to M, 490 mM Trisodium citrate, 10% (v/v) DMSO) B1 (many S to L, 500 mM Trisodium citrate, 10% (v/v) DMSO) B2 (v. many S to M, 510 mM Trisodium citrate, 10% (v/v) DMSO) B3 (v. many S, 520 mM Trisodium citrate, 10% (v/v) DMSO) B4 (v. many v. S, 530 mM Trisodium citrate, 10% (v/v) DMSO) B5 (v. many vv. S, 540 mM Trisodium citrate, 10% (v/v) DMSO) B6 (inf tiny, 550 mM Trisodium citrate, 10% (v/v) DMSO) C6 (many S, seem to float in drop instead of on surface, 600 mM Trisodium citrate, 20% (v/v) DMSO)
		1 + 1	24-well hanging drop: 100-600 mM Trisodium citrate, 0.1 M HEPES pH 7.4, 20% (v/v) Glycerol	4°C	A5 (few M to L, 500 mM Trisodium citrate, 0.1 M HEPES pH 7.4, 20% (v/v) Glycerol)
			100-600 mM Trisodium citrate, 0.1 M HEPES pH 7.4, 30% (v/v) Glycerol		---
		0.2 + 0.2	Additive screen: 600 mM Trisodium citrate, 0.1 M HEPES pH 7.4		field v. S crystals in A1, A4, A11, A7, B7, C12, D2, D8, D9, D11-12, E2, E5, E11, F8, G12 S/M/L crystals in A6-9, A12, B9, C4-6, G5-6, H11
			Additive screen: 800 mM Trisodium citrate, 0.1 M HEPES pH 7.4		---
Gea1ΔHis-tag		1 + 1	24-well hanging drop: 450-575 mM Trisodium citrate, 0.1 M HEPES pH 7.4		A4 (several M, 525 mM Trisodium citrate), A5 (few M, 550 mM Trisodium citrate)
			24-well hanging drop: 450-575 mM Trisodium citrate, 0.1 M HEPES pH 7.4	RT	---
Gea2ΔC50		0.2 + 0.2	50% MCSG-1	4°C	E12 (cluster of needles, 1.2 M sodium malonate pH 7.0)
			50% MCSG-2		---
			50% MCSG-3		
			50% MCSG-4		
Gea2ΔC+24			50% MCSG-1		
			50% MCSG-2		
			50% MCSG-3		
			50% MCSG-4		
Gea2ΔC50		1 + 1	24-well hanging drop: 750-1500 mM Sodium malonate pH 6		
			24-well hanging drop: 750-1500 mM Sodium malonate pH 7		
			24-well hanging drop: 750-1500 mM Sodium malonate pH 8		
			24-well hanging drop: 250-750 mM Sodium malonate pH 6		
			24-well hanging drop: 250-750 mM Sodium malonate pH 7		
			24-well hanging drop: 250-750 mM Sodium malonate pH 8		
			24-well hanging drop: 550-950 mM Sodium malonate pH 7		
			24-well hanging drop: 550-950 mM Sodium malonate pH 8		

Table 3.2. (continued)

Construct	[Protein] (mg/ml)	Drop size (µl)	Kit screen or followup	Temp.	Hit conditions
Gea2ΔC50	10	0.2 + 0.2	Additive screen: 650 mM Sodium malonate pH 7.5	4°C	G1 (bowties/clusters of needles, 30% (w/v) Trimethylamine N-oxide dihydrate) B11 (one bowtie) D10 (long, thin needles, 0.1 M ATP) H10 (possible bundle of long, thin needles, 7% (v/v) 1-butanol)
			Additive screen: 1.2 M Sodium malonate pH 7.5		---
		1 + 1	24-well hanging drop: 650 mM Sodium malonate pH 7.5, 0-100 mM ATP		stubby needles at low ATP or 1-butanol; thin, spiky clusters at high ATP
			650 mM Sodium malonate pH 7.5, 0-10% (v/v) 1-butanol		---

Table 3.3. Cryoprotectant strategies and crystals looped and shot. Condition for which full dataset was collected is emphasized in **bold.**

CHESS date	Construct	Crystal condition	Crystal type	#	Crystal size	Cryoprotectant condition/strategy	File name if shot	Notes
11/22/2013	Gea1ΔHis-tag	540 mM Trisodium citrate, 0.1 M HEPES pH 7.4	Rhomboid prism	1	M	325 mM Trisodium citrate, 50 mM HEPES pH 7.4, 30% (v/v) DMSO	---	
				2	L		---	
				3	L		---	
				4	M		---	
				5	M	425 mM Trisodium citrate, 50 mM HEPES pH 7.4, 30% (v/v) DMSO	---	
				6	M		---	
				7	M		---	
				8	M	525 mM Trisodium citrate, 50 mM HEPES pH 7.4, 30% (v/v) DMSO	---	
				9	S		---	

Table 3.3. (continued)

CHESS date	Construct	Crystal condition	Crystal type	#	Crystal size	Cryoprotectant condition/strategy	File name if shot	Notes
11/22/2013	Gea1ΔHis-tag	500 mM Trisodium citrate, 0.1 M HEPES pH 7.4	Rhomboid prism	10	M	625 mM Trisodium citrate, 50 mM HEPES pH 7.4, 30% (v/v) DMSO	---	
				11	L		---	
				12	L	725 mM Trisodium citrate, 50 mM HEPES pH 7.4, 30% (v/v) DMSO	48-50	
				13	M	425 mM Trisodium citrate, 50 mM HEPES pH 7.4, 30% (v/v) DMSO	---	
				14	L		---	
				15	L	325 mM Trisodium citrate, 50 mM HEPES pH 7.4, 30% (v/v) DMSO	---	
				16	L		---	maybe cracked?
				17	L		---	
		540 mM Trisodium citrate, 0.1 M HEPES pH 7.4		18	M		---	
		500 mM Trisodium citrate, 0.1 M HEPES pH 7.4		19	L	525 mM Trisodium citrate, 50 mM HEPES pH 7.4, 20% (v/v) DMSO	---	
				20	M		---	
				21	M		---	

Table 3.3. (continued)

CHESS date	Construct	Crystal condition	Crystal type	#	Crystal size	Cryoprotectant condition/strategy	File name if shot	Notes
11/22/2013	Gea1ΔHis-tag	500 mM Trisodium citrate, 0.1 M HEPES pH 7.4	Rhomboid prism	22	M	625 mM Trisodium citrate, 50 mM HEPES pH 7.4, 20% (v/v) DMSO	---	maybe cracked?
				23	L		---	
		540 mM Trisodium citrate, 0.1 M HEPES pH 7.4		24	L	625 mM Trisodium citrate, 50 mM HEPES pH 7.4, 20% (v/v) DMSO	---	
				25	L	725 mM Trisodium citrate, 50 mM HEPES pH 7.4, 20% (v/v) DMSO	13-14	cryo looked grainy
				26	M		15-16	
		500 mM Trisodium citrate, 0.1 M HEPES pH 7.4		27	L		44-45	
				28	L	525 mM Trisodium citrate, 50 mM HEPES pH 7.4, 20% (v/v) DMSO	---	destroyed crystal while loading
				29	L	425 mM Trisodium citrate, 50 mM HEPES pH 7.4, 20% (v/v) DMSO	46-47	
				30	M	325 mM Trisodium citrate, 50 mM HEPES pH 7.4, 20% (v/v) DMSO	48-50	
		650 mM Sodium malonate, 0.05 M HEPES pH 7.4, 0.25% (v/v) Jeffamine ED-2000	Rod	31	v. S	700 mM Sodium malonate, 50 mM HEPES pH 7.4, 30% (v/v) Glycerol	32-35	cryo looked streaky

Table 3.3. (continued)

CHESS date	Construct	Crystal condition	Crystal type	#	Crystal size	Cryoprotectant condition/strategy	File name if shot	Notes
11/22/2013	Gea1ΔHis-tag	700 mM Sodium malonate, 0.05 M HEPES pH 7.4, 0.25% (v/v) Jeffamine ED-2000	Rod	32	v. S	700 mM Sodium malonate, 50 mM HEPES pH 7.4, 30% (v/v) Ethylene glycol	36-39	
		525 mM Trisodium citrate, 0.1 M HEPES pH 7.4	Rhomboid prism	33	L	525 mM Trisodium citrate, 50 mM HEPES pH 7.4, 30% (v/v) Glycerol	24-26	
				34	M		27-28	
		600 mM Sodium malonate, 0.05 M HEPES pH 7.4, 0.25% (v/v) Jeffamine ED-2000		35	M	700 mM Sodium malonate, 50 mM HEPES pH 7.4, 30% (v/v) Glycerol	29-31	collected 10 Å dataset, refroze and returned to cane
		525 mM Trisodium citrate, 0.1 M HEPES pH 7.4		36	L	650 mM Trisodium citrate, 50 mM HEPES pH 7.4, 30% (v/v) Ethylene glycol	17-19	
				37	M		20-23	cryo looked streaky
				38	L	700 mM Trisodium citrate, 50 mM HEPES pH 7.4, 1.5 M Sodium malonate	6-10	
				39	M		11-12	
		Crystal condition	Crystal type	#	Crystal size	Cryoprotectant condition/strategy	File name if shot	Notes

Table 3.3. (continued)

CHESS date	Construct	Crystal condition	Crystal type	#	Crystal size	Cryoprotectant condition/strategy	File name if shot	Notes
5/28/2014	Gea1ΔN14	500 mM Trisodium citrate, 0.1 M HEPES pH 7.4	Rhomboid prism	40	L	700 mM Trisodium citrate, 100 mM HEPES pH 7.4, 1.4 M Sodium malonate (gradual transfer)	snap_99_001-3	diffraction completely smeared out; reshot after soaking in RT cryo solution for ~80 min., remained smeary
				41	S		snap_02_001-2;3	two crystals in loop (one stuck on edge), both completely smeared out
		520 mM Trisodium citrate, 0.1 M HEPES pH 7.4		42	M	700 mM Trisodium citrate, 100 mM HEPES pH 7.4, 1.7 M Lithium sulfate (gradual transfer)	snap_03_001-2;3	two crystals in loop (one stuck v. S), one completely smeared out, other nothing
				43	M		snap_04_001-2	smear
				44	M	700 mM Trisodium citrate, 100 mM HEPES pH 7.4, 20% (v/v) MPD (gradual transfer)	snap_05_001-2	nothing
				45	M		snap_06_001-2	nothing
				46	M	700 mM Trisodium citrate, 100 mM HEPES pH 7.4, 15% (v/v) PEG 400 (gradual transfer)	snap_07_001-3;4-5	two crystals; faint smears for each
				47	M		snap_08_001-2	hard water line, poor diffraction, smeary
				48	M	700 mM Trisodium citrate, 100 mM HEPES pH 7.4, 1.4 M Sodium malonate (soaked 8 hours)	snap_09_001-2;3	some smearing; reshot after "annealing" (blocking LN_2 briefly), smears disappeared
		540 mM Trisodium citrate, 0.1 M HEPES pH 7.4		49	L		snap_11_001-2	smearing
				50	L	700 mM Trisodium citrate, 100 mM HEPES pH 7.4, 1.7 M Lithium sulfate (soaked 8 hours)	snap_15_001-2	faint smearing
				51	M		---	

Table 3.3. (continued)

CHESS date	Construct	Crystal condition	Crystal type	#	Crystal size	Cryoprotectant condition/strategy	File name if shot	Notes
5/28/2014	Gea1ΔN14	540 mM Trisodium citrate, 0.1 M HEPES pH 7.4	Rhomboid prism	52	M	700 mM Trisodium citrate, 100 mM HEPES pH 7.4, 15% (v/v) PEG 400 (gradual transfer)	---	
				53	L		---	
				54	M		---	
		530 mM Trisodium citrate, 0.1 M HEPES pH 7.4		55	L	700 mM Trisodium citrate, 100 mM HEPES pH 7.4, 1.4 M Sodium malonate (direct to final)	snap_17_001-2	completely smeared out; reshot after soaking in RT cryo solution for ~50 min., still smeared/nothing
				56	L		snap_18_001-2	completely smeared out
				57	S		snap_19_001-5	nothing/smear
				58	M	700 mM Trisodium citrate, 100 mM HEPES pH 7.4, 1.4 M Sodium malonate (gradual transfer)	snap_20_001-2;3-4	mostly smear; reshot after soaking in RT cryo solution for ~30 min., smears disappeared

Table 3.3. (continued)

CHESS date	Construct	Crystal condition	Crystal type	#	Crystal size	Cryoprotectant condition/strategy	File name if shot	Notes
6/16/2014	Gea1ΔN14	550 mM Trisodium citrate, 0.1 M HEPES pH 7.4	Rhomboid prism	59	M	600 mM Trisodium citrate, 100 mM HEPES pH 7.4, 1.5 M Sodium malonate (gradual transfer)	snap_01_001-4	some dots at some angles, possibly damaged loop
				60	M		snap_02_001-2	couldn't see crystal well, no diffraction
				61	M	100 mM HEPES pH 7.4, 1.5 M Sodium malonate (gradual transfer)	snap_03_001-2	no diffraction, probably didn't cryoprotect
				62	M		---	crystal may be flawed?
				63	M		---	crystal may be flawed?
				64	M	600 mM Trisodium citrate, 100 mM HEPES pH 7.4, 17% (v/v) DMSO (gradual transfer)	snap_06_001-2; smallset_06_1-6	clear, can see crystal, little ice, ~9.4 Å dataset at best; collected small dataset
				65	M		snap_07_001-2	clear can see crystal, no ice, ~9.5 Å dataset at best at 0° angle
				66	M	600 mM Trisodium citrate, 100 mM HEPES pH 7.4, 25% (v/v) Glycerol (gradual transfer)	snap_08_001-2; smallset_08_1-6	clear, can see crystal, little ice, ~9.5 Å dataset at best; collected small dataset
				67	M		snap_09_001-2	clear can see crystal, no ice, ~9.5 Å dataset at best
		500 mM Trisodium citrate, 0.1 M HEPES pH 7.4, 10% (v/v) DMSO		68	M	500 mM Trisodium citrate, 100 mM HEPES pH 7.4, 25% (v/v) DMSO (gradual transfer)	snap_10_001-2	clear drop, obvious crystal, some spots at 0° angle, none at 90° angle
				69	M		snap_11_001-2	few dots and smearing
				70	L	550 mM Trisodium citrate, 100 mM HEPES pH 7.4, 15% (w/v) PEG 400 (gradual transfer)	snap_12_001-3	few dots and smearing

Table 3.3. (continued)

CHESS date	Construct	Crystal condition	Crystal type	#	Crystal size	Cryoprotectant condition/strategy	File name if shot	Notes
6/16/2014	Gea1ΔN14	550 mM Trisodium citrate, 0.1 M HEPES pH 7.4	Irregular prism	71	M	dehydrated by transfer over increasing [PEG 3350] solutions over 4 days; 700 mM Trisodium citrate, 100 mM HEPES pH 7.4, 1.4 M Sodium malonate (direct to final)	snap_13_001-3	unusually shaped crystal (5-sided); no diffraction
			Rhomboid prism	72	M		snap_14_001-2	better than crystal 71, but not much; some dots and smears
				73	M	dehydrated by transfer over increasing [PEG 3350] solutions over 4 days; 700 mM Trisodium citrate, 100 mM HEPES pH 7.4, 25% Glycerol (direct to final)	snap_15_001-2	crystal may be damaged; some dots, smearing
				74	M		---	crystal may be damaged
				75	M		snap_17_001-2	v. few dots
				76	M	dehydrated by transfer over increasing [PEG 400] solutions over 4 days; looped directly from drop	snap_18_001-4; smallset_18_1-6	lots of film, first trial dissolved in well solution, so looped directly from drop; clear drop, ~10 Å at best; collected small dataset
				77	M		snap_19_001	lots of film, first trial dissolved in well solution, so looped directly from drop; no apparent crystal in loop
		550 mM Trisodium citrate, 0.1 M HEPES pH 7.4, 10% (w/v) PEG400		78	M		---	lots of film, first trial dissolved in well solution, so looped directly from drop
				79	S		snap_21_001-3	lots of film, first trial dissolved in well solution, so looped directly from drop; few dots, smearing; file 3 is a 3 min exposure
		550 mM Trisodium citrate, 0.1 M HEPES pH 7.4		80	L	no freezing: 4°C, pipet into capillary	snap_27_001-2	maybe two dots; file 1 is a 3 min exposure
				81	L		snap_28_001-2	lots of plastic smears from capillary, little dots
		480 mM Trisodium citrate, 0.1 M HEPES pH 7.4, 10% (v/v) DMSO		82	L		snap_29_001-2	lots of plastic smears from capillary, little dots
				83	M		snap_30_001-2	v. few dots, 10 Å smear

test a method developed at Cornell called high pressure cryocooling, which eliminates the need for cryoprotectants, but this technique proved fruitless for my crystals.

I collected a 10 Å dataset of a Gea1ΔHis-tag crystal grown in 600 mM sodium malonate, 0.05 M HEPES pH 7.4, and 0.25% (v/v) jeffamine ED-2000 and cryoprotected in 700 mM sodium malonate, 50 mM HEPES pH 7.4, and 30% (v/v) glycerol (Figure 3.1). Aside from the low resolution, I was unable to confidently index the crystal lattice indicating microscopic heterogeneity of the crystals. None of the optimization strategies that I attempted after this dataset improved diffraction, as diffraction resolution from additional crystals frozen under different conditions approached 9.5 Å at best, still well short of useful resolution (Table 3.3).

Discussion

A full length structure of Gea1 or Gea2 remains a tantalizing objective, given the enormous advantage such information would provide in understanding how the structure of Gea relates to its function and regulation. My own 10 Å dataset may prove useful in assessing alternate conformations of Gea by molecular replacement once a higher resolution structure is solved.

Improving yields of Gea1 and Gea2 might permit more extravagant testing of obscure crystallization and cryoprotectant strategies. It is noteworthy that neither Gea1 nor Gea2 expressed in the Bac-to-Bac baculovirus expression system, but this approach may be worth

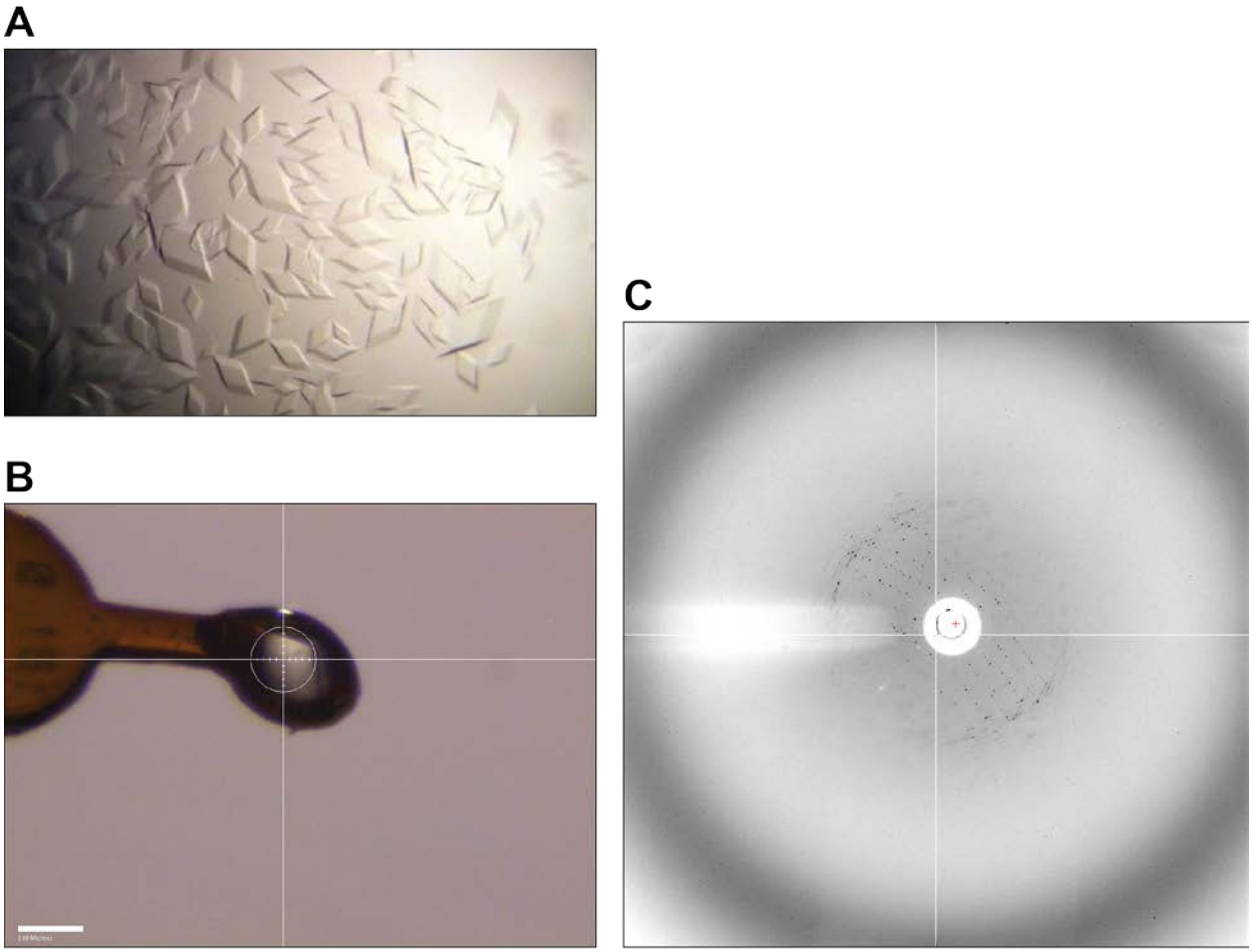

Figure 3.1. Gea1 rhomboid prism crystals produce diffraction at 10 Å resolution. (A) Gea1 rhomboid prism crystals grown in Trisodium citrate and HEPES pH 7.4. (B) The Gea1 crystal (#35) which yielded the dataset mounted on a loop for data collection. This crystal was grown in 600 mM Sodium malonate, 0.05 M HEPES pH 7.4, 0.25% (v/v) Jeffamine ED-2000 and cryoprotected in 700 mM Sodium malonate, 50 mM HEPES pH 7.4, 30% (v/v) Glycerol. (C) Diffraction pattern of the 10 Å dataset, which shows a relatively narrow field of scattering.

revisiting with different constructs to obtain greater yields of protein. Overexpression and purification from yeast may also provide an avenue for improved yields, with optimization.

Additional species may provide opportunities for crystallizing Gea homologs. The sole Gea homolog in the thermophilic yeast *T. terrestris* (the species from which our N-terminal Sec7 structure was solved (Richardson et al. 2016)) represented a challenge in cloning, as it contains four introns and one very short exon. Renewed efforts at cloning this gene into a bacterial expression vector, either through improved PCR approaches or by generating cDNA, might supply a Gea construct more amenable to crystallization. Beyond this, I did not test mammalian Gea homologs, which generally contain longer loops, nor homologs from common model organisms such as *C. elegans*, *D. melanogaster*, or *A. thaliana*. Any of these species or others might deliver a successful Gea/GBF structure to a determined crystallographer.

Last but not least, developments in the field of cryo-electron microscopy may provide an avenue for successfully solving a structure of Gea. Gea1 and Gea2 reside near the low end of the size spectrum for cryo-EM, but optimization of sample preparation and the ever advancing technology in this approach bring us closer to a structure every day. With a structure in hand, future researchers will have a powerful toolbox for asking and answering questions about Golgi recruitment, membrane- and protein- interactions, and autoregulation of the Golgi Arf-GEFs.

- CHAPTER 4 -

THE DOMAINS OF GEA1 AND GEA2 REGULATE LOCALIZATION AND FUNCTION

Introduction

Gea1 and Gea2 are large proteins, but only one 200-residue domain out of 1400 amino acids is devoted to catalysis. The remaining predicted domains likely regulate Gea in some way, either catalytically or by controlling Gea recruitment to membranes. Without homologous domains in the literature or a solved protein structure, characterization of the relationship between the domains and regulation of Gea represents a challenge.

Gross truncations of C-terminal domains have proven informative, as shown in Chapter 2. Dissecting how the structures and residues comprising those domains relate to their functions is more difficult. Random mutagenesis has revealed temperature sensitive alleles of Gea1 and Gea2 (Peyroche, Paris, and Jackson 1996; S.-K. Park, Hartnell, and Jackson 2005), although the reason for phenotypes of these mutants is not always obvious. Studies of mutants which impact domain interactions and membrane targeting have relied heavily upon yeast two-hybrid approaches which may be prone to artefacts (Bouvet et al. 2013; Ramaen et al. 2007). More concrete information about the roles of domains and key amino acids of Gea1 and Gea2 is required to resolve a full picture of Gea regulation.

Lastly, differences between Gea1 and Gea2 have rarely been addressed in the field. We showed in Chapter 2 that main difference previously reported was an artefact of differences in expression levels between Gea1 and Gea2, but we also revealed that Gea1 and Gea2 do not

show identical colocalization patterns with Golgi markers. Gea1 and Gea2 may represent *in situ* separation of function mutants for higher order eukaryotic Arf-GEFs like human GBF1, facilitating dissection of the tasks achieved by this Sec7 GEF subfamily.

Results

The HDS3 domain of Gea2 is a regulator of Gea2 membrane binding and catalytic activity.

As shown in Figure 2.6, the HDS3 domain of Gea1 and Gea2 is dispensable for both the essential function of Gea1/2 and for localization to the Golgi. As this domain is highly conserved across eukaryotes, we hypothesized that it might play a regulatory role, fine-tuning Gea localization or function. Therefore, I purified Gea2ΔHDS3 for use in biochemical studies.

When tested in membrane pelleting assays, Gea2ΔHDS3 bound membranes about two-fold better than Gea2 FL (Figure 4.1 A), an effect similar to that observed for Gea2ΔC in Figure 2.7 A. Interestingly, Gea2ΔHDS3 had a milder effect on the catalytic activity of Gea2 than Gea2ΔC, activating Arf1 significantly but subtly faster than Gea2 FL on membranes (Figure 4.1 B). When activating Arf1 in solution, removing the HDS3 domain or the entire C-terminus had a similar effect on catalytic activity: both Gea2ΔHDS3 and Gea2ΔC show about half the catalytic rate of Gea2 FL when activating Arf1ΔN17. The effect of removing the HDS1 and HDS2 domains is not additive with the removal of HDS3. This suggests that whatever beneficial effect the C-terminus has on catalysis of Arf1 exchange is conferred by the HDS3 domain. Further investigation is required uncover the precise structural or functional role that this domain plays in Gea regulation.

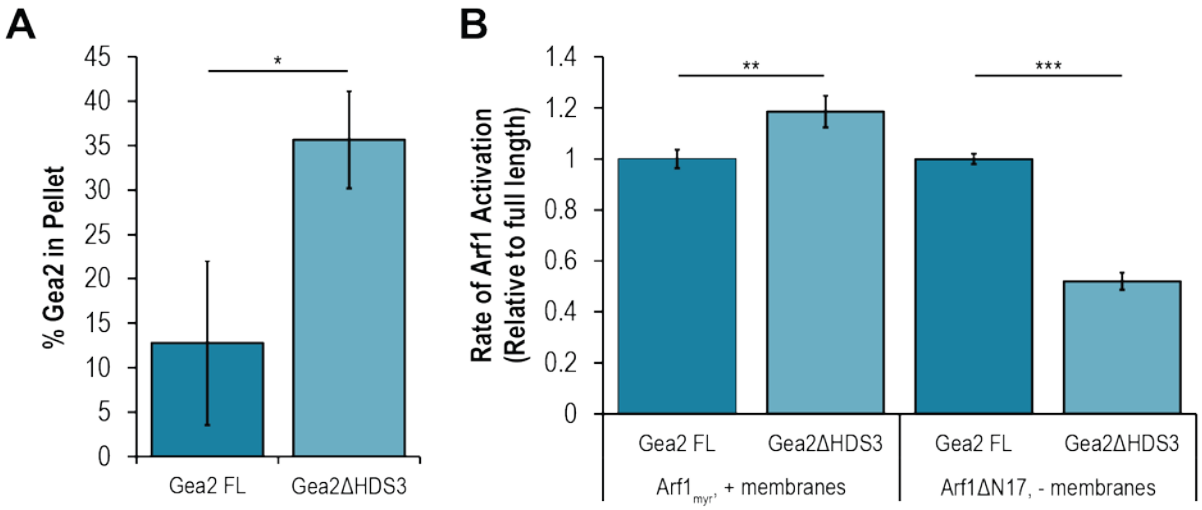

Figure 4.1. The HDS3 domain opposes membrane binding but is required for full catalytic activity of Gea2 *in vitro*. (A) Percent of Gea2 FL or Gea2ΔHDS3 in membrane pellet after incubation with either PC-Ni^{2+} liposomes. n = 3. Rates of Arf1 activation by Gea2 FL or Gea2ΔHDS3 on PC-Ni^{2+} liposomes ($Arf1_{myr}$) or in solution (Arf1ΔN17). Rates are shown relative to Gea2 FL for each experimental condition. n = 3. *, $P < 0.05$; **, $P < 0.01$; ***, $P < 0.0001$.

An extra α-helix is required for stability of Gea1ΔC and Gea2ΔC.

My early attempts to purify constructs of Gea1 and Gea2 truncated after the GEF domain failed, yielding no stably expressed protein and suggesting that our *in vivo* constructs were similarly unstable. In reviewing secondary structure prediction maps of Gea1 and Gea2, I noticed a predicted 11-residue α-helix downstream of the GEF domain but before the unstructured loop leading to the HDS1 domain (Figure 4.2 A), which had been excluded from the previously predicted GEF domain sequence (Bui, Golinelli-Cohen, and Jackson 2009). This helix, as well as the 12 residues preceding it, is perfectly conserved between Gea1 and Gea2, but not in GBF1 (Figure 4.2 B). Two more residues are well-conserved between Gea1 and Gea2 after the helix, beyond which the sequence conservation degenerates into a predicted loop. I therefore designed Gea1ΔC and Gea2ΔC constructs with an additional 8 (included in reported structure of Gea2 GEF domain (Renault et al. 2002), excludes the helix) or 24 (including the helix) residues C-terminal to the GEF domain. As demonstrated in Figure 2.6 B, the Gea2ΔC+8 construct expressed well in yeast cells. The Gea2ΔC+24 construct purified relatively well from *E. coli*, allowing me to carry out the biochemical studies presented in Chapter 2. Gea1ΔC+24 was not as stable in purification, which is not surprising, as Gea1 has consistently proven less amenable to purification than Gea2. Further optimization of the Gea1ΔC construct or purification strategy may produce a stable version for biochemistry. It is possible that the additional helix included in my constructs packs onto the GEF domain, stabilizing it when truncated, or that this sequence is important for folding. Structural studies of this helix relative to the GEF domain may provide insight into the question of its biological importance.

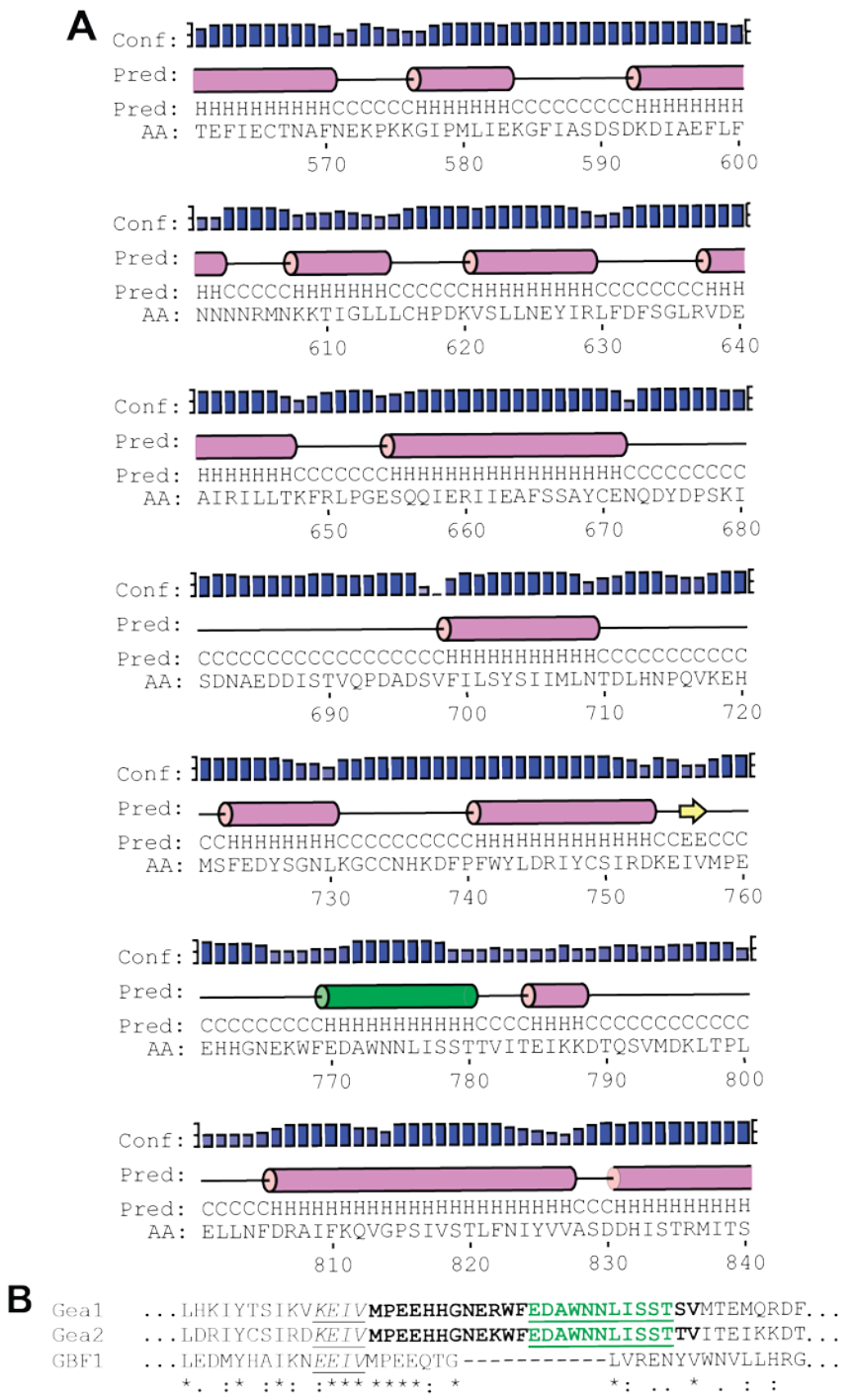

Figure 4.2. Secondary structure predictions identify a previously undocumented α-helix C-terminal to the GEF domain of Gea1 and Gea2. (A) Predicted secondary structure map of Gea2 places an α-helix (green) after the reported GEF domain ends. (B) Sequence alignment of the C-terminus of the GEF domain in Gea1, Gea2, and human GBF1. Previously described end of the GEF domain is marked with *underlined italics*, additional sequence conserved between Gea1 and Gea2 is marked in **bold**, and new predicted α-helix in Gea1 and Gea2 is marked in **green, underlined bold**.

Reported point mutants represent an opportunity for isolating regulatory mechanisms.

In combination with large scale truncations of domains, we turned to the analysis of the effects of point mutations to understand Gea1/2 regulation. However, it is not trivial to identify potentially informative point mutants in 160 kD proteins with no known domain homology to proteins outside their family. For such large proteins, or even the individual domains, traditional approaches such as comprehensive alanine scanning represent a considerable undertaking. Therefore, we turned to mutations described in the literature to pursue biochemical mechanisms for cellular phenotypes (Table 4.1).

A set of three point mutants in mammalian GBF1 was reported to disrupt dimerization through the DCB domain (Ramaen et al. 2007). These results were obtained through yeast two-hybrid analysis of constructs of the DCB domain alone, either wild type or with each mutation. Based on our 2016 structure of *T. terrestris* Sec7 DCB/HUS (Richardson et al. 2016), which showed that the DCB and HUS domains fold as a single domain, it is surprising that these constructs would be stable in cells. While I successfully mapped these mutations onto Gea1 and Gea2 and cloned each construct individually, it seems likely that disruption of dimerization in full length Gea1 or Gea2 may require a combination of these mutations, so these mutants were not tested. A combination of these mutations could provide a way to disrupt dimerization of Gea1 and Gea2,

Table 4.1. Tests of reported point mutants.

Mutant	Inspiration	Purified?	Experimental results
Gea1 K127A	Ramaen et al, 2007	---	---
Gea1 D166A		---	---
Gea1 D467A		---	---
Gea2 K124A		yes	Did not test
Gea2 D163A		---	---
Gea2 D485A		---	---
Gea1 W931S	Bouvet et al, 2013	---	---
Gea2 W943S		yes	No effect on membrane binding
Gea1 Y991C	Arst Jr. et al, 2014	yes	Cannot replace Sec7 *in vivo*
Gea2 Y1001C		yes	Cannot replace Sec7 *in vivo*

and further investigation of these mutants may offer mechanistic insight into the role of dimerization in regulation of Gea1/2.

Membrane targeting of GBF1 to lipid droplets and the Golgi has been attributed to the HDS1 domain (Bouvet et al. 2013). A single amphipathic helix and an individual point mutant in that helix, W1028S, were identified as important for membrane binding. I mapped this mutation into Gea1 and Gea2 and purified Gea2 W943S from *E. coli*, but observed no effect on membrane binding of Gea2 in our membrane pelleting assays (Table 4.1, data not shown).

Finally, another intriguing mutant has been described which allows Gea/GBF to substitute for Sec7/BIG *in vivo* (Arst Jr. et al. 2014). In this study, a single residue substitution, Y1022C, in the HDS1 domain of *A. nidulans* GeaA (Gea/GBF) was shown to suppress *hypBΔ* (Sec7/BIG), implicating this residue as a potential key to understanding regulatory differences between Gea and Sec7. I mapped this mutation onto Gea1 and Gea2 and cloned each mutant into both bacterial and yeast expression vectors. Ultimately, this fascinating phenotype is not conserved in *S. cerevisiae*: neither Gea1 Y991C nor Gea2 Y1001C could rescue the deletion of Sec7. Gea1 Y991C and Gea2 Y1001C were both purified, but I did not test them in biochemical assays. *In vitro* studies could be revisited to ascertain whether these mutants cause any changes in the catalytic rate or lipid preferences of Gea1 and Gea2.

Gea1 and Gea2 colocalize with different Golgi markers.

As Gea1 and Gea2 are genetically redundant, it could be assumed that they share sub-cellular localization. In addition to the experiments presented in Figure 2.1, I attempted to colocalize Gea1 and Gea2 with additional Golgi markers. Gea2 colocalized better than Gea1 with the Golgi marker Kex2, which cycles between the endosome and the TGN (Figure 4.3 A, C). However, Gea1 and Gea2 both show lower colocalization with the early Golgi marker Svp26 (Figure 4.3 B, C), suggesting that Svp26 perhaps resides at a compartment which neither Gea1 nor Gea2 fully occupies.

Different localization of Gea1 and Gea2 is directed by the N-terminus of each.

After observing that Gea1 and Gea2 show different patterns of colocalization with Golgi markers Figure 2.1, I wanted to measure how much Gea1 and Gea2 colocalize with one another. As a control, Gea2-Mars and Gea2-GFP colocalize well (Figure 4.4 A, B). Surprisingly, Gea1 and Gea2 hardly ever colocalize, and this observation is confirmed by Pearson's analysis.

The collection of these data was complicated by the low abundance and fluorescent signal of Gea1. Increasing exposure times to improve Gea1 signal left enough time for highly dynamic Golgi puncta to move between capturing each channel, hopelessly confounding the interpretation of colocalized puncta. To overcome this problem, I collected these data using a dual-capture system, which allowed simultaneous imaging in both channels and eliminated issues with Golgi puncta moving during capturing. However, there is some degree of signal bleed-through from the green channel into the red. I corrected for this by measuring red channel signal intensity at puncta in a strain only expressing a GFP-fusion and subtracting that

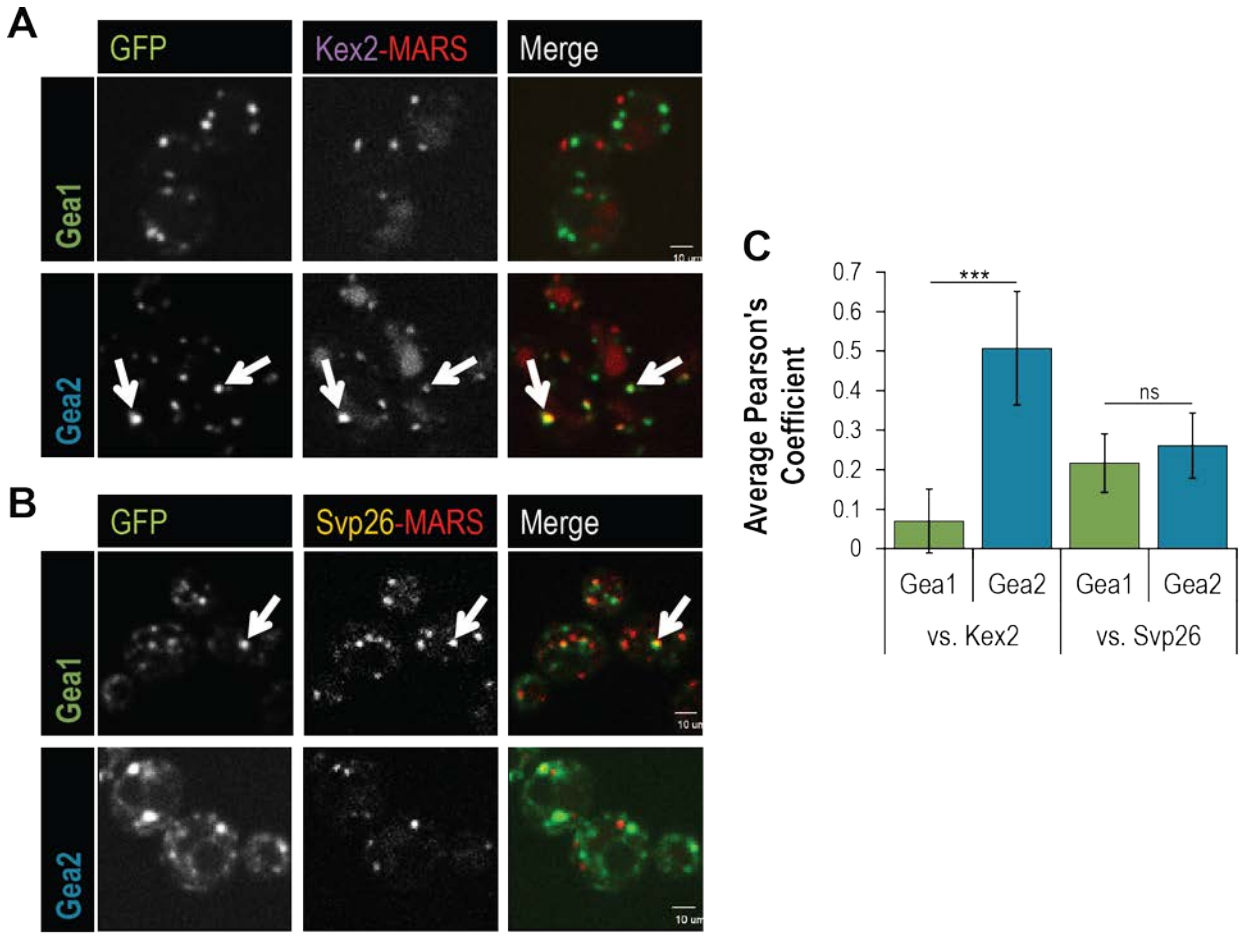

Figure 4.3. Gea1 and Gea2 display different colocalization patterns. Subcellular localization of Gea1-GFP and Gea2-GFP coexpressed with (A) Sec7-Mars, (B) Kex2-Mars, and (C) Svp26-Mars. (D) Quantification of colocalization of Gea1 or Gea2 with each marker at puncta. Error bars represent standard deviations for n = 45 (Gea1 v. Sec7), n = 16 (Gea2 v. Sec7), n = 51 (Gea1 v. Kex2), n = 54 (Gea2 v. Kex2), n = 35 (Gea1 v. Svp26), and n = 51 (Gea2 v. Svp26) cells analyzed. Yellow indicated overlap between channels. Arrows indicate points of colocalization. n.s., not significant; ***, $P < 0.0001$.

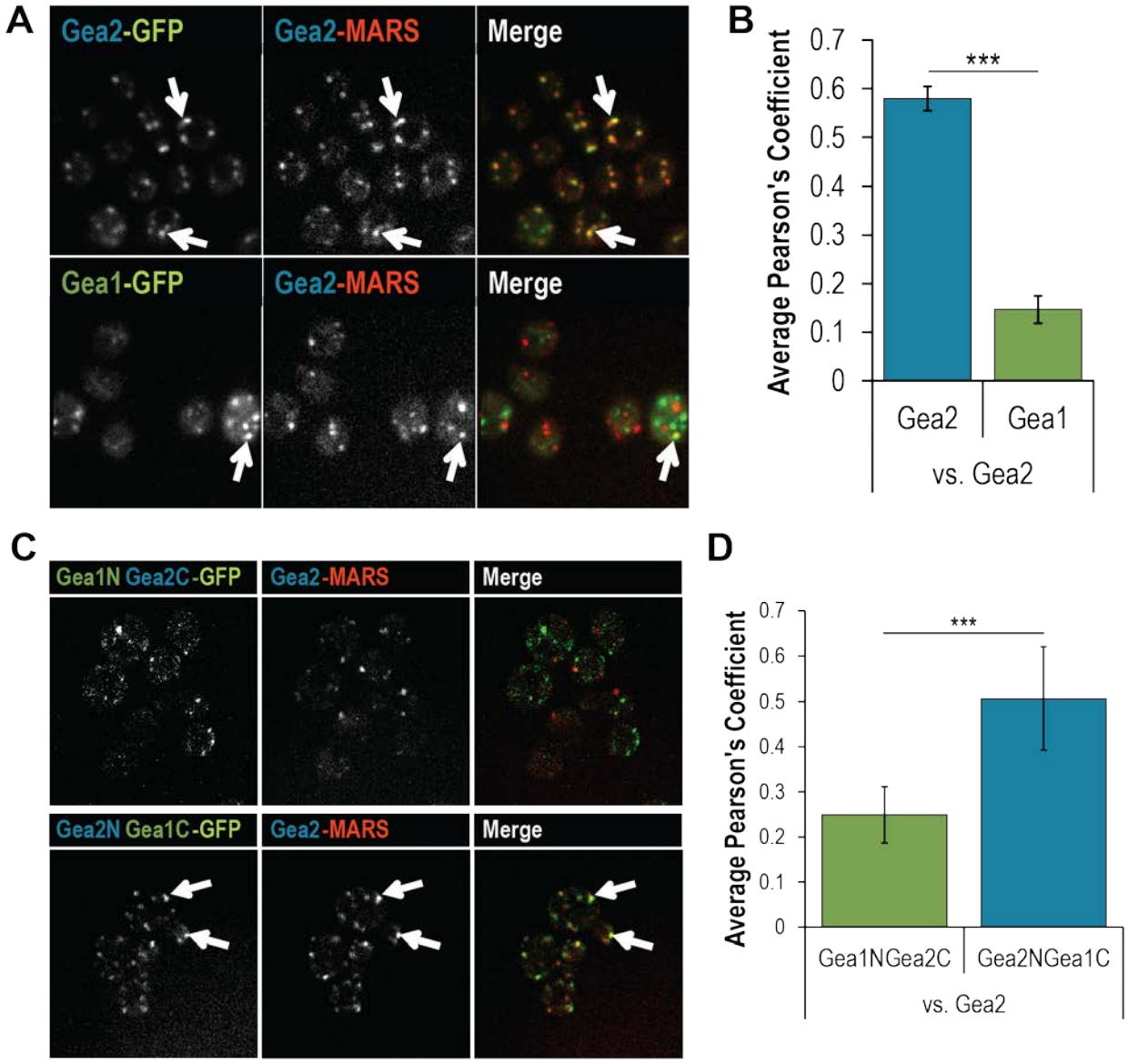

Figure 4.4. Differential localization of Gea1 and Gea2 is determined by their N-terminal domains. (A) Subcellular localization of Gea2-Mars coexpressed with Gea2-GFP or Gea1-GFP. (B) Quantification of colocalization of Gea2 with Gea2 and Gea1 at puncta. Error bars represent 95% confidence intervals for n = 79 (Gea2 v. Gea2) and n = 42 (Gea2 v. Gea1) cells analyzed. (C) Subcellular localization of Gea2-Mars coexpressed with Gea1NGea2C-GFP or Gea2NGea1C-GFP. (D) Quantification of colocalization of Gea1 or Gea2 with each marker at puncta. Error bars represent standard deviations for n = 20 (Gea2 v. Gea1NGea2C) and n = 26 (Gea2 v. Gea2NGea1C) cells analyzed. Yellow indicated overlap between channels. Arrows indicate points of colocalization. ***, $P < 0.0001$. Data collection assisted by J.E. Manzi.

value before carrying out channel math to calculate Pearson's coefficients for these data. Nevertheless, this dataset should be considered preliminary, and follow-up experiments using brighter Gea tags, sequential channel imaging, and time-lapse imaging are warranted to confirm this result.

After the observation that Gea1 and Gea2 occupy different Golgi compartments, I wanted to identify which domains in Gea1 and Gea2 are responsible for this difference. I designed chimeras of Gea1 and Gea2 in which the C-terminus of Gea2 was fused with the N-terminus of Gea1 (Gea1NGea2C, and vice versa (Gea2NGea1C). I chose the highly conserved 24-residue stretch immediately downstream of the GEF domain (shown in Figure 4.2) as the junction, to avoid amino acid changes that might prevent folding. Working with J.E. Manzi, I cloned these constructs with GFP tags into yeast expression vectors. First, we confirmed that these constructs are viable as the only copy of Gea in cells, as it was very possible that in creating the chimeras we would interfere with folding or domain-domain interactions. Reassuringly, each chimera was able to support growth. Yeast shuffled to contain only one chimera or the other grew in the same pattern as their respective N-terminal wild type cells, as each chimera was driven under the promoter that matched its N-terminus.

Next, I compared the subcellular localization of each chimera to wild type Gea2-Mars. We found that while Gea1NGea2C rarely colocalizes with wild type Gea2, Gea2NGea1C and wild type Gea2 frequently colocalize (Figure 4.4 C, D). This result shows that the N-terminus is responsible for dictating the differential localization of Gea1 and Gea2. It remains a formal, but

very unlikely, possibility that the observed localization arises through heterodimerization of the N-terminus of the chimera with the N-terminus of the endogenous protein.

J.E. Manzi began cloning and testing further N-terminal domain chimeras, but this work remains unfinished. Additional experiments may pinpoint which N-terminal domain confers specific localization to Gea1 and Gea2, although such experiments may be confounded by protein instability if mutating the interface between the DCB and HUS domains disrupts folding or packing.

Point chimeras represent divergence between Gea1 and Gea2 which may dictate localization specificity.

To try to understand which residues in the N-terminus of Gea1/2 are important for localization, I worked with J.E. Manzi to identify residues in the N-termini of Gea1 and Gea2 which are highly conserved across the Gea/GBF family but at which either Gea1 or Gea2 diverges (Table 4.2). We prioritized residues in this category which represented dramatic differences between Gea1 and Gea2: charge inversions, large differences in side chain length, and differences in backbone rigidity. We then designed single point chimeras in Gea1 and Gea2, and J.E. Manzi began to clone each into yeast expression vectors. He successfully cloned one mutant (Gea2 Q158K) and found that it could support growth as the only copy of Gea in the cell, but did not have time to test whether this mutant colocalizes with wild type Gea2. The completion of cloning for the full set of chimeras, as well as some combinations, may provide a toolbox for isolating which residues are essential for the differential localization of Gea1 and Gea2. If these

Table 4.2. N-terminal reciprocal point chimeras in Gea1 and Gea2.

Mutant	Cloned?	Experimental results
Gea1 V145H	---	---
Gea2 H142V	---	---
Gea1 K161Q	---	---
Gea2 Q158K	yes	No effect on cell growth in *arf1Δ* background
Gea1 Q208R	---	---
Gea2 R205Q	---	---
Gea1 K215N	---	---
Gea2 N212K	---	---
Gea1 T315P	---	---
Gea2 P330T	---	---
Gea1 G322N	---	---
Gea2 N337G	---	---
Gea1 T338Y	---	---
Gea2 Y353T	---	---
Gea1 P409Q	---	---
Gea2 Q424P	---	---
Gea1 E482A	---	---
Gea2 A500E	---	---

residues can be isolated, the resulting mutants may be used in turn to help identify the recruiting interactions, either protein-protein or lipid-protein, which direct Gea1 and Gea2 to their separate Golgi compartments.

Discussion

Between the findings discussed in Chapter 2 and those presented here, we have developed a clearer picture of the roles played by the HDS domains of Gea1 and Gea2. The C-terminus as a whole plays conflicting roles in different cellular environments. When cytosolic, the C-terminus prevents inappropriate membrane binding by Gea. Once actively recruited by protein binding, the C-terminus is required for optimal catalytic function. Assigning these two roles to individual domains or even specific residues will require further investigation. Indeed, as most all point mutants tested have caused no apparent effect *in vitro*, it is likely that overall domain interactions or surface patches are responsible for regulating Gea localization and activity. A solved structure of the C-terminus of Gea will permit identification and study of such interactions or surfaces.

Placing Gea1 and Gea2 spatially and temporally within the Golgi complex will provide useful context for understanding their roles and regulation, but has largely proven difficult due to the low expression levels (and low fluorescent signal) of the early Golgi Arf-GEFs, especially Gea1. We now have a brighter green fluorescent tag, mNeonGreen, which will enable more reliable colocalization experiments and quantification and hopefully allow us to develop a meticulous timeline of Gea Golgi recruitment. Combining such studies with chimeras or deletion mutants

will reveal not only the different pathways in which Gea1 and Gea2 participate, but also the essential function in which they are redundant.

Our finding that the specificity of Gea1 v. Gea2 recruitment is dictated by the N-terminus is especially interesting when compared with Figure 2.6 C, which shows that the N-terminus alone is insufficient to target Gea to Golgi membranes. This suggests that a C-terminal interaction is required for recruitment to the Golgi, while an N-terminal interaction provides specificity between compartments. It is also possible that the C-terminus is required to facilitate the specific N-terminal recruiting interactions, as I showed with the Ypt1 interaction in Figure 2.10. Perhaps the C-terminus provides structural interactions to improve geometry relative to the membrane surface, or stabilizes a weak interaction with protein recruiters. Further investigation is required to resolve hypotheses into a model of Gea regulation by its domains and interacting partners.

- CHAPTER 5 -

INTERACTING PARTNERS OF GEA1 AND GEA2 DIRECT LOCALIZATION

Introduction

In the absence of canonical membrane binding domains, Gea1 and Gea2 must rely on protein or membrane interactions for recruitment to the appropriate Golgi compartments. While several protein interactions with Gea/GBF1 have been described (Jones et al. 1999; Monetta et al. 2007; Chantalat et al. 2003; Chantalat et al. 2004; Deng et al. 2009; Tsai et al. 2013), none have been shown to function as recruiting interactions. Identification of the protein or lipid interactions which recruit Gea1 and Gea2 to the Golgi and specifically to different cisternae will permit mechanistic studies of Gea regulation and shed light on the different mechanisms which regulate anterograde and retrograde Golgi traffic.

After employing both targeted and blind screens to discover new Gea interactors and testing reported interactions for *in vitro* recruitment, a complex model of recruitment has emerged for Gea1 and Gea2, requiring coordinated interactions. In addition to the Ypt1 interaction documented in Chapter 2, we have uncovered novel potential recruiting partners: Golgi SNAREs. Future investigations will focus on describing these interactions and dissecting the mechanism of Gea1 and Gea2 participation in different Golgi pathways.

Results

No single Golgi protein tested is required for Gea localization.

Sec7 is recruited by interactions with activated Arf1, Arl1, and Ypt1, and its activity is stimulated by Ypt31. Considering the conservation between Sec7 and Gea1/2, we hypothesized that Gea would be recruited and regulated in a parallel manner, though possibly with different interacting partners. Therefore, we carried out a targeted screen for mislocalization of Gea1 and Gea2 in a selected set of single deletion mutants, focusing on Golgi proteins which would be likely to encounter Gea1 and Gea2 (Table 5.1). Minimally localized truncations lacking the HDS3 domain were used to increase the odds of identifying an essential recruiter. *GEA1ΔHDS3-GFP* and *GEA2ΔHDS3-GFP* were cloned into *LEU2 CEN* plasmids and transformed into each deletion strain. Log phase cells were screened for loss of punctate Golgi signal.

Most deletions failed to reveal an obvious mislocalization phenotype. Subtle phenotypes (partial mislocalization) are difficult to perceive with certainty for Gea1 and Gea2, which show a constitutive pool of cytosolic signal. Therefore, only a complete loss of punctate GFP signal qualifies as a sure phenotype. Only deletion of Ypt6 or its GEF complex proteins, Rgp1 and Ric1, and a temperature sensitive mutant for the essential Ypt1 showed such loss of punctate signal. However, when I sought to confirm these results by observing the localization of the Golgi marker Sys1-dsRed in *ypt6Δ* and *ypt1-3* mutants, I found that Sys1 signal was no longer punctate, suggesting gross disruption of the Golgi complex (Table 5.1, data not shown). It is

Table 5.1. Gea localization in single deletion strains. *, Golgi disrupted.

GEF-GFP	Strain	Phenotype
Gea1ΔHDS3	*cog5Δ*	intermediate
	cog6Δ	intermediate
	cog7Δ	intermediate
	cog8Δ	intermediate
	gyp8Δ	intermediate
	rgp1Δ	mislocalized
	ric1Δ	mislocalized*
	rud3Δ	normal
	vps51Δ	intermediate
	vps52Δ	intermediate
	vps53Δ	normal
	vps54Δ	normal
	arl1Δ	normal
	arl3Δ	normal
	arf1Δ	normal
	sys1Δ	normal
	syt1Δ	normal
	ypt31-101/ypt32Δ	normal
	ypt6Δ	mislocalized*
	ypt10Δ	normal
	ypt11Δ	normal
	ypt1-3	intermediate*
Gea2 FL and Gea2ΔHDS3	*ypt6Δ*	mislocalized*
	ypt1-3	intermediate*
	drs2Δ	normal
	sgt2Δ	normal
	gyp1Δ	normal
	ypt10Δ	normal
	trs85Δ	normal
	trs86Δ	normal
	trs65Δ	normal
	ycp4Δ	normal
	smy1Δ	normal
	gyp2Δ	normal
	trs33Δ	normal
	syt1Δ	normal
	vps51Δ	normal
	vps52Δ	normal
	vps53Δ	normal
	vps53Δ	normal

therefore impossible to know from these *in vivo* experiments whether Gea1 or Gea2 require Ypt1 or Ypt6 for recruitment. Further genetic analysis may provide insight into this question.

Of the Golgi GTPases, only Ypt1 can increase the catalytic activity of Gea.

In the absence of definitive data about possible recruitment of Gea1 or Gea2 by Golgi GTPases, I carried out a more focused target screen for an effect on membrane binding or catalytic activity of Gea1 and Gea2 *in vitro*. Myristoylated Arf1 or Arl1 were preloaded onto membranes by incubation with excess GTP in the presence of PC-Ni^{2+} liposomes, and Ypt1-His_7 and Ypt6-His_7 were membrane bound by their interaction Ni^{2+}-DOGS and activated by incubation with GTP. I measured the catalytic activity of Gea1 and Gea2 on PC-Ni^{2+} liposomes alone or with each of the small GTPases (Figure 5.1). I observed that no small GTPase could increase Gea2 activity above mock, and that only Ypt1 could increase the activity of Gea1 significantly. These results were probed further in the experiments documented in Chapter 2, Figures 6 and 7.

Arl1 showed a statistically insignificant effect on the activity of Gea1 nearly as great as the effect of Ypt1, which may merit further investigation. However, Arl1 does not increase Gea membrane binding *in vitro* (Figure 2.9), so this effect seems unlikely to represent a recruiting interaction. The Ypt6 result may also bear further scrutiny, as our Ypt6-His_7 construct purifies poorly for a small GTPase and seems less than perfectly stable in solution. It should be noted that the Rab GTPase homologs Ypt31/32 were excluded from this screen because they are never seen to colocalize with Gea1 or Gea2 in fluorescence microscopy, so they seemed unlikely

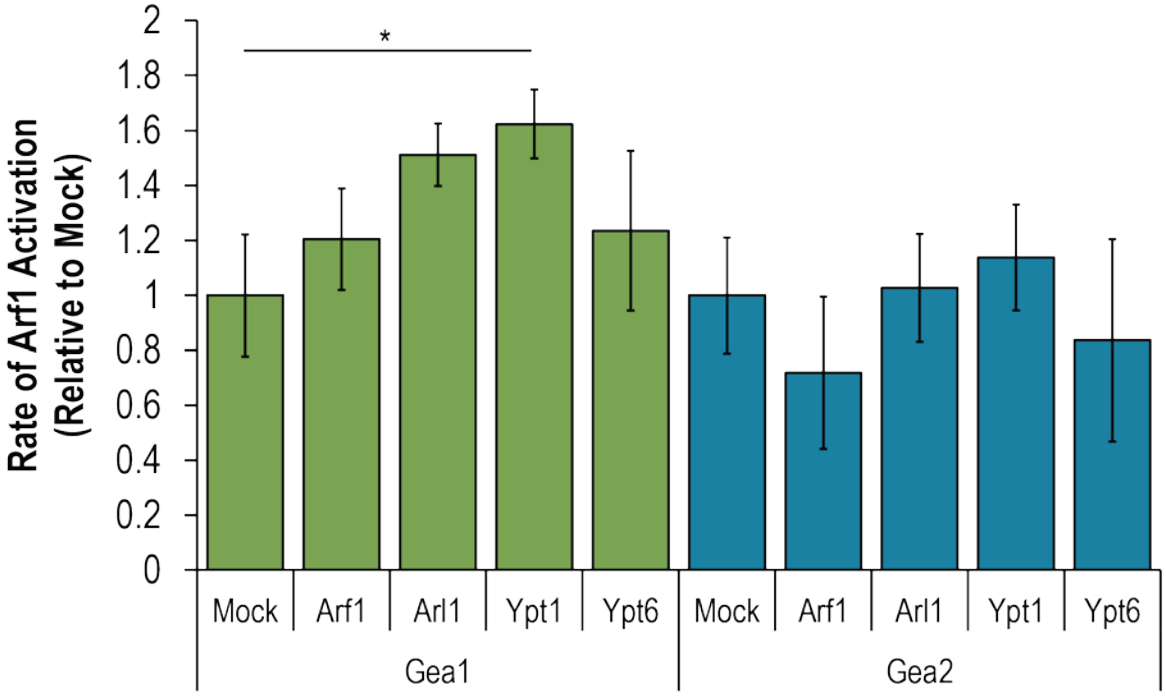

Figure 5.1. Of the Golgi GTPases, only Ypt1 improves Arf1 activation by Gea. Arf1 activation by Gea1 and Gea2 was measured in real time in the presence of PC-Ni^{2+} liposomes alone (Mock) or preloaded with Arf-GTP, Arl1-GTP, Ypt1-His_7, or Ypt6-His_7. Rates are graphed relative to Mock. All unmarked comparisons are n.s. (not significant). *, $P < 0.05$.

recruiters. The GTPase Arl3 was excluded because our lab has not purified it to date, but may be a good target for future testing.

Conservation and molecular replacement were used to identify potential Ypt1-binding mutants of Gea2.

It has been reported that human Rab1b (Ypt1) interacts with the N-terminus of GBF1 (Gea1/2). Therefore, we set out to identify highly conserved residues that might participate in that interaction in Gea2. First, I generated a weblogo of the N-terminus of Gea2 (Figure 5.2 A), which displays highly conserved residues as larger letters. From this weblogo, we selected residues which are both highly conserved and unlikely to be involved in helix stability or packed within the protein (hydrophobic). These chosen clusters of residues were verified further by mapping onto a rough structural model of Gea2 based on *T. terrestris* Sec7 (Richardson et al. 2016). Conservation mapping on the model identified a few conserved patches, notably that surrounding YBmut4 (Figure 5.2 B).

Mutants were cloned into a bacterial expression vector by Y.F. Chen, tested for expression, purified, and used in biochemical assays for membrane recruitment by Ypt1 (Table 5.2). Expression tests of each mutant showed expression in *E. coli* similar to wild type. YBmut3 and YBmut4 were purified and tested for any effect on membrane recruitment by Ypt1, relative to wild type Gea2. YBmut3 had no effect, while YBmut4 seemed have subtly reduced membrane recruitment by Ypt1. Results were confounded by unusually high background membrane binding by both wild type and mutant Gea2, possibly due to issues with lipid stocks. Despite

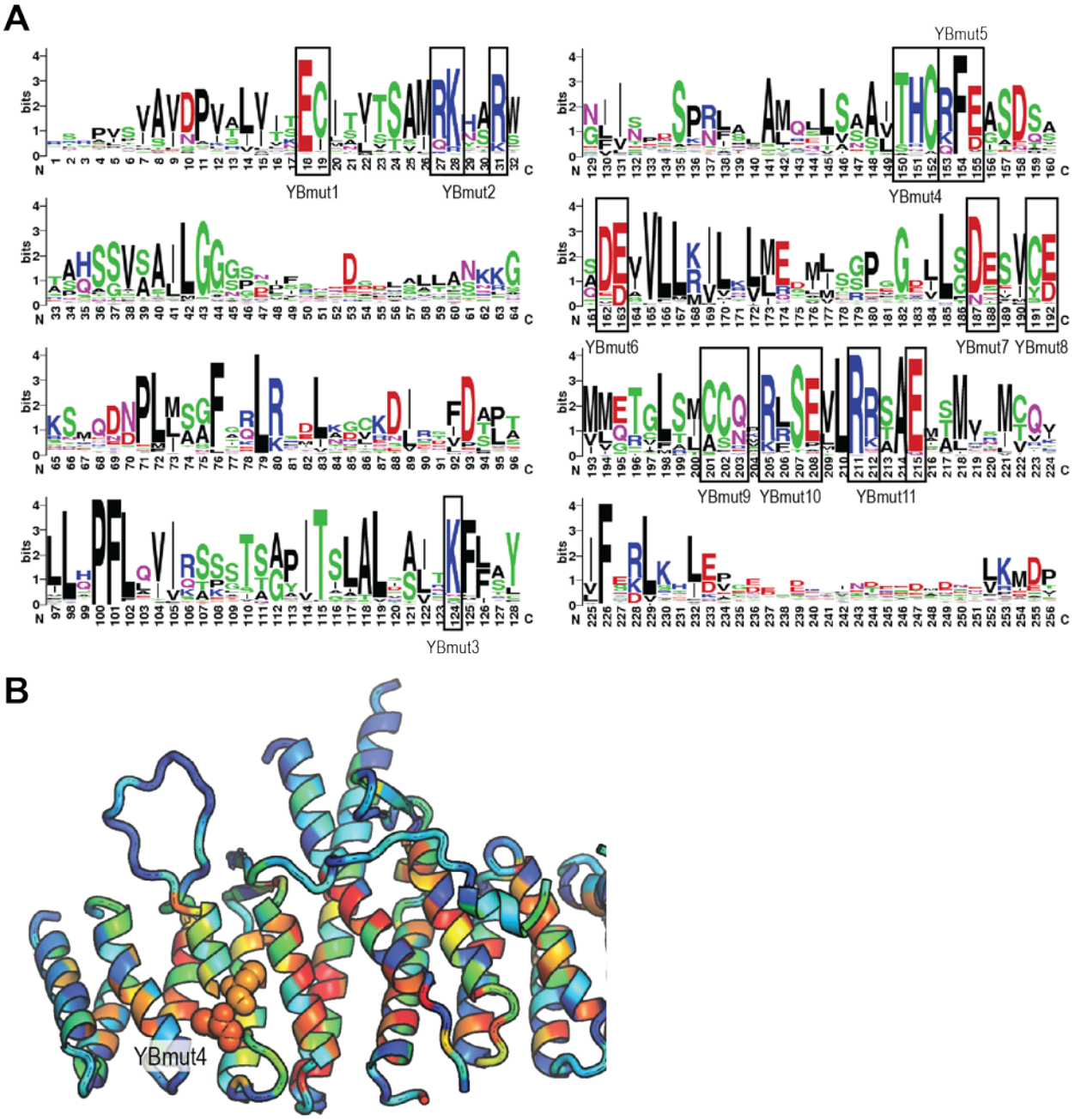

Figure 5.2. Sequence conservation and molecular replacement were used to predict possible Ypt1-binding residues in Gea2. (A) Weblogo showing conservation of residues in the N-terminus of Gea2. Size of letters is proportionate to degree of conservation. Planned mutations are boxed and labeled. (B) A rough structural model of the N-terminus of Gea2 colored for conservation (red to blue, high to low conservation) was used to confirm that planned mutations were in likely surface residues and to identify conserved patches. Conserved patch surrounding YBmut4 is emphasized here by space filled modeling of residues as an example.

Table 5.2. Potential Ypt1 binding mutants.

Name	Mutation	Expression	Experimental results
YBmut1	Gea2 E18A, C19A	good	---
YBmut2	Gea2 R27A, K28A, K31A	good	---
YBmut3	Gea2 K124A	good	Reduced membrane binding? Pelleting expt a little suspect. Conflicting Arf1 activation results.
YBmut4	Gea2 T150A, H151A, C152A	good	No effect on membrane binding.
YBmut5	Gea2 R153A, F154A, E155A	good	---
YBmut6	Gea2 D162A, D163A	good	---
YBmut7	Gea2 N187A, S188A	good	---
YBmut8	Gea2 Y191A, D192A	good	---
YBmut9	Gea2 C202A, N203A	good	---
YBmut10	Gea2 R205A, R206A, S207A, E208A	good	---
YBmut11	Gea2 R211A, N212A, Q215A	good	---

this, we tested YBmut4 for an effect on catalytic activity relative to wild type in the presence of Ypt1. Across multiple sets of experiments, results are conflicting, possibly due to the same issues with lipid stocks or to issues with the fluorometer lamp. Due to scheduling, not all constructs were purified and tested, and YBmut3 and YBmut4 have not been retested with new lipids and a new lamp. As these mutants, especially YBmut4, have not been ruled out as affecting Ypt1 binding by Gea2, they may merit future investigation.

Finally, Y.F. Chen also employed several temperature sensitive mutants of Gea1 and Gea2 in experiments to pursue additional *in vivo* phenotypes for these mutants which might reveal their mechanistic roles. He observed that *gea1-6*, which carries two point mutations (L862S and F1135S) in the HDS1 and HDS2 domains, is partially mislocalized at restrictive temperature. A rotation student who worked with me, A.M. Miller, attempted to purify *gea1-6* for biochemical studies, but found it to be insoluble under normal Gea purification conditions. Further optimization to purify this mutant will be required to allow biochemical analysis of its effect on Gea1. A combination of additional *in vivo* and *in vitro* experiments may clarify both the molecular mechanism of the *gea1-6* mutant and whether the Ypt1 interaction with this mutant is direct or indirect.

Known Gea interactor Gmh1 fails to recruit Gea2 to membranes in vitro.

As mentioned in Chapters 2 and 4, Ypt1 cannot be the only recruiting signal for Gea1 and Gea2, as Ypt1 also recruits Sec7, and all three Golgi Arf1-GEFs localize to different subcompartments. Therefore, we mined the literature for Gea interactors that might provide a recruiting effect.

The early Golgi protein Gmh1 was identified as a multicopy suppressor of *gea1-6*, and Gea1 and Gea2 were shown to coimmunoprecipitate with Gmh1 (Chantalat et al. 2003). However, to date no function has been ascribed to Gmh1 and, as a multi-transmembrane domain protein, Gmh1 is likely to be difficult to manipulate *in vitro*. In addition to Gmh1, we postulated that another transmembrane Golgi protein of unknown function, Sft2, might be a Gea recruiter.

The cytosolic tails of Gmh1 and Sft2 were cloned with His_7 tags and purified by a rotation student who worked with me, D.J. Wasilko. We then tested the ability of these cytosolic tails to recruit Gea2 or Gea2ΔHDS3 to PC-Ni^{2+} liposomes using a membrane pelleting assay. We found that neither the cytosolic tail of Gmh1 nor that of Sft2 was able to recruit Gea2 or Gea2ΔHDS3 to membranes above the intrinsic membrane binding of Gea2 (Figure 5.3). In fact, it seems likely that Gmh1 reduced membrane binding of Gea2 by crowding the liposome surface, preventing the native binding of Gea2 to the membrane. Taken at face value, these results suggest that the reported interaction with Gmh1 occurs downstream of Gea2 recruitment and does not regulate Gea localization.

However, we cannot definitively conclude from these experiments that Gmh1 and Sft2 are not recruiters of Gea1 or Gea2, as these cytosolic tail constructs are highly artificial. They may lack the proper orientation or geometry relative to the membrane, or the interaction with Gea may occur in the loops between the transmembrane domains. Further study of Gmh1 in particular, while non-trivial, may answer this question in a more biologically relevant manner.

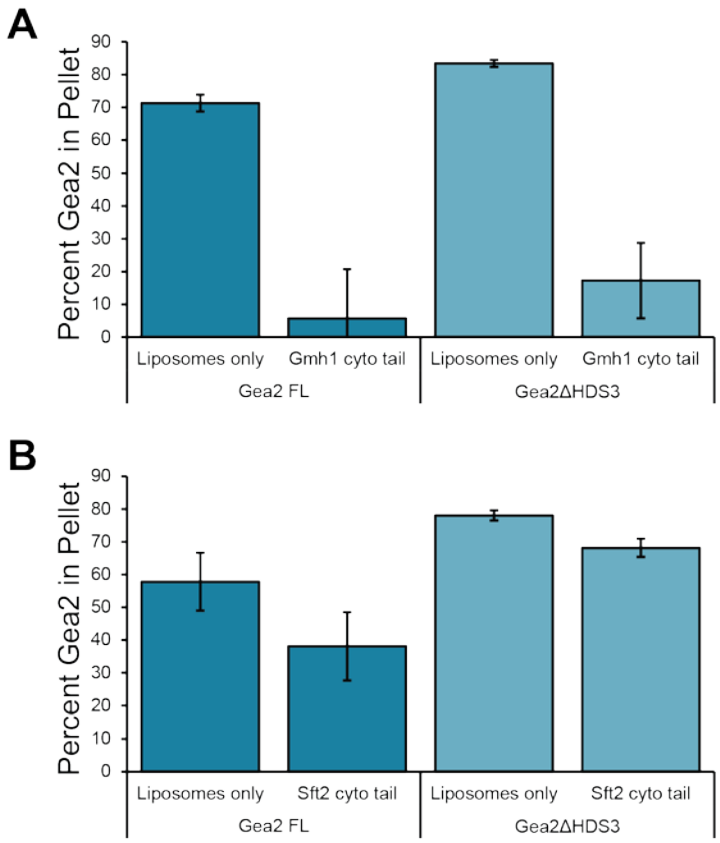

Figure 5.3. The cytosolic tails of documented Gea2 interactors Gmh1 and Sft2 fail to recruit Gea2 to membranes *in vitro*. Percent of Gea2 FL or Gea2ΔHDS3 in membrane pellet after incubation with either PC-Ni^{2+} liposomes alone or with His7-tagged cytosolic tails of Gmh1 (A) or Drs2 (B). n = 3. Data collected by D.J. Wasilko.

Nevertheless, we can safely conclude from these experiments that the sequence of the cytosolic tails of Gmh1 or Sft2 alone are insufficient to recruit Gea2 to membranes *in vitro*.

SILAC-MS revealed Gea2 interactions with Golgi SNAREs.

As targeted screens had failed to uncover the unique protein interactors which target Gea1 and Gea2 to different compartments, we chose to employ SILAC-MS to identify new interactions. We grew yeast with or without Gea2-HA in parallel cultures with light and heavy media, then formaldehyde crosslinked both cultures with low concentrations of formaldehyde (0.375%) to crosslink any interacting proteins. After pulldown with HA and trypsin digestion, the samples were analyzed by mass spectrometry by D.S. Kim in the Smolka Lab. Note that the low cellular levels of Gea1 have precluded collection of useful SILAC-MS data, despite efforts to scale up the cultures and preparations. Further optimization of Gea1 SILAC-MS, perhaps by overexpression of Gea1, may prove valuable in the future.

In addition to several other Golgi proteins, the top hits for Gea2 include two Golgi SNAREs: Gos1 and Sed5 (Figure 5.4 A). A third interesting hit is the SM protein Sly1, which is known to interact with the Habc domains of certain SNAREs, such as Gos1 and Sed5, and regulate SNARE complex assembly (Kosodo et al. 2002). Sed5 participates as the Qa in two SNARE complexes at the Golgi: one at the early Golgi receiving ER-Golgi vesicles and one at the medial Golgi receiving intra-Golgi and endosomal vesicles (Fasshauer et al. 1998; Hardwick and Pelham 1992; Volchuk et al. 2004). Gos1 participates as the Qb in only the complex at the

A

Gene	Z-score	"Molar Ratio"
GEA2	6.63	1.00
GEA1	3.80	0.05
GOS1	3.01	0.35
SED5	2.58	0.22
SLY1	2.31	0.08
COG7	2.08	0.05
MNN10	1.38	0.17
USO1	1.37	0.03
TLG2	1.25	0.08
COY1	1.14	0.15
VPS53	1.08	0.04
EMP47	0.83	0.13
PMR1	0.80	0.09
MON2	0.74	0.03
SEC7	0.58	0.03

B

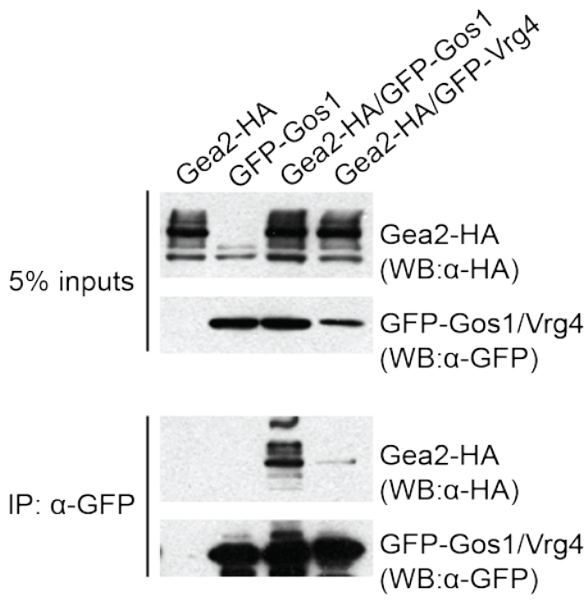

Figure 5.4. Gea2 interacts directly with the Golgi SNARE Gos1 *in vivo*. (A) Tops hits from SILAC-MS analysis with Gea2-HA as bait, sorted using a custom Z-score. (B) Western blots of GFP-Gos1 IP using anti-GFP to detect Gos1 and anti-HA to detect HA-tagged Gea2. GFP-Vrg4 IP serves as a negative control. Data collected by D.S. Kim, M.B. Smolka, and J.C. Fromme.

medial Golgi, making it an attractive prospect for the role of differentiating Gea1 and Gea2 localization (McNew et al. 1998).

An *in vivo* interaction between Gea2 and Gos1 was confirmed through co-immunoprecipitation of Gea2 in an IP of GFP-Gos1 (Figure 5.4 B). Gea2 was pulled down specifically by Gos1 and not by another Golgi protein, Vrg4. However, preliminary microscopy experiments showed that Gea2 is not mislocalized in a *gos1Δ* strain, indicating that the Gos1 interaction is not required for Gea2 recruitment to Golgi surfaces (data not shown).

Gea1 colocalizes with early Golgi Bos1, Gea2 with medial Golgi Gos1.

To test whether Gos1 is truly a specific interactor of Gea2 and not Gea1, we decided to test colocalization of Gea1 and Gea2 with both Gos1 and the early Golgi SNARE complex Qb SNARE, Bos1. When we co-expressed Gea1-3xMars or Gea2-3xMars with GFP-Gos1, we observed that Gea2 colocalized very well with Gos1, while Gea1 rarely did (Figure 5.5 A, B). Conversely, Gea1 colocalized very well with GFP-Bos1, while Gea2 showed no apparent colocalization with Bos1 (Figure 5.5 C, D).

A caveat of these experiments is that the method for integrating the *GFP-GOS1* and *GFP-BOS1* fusion genes introduces a second copy of each gene at the *LEU2* locus and that second copy is driven by the high expression *ACT1* promoter, so Gos1 and Bos1 are considerably overexpressed in these strains. It was reported previously that overexpression of Gos1 in particular alters Golgi number and morphology (Losev et al. 2006), so it is possible that our data

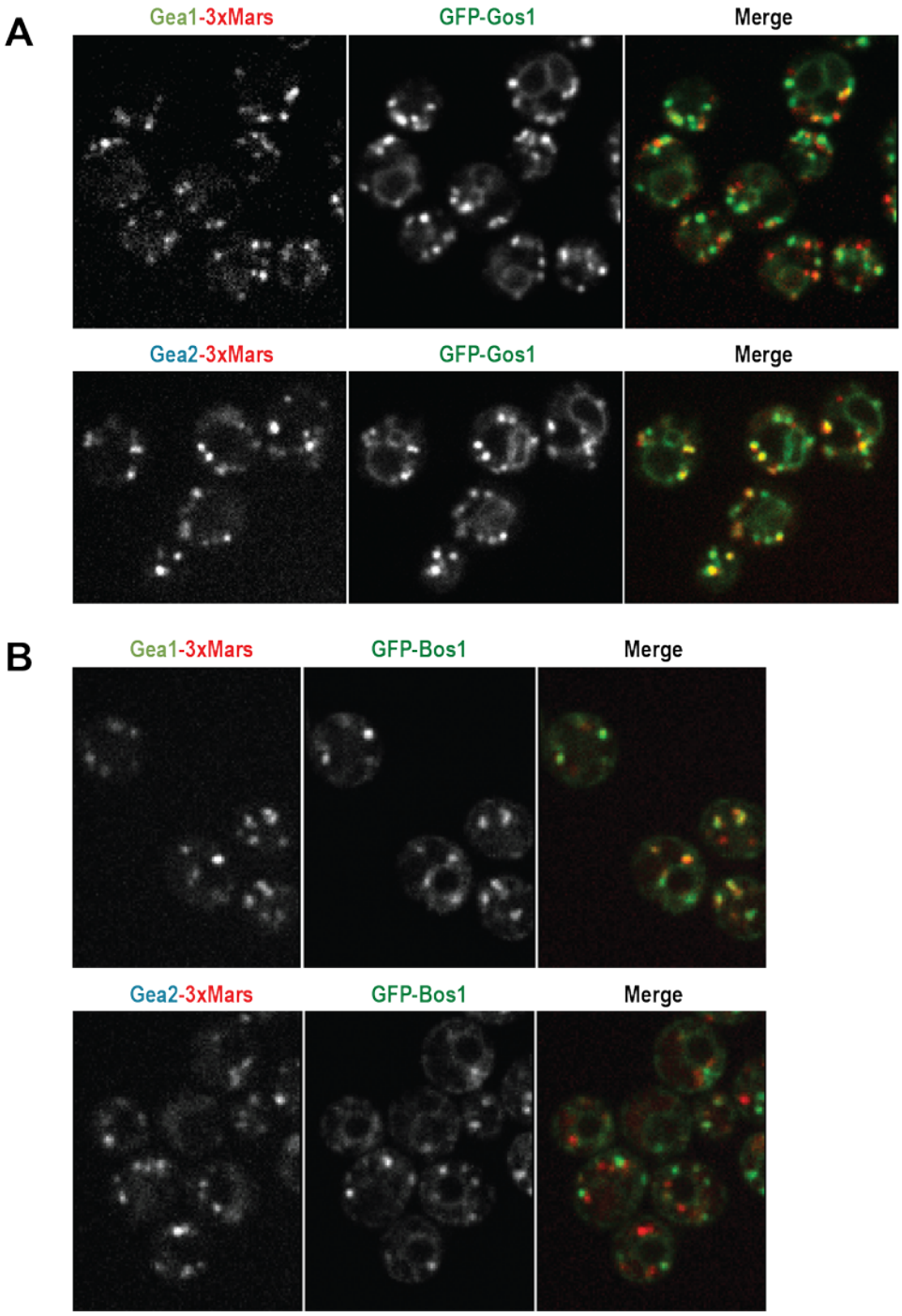

Figure 5.5. Colocalization patterns show that Gea2, but not Gea1, colocalizes with Gos1. Intracellular colocalization assessed by coexpression of RFP-labeled Gea1 (A, C) or Gea2 (B, D) with GFP-labeled Gos1 (A, B) or the early Golgi SNARE Bos1 (C, D). Yellow indicates overlap of green and red channels. Data collected by J.C. Fromme.

are confounded by this effect. Further experiments to confirm these preliminary results are necessary.

Purified Gos1 cytoplasmic domain is not monomeric, but can recruit Gea2 to membranes in vitro.

To improve our understanding of the physical interaction between Gos1 and Gea2, and to ascertain whether Gos1 serves as a regulator of Gea2 or vice versa, I set out to purify Gos1 for biochemical studies. We designed constructs encompassing the entire Gos1 cytoplasmic domain (1-204), the Gos1 Habc domains (1-129), and the Gos1 SNARE helix (130-20), each with a C-terminal His tag to replace the transmembrane domain, and introduced them into bacterial expression vectors. The SNARE helix construct proved insoluble during purification, but I was able to purify both the cytoplasmic domain and the Habc domain with good yields.

To test whether Gos1 is a membrane recruiter for Gea2, I carried out membrane pelleting assays with PC-Ni^{2+} liposomes and Gea2 alone or with Ypt1-GTP, Gos1 cytoplasmic domain, or Gos1 Habc domain. Interestingly, the Gos1 cytoplasmic domain recruited Gea2 to membranes as well as Ypt1, while the Habc domain did not increase membrane binding (Figure 5.6 A). This preliminary results suggests that Gos1 can recruit Gea2 to membranes and that the SNARE helix is required for this recruitment.

These results were somewhat confounded by the fact that Gos1 cytosolic tail fractionated into two distinct pools during gel filtration, one around the molecular weight of monomeric Gos1

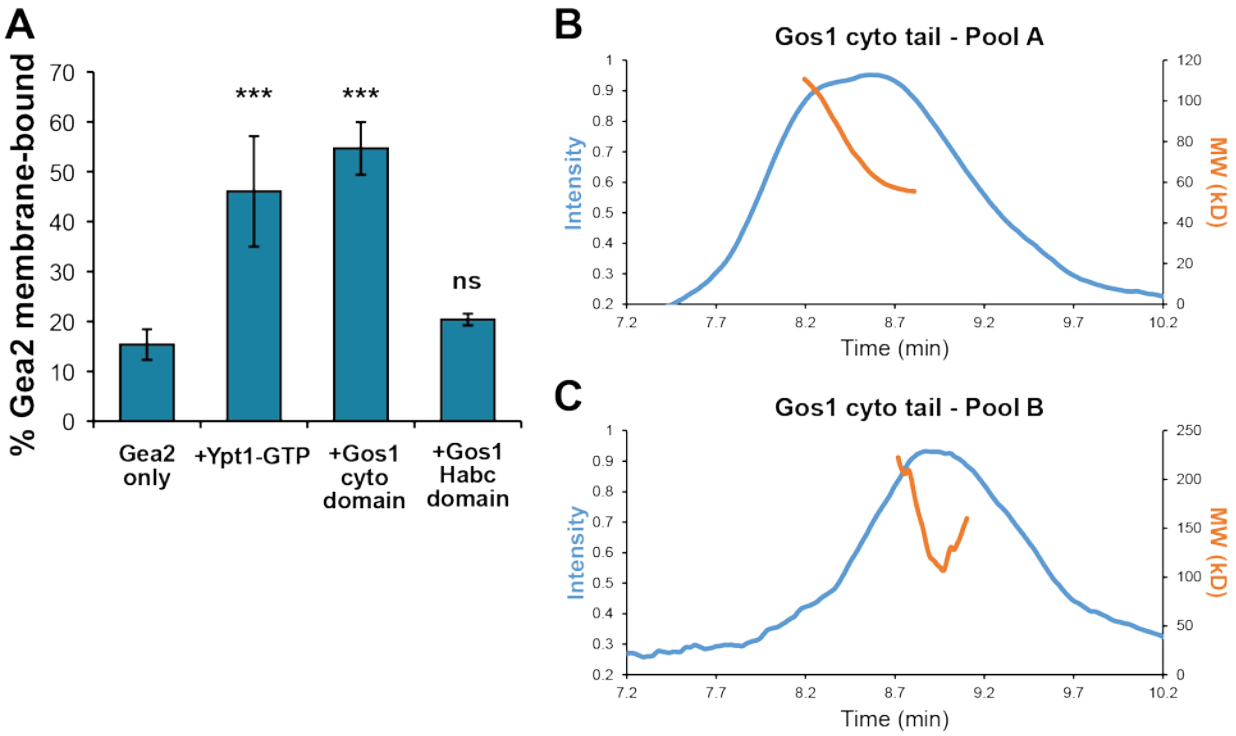

Figure 5.6. The purified cytoplasmic domain of Gos1 recruits Gea2 to membranes *in vitro*. (A) Percent of Gea2 FL in membrane pellet after incubation with either PC-Ni^{2+} liposomes alone (Gea2 only) or with Ypt1-His_7-GTP, His-tagged Gos1 cytoplasmic (cyto) domain, or His-tagged Gos1 Habc domain. n = 3. (B, C) MALS analysis of two pools recovered from gel filtration of the purified Gos1 cytoplasmic domain of Gos1. Error bars represent 95% confidence intervals. n.s., not significant; ***, P < 0.0001. MALS data collected by S.L. Halaby.

(Pool B) and one at a higher molecular weight (Pool A). The pelleting data from Pool B is shown in Figure 5.6 A. A comparison of the effect on pelleting of Pool A and Pool B shows that Pool A has a significantly smaller effect on Gea2 membrane binding than Pool B (data not shown). To understand the nature of these two pools, each was analyzed by MALS to measure the molecular weight of proteins in solution.

Interestingly, both pools of Gos1 cytosolic tail returned similar MALS data (Figure 5.6 B, C). Neither was monodispersed, as evident from the deviation of each molecular weight trace from a straight, horizontal line. This deviation makes estimating molecular weight unreliable, but we can roughly estimate a range based on each trace. Pool A returns a molecular weight range of about 80-100 kD if judged from the trace or 720 kD as calculated by the software. This calculated value differs drastically from an obvious estimate based on the trace, likely due to the fact that the sample was not monodispersed. Pool B returns a molecular weight range of about 150-200 kD based on the trace or 150 kD as calculated by the software. Regardless of the reason, all of these estimates are considerably higher than the approximately 25 kD molecular weight expected for a monomer of this construct. These results suggest homo-multimerization and perhaps aggregation of the Gos1 cytoplasmic tail construct.

It is telling that both pools recovered from gel filtration yielded similar traces from MALS analysis, despite the fact that Pool B should have a lower molecular weight as it eluted later from the gel filtration column. This suggests that the equilibrium between monomeric and multimeric states favors multimers and that any monomer from Pool B disappeared into the

mix of multimers observed by MALS. It is notable that we also observed slightly larger than normal aggregation peaks in the MALS data, again hinting at the instability of this construct in solution.

Before completing MALS analysis, I also prepared preliminary crystallization screens of the Gos1 cytosolic tail construct, but they failed to produce any hits, likely because the protein was not mono-dispersed in solution, but rather a mixture of monomers and various multimers.

Further troubleshooting will be necessary to attain biologically relevant, stable SNAREs and SNARE complexes for use in biochemistry with Gea1 and Gea2.

Discussion

The evidently complex nature of regulating interactions and recruitment of Gea1 and Gea2 has complicated characterization. Based on screens for mislocalization in single deletion strains, it seems plausible that no single interaction is either required or sufficient for Gea recruitment *in vivo*. Instead, Gea1 and Gea2 may utilize coincidence detection in their decision-making process for activating Arf1. In this model, Gea1 and Gea2 are recruited by weak or transient interactions with multiple factors. While I cannot completely rule out the possibility that a single strong interaction might be required or sufficient to recruit Gea to the Golgi, we have been unable to uncover such an interaction, and our current evidence of protein and lipid interactions seems to point in the direction of cooperative recruitment.

Further characterization of the interaction between Gea and Ypt1 *in vitro* and *in vivo*, especially in concert with the recently discovered SNARE interaction, offers an opportunity for a thorough mechanistic model of both Gea recruitment and possible tethering to the membrane by its recruiting interactions, as well as exploration of conformation changes in Gea upon recruitment.

The SILAC-MS hits of Golgi SNARE proteins present an intriguing line of inquiry. While preliminary results are not without caveats, it is promising that the colocalization patterns of Gea1 and Gea2 are so distinctly opposite relative to Bos1 and Gos1; the difference is quite striking. Further investigation is warranted to ascertain whether this difference persists with endogenous expression of the SNAREs and how the SNAREs themselves relate to one another, spatially or temporally, within the Golgi. If the observation holds water, it should prompt additional tests for a direct interaction between Gea1 and Bos1, or other members of the early Golgi SNARE complex, and will bring us closer to an understanding of the different pathways in which Gea1 and Gea2 participate.

We have begun efforts to improve purification of Gos1, as well as the other SNAREs of its complex, by using stabilizing protein fusions. Additional measures, such as coexpression of the complex or expression with additional factors, such as the SM protein Sly1, may prove helpful in isolating stable SNARE complexes or monomeric SNAREs for further biochemical studies. It seems likely that Gea2 interacts with at least a partially assembled SNARE bundle, in light of the fact that both Gos1 and Sed5 were identified in the SILAC-MS screen. Developing the tools to test this and other hypotheses will allow us to form a detailed picture of the molecular

interactions between Gea2 and the SNAREs, as well as a broader understanding of the cellular context in which these interactions occur and their implications for coordination between incoming and outgoing Golgi vesicle traffic.

- CHAPTER 6 -

FUTURE DIRECTIONS

Both cellular and molecular models of Golgi Arf-GEF regulation emerge from this work. Gea1, Gea2, and Sec7 each occupy different compartments within the Golgi, with Gea2 likely functioning later in the Golgi than Gea1. This specificity is achieved through a combination of affinities for different membranes and protein interactions. The regulatory domains of Gea1 and Gea2 function differently from those of Sec7, as Gea1 and Gea2 show no catalytic autoinhibition or positive feedback. The C-terminus of Gea functions in both masking membrane binding and facilitating catalysis, both the N- and C-termini are required for recruitment by the GTPase Ypt1, and the N-terminus is responsible for directing Gea1 and Gea2 to different Golgi compartments. A novel Gea2 interactor, the SNARE Gos1, presents a possible recruiter specific to Gea2, perhaps paralleled by recruitment of Gea1 by the early Golgi SNARE Bos1.

Many of the details of this model remain unresolved. The *in vivo* composition of the cis-Golgi has been difficult to measure, leaving the role of lipids in recruiting Gea somewhat undefined beyond "not anionic." While the preferences *in vitro* of each Golgi Arf-GEF seem to fit logically with their localization *in vivo*, further evidence will be required to prove once and for all that membrane identity plays a role in directing the Arf-GEFs.

The effect of positively charged artificial lipids is also striking. It may represent an artefact, as there are no physiological positively charged lipids. Preliminary studies by A.M. Joiner during his rotation and after showed that other artificial positive lipids had a similar or stronger effect on Gea recruitment to membranes and catalytic activity. While this effect may be artefactual, its possible physiological interpretations are intriguing.

One hypothesis we have considered attributes the membrane proximal positive charge to the di-lysine motif found in COPI cargos. A.M. Joiner attempted anchor away experiments with the cytoplasmic tail of two COPI cargos used to lure Gea to the mitochondria, but he did not observe a change in Gea localization. It is not unlikely that the greater concentration of COPI cargoes at the Golgi would confound a single di-lysine motif sent to the mitochondria, and other recruiting signals such as Ypt1 remained at the Golgi as well. While this hypothesis is not trivial to test, it cannot be ruled out based on our experiments so far.

Another tempting hypothesis points to the SNARE Gos1, which bears two membrane-proximal lysines as well as two arginines between its transmembrane and SNARE domains. If Gos1 proves to be a true recruiter of Gea2, this positively enriched motif might explain Gea2's *in vitro* preference for Ni^{2+}-containing liposomes.

In terms of Gea regulation through its own domains, the next frontiers are domain- and residue-level mechanisms. Continuation of studies using conservation-selected mutants and chimeras

represent a potentially useful avenue for this work, but such studies may ultimately prove too simplistic to untangle the complex interactions regulating Gea.

A full length structure of Gea, either solved through x-ray crystallography or cryo-EM, will provide a wealth of information for future dissection of atomic-level interactions which regulate Gea1 and Gea2. Additionally, a structure of the GEF domain including the extra conserved helix may prove help explain why that helix has such a dramatic effect on the stability of Gea2ΔC.

Our most promising current line of research revolves around the SNARE protein interactions discovered in our SILAC-MS experiments with Gea2. Additional work is aimed at verifying whether this interaction is a recruiting interaction, and if so, whether Gea2 interacts with Gos1 as a monomer, or with Gos1 and Sed5 as part of their assembled SNARE complex. The implications of each hypothesis are fascinating. If Gea2 is recruited by Gos1 alone, then Gea2 is recruited to the Golgi membrane surface before the arrival of incoming vesicles from endosomes. If Gea2 interacts with the assembled Gos1/Sed5/Ykt6/Sft1 SNARE helix, this points to a very specific moment in the life cycle of those SNAREs: after vesicle fusion but before unzipping of the SNARE complex. This hypothetical model suggests that the arrival of incoming vesicles with cargo may be coupled to preparations for packaging into COPI vesicles for retrograde transport, and that the interaction between Gea2 and the SNARE complex might mediate this coordination of events.

If Gea2 is recruited by Gos1, or the Gos1 SNARE complex, it is tempting to hypothesize that Gea1 may be recruited in a parallel manner by Bos1 or its SNARE complex. So far our preliminary evidence for this hypothesis is the excellent colocalization of Gea1 with Bos1. Down the line, biochemical studies can be used to test the preferences of Gea1 and Gea2 for Gos1 and Bos1 *in vitro*. This line of inquiry also raises interesting questions about the functional redundancy of Gea1 and Gea2. If Gea1 is deleted, does Gea2 spread into Bos1 compartments to take up the tasks which Gea1 normally handles? Can the opposite happen when Gea2 is deleted? What function does Gea2 serve at the late Golgi, were it overlaps with Sec7? Perhaps it relates to the interaction between Gea2 and Drs2, flipping of phosphatidylserine to help create the anionic lipid environment to which Sec7 is recruited. In that vein, what is the source of the seed Arf1-GTP required for Sec7 positive feedback (Richardson, McDonold, and Fromme 2012)? Possibly Gea2 activates small amounts of Arf1 at the TGN to prepare the way for rapid secretory vesicle formation. While these hypotheses are highly speculative, they focus on the way in which trafficking is orchestrated across the entire Golgi, rather than as distinct events. The more we learn about the recruitment and regulation of Gea1 and Gea2, the better we can model the overall system.

Ultimately these types of questions target a fundamental gap in our understanding of the Golgi Arf-GEFs. We know that they activate Arf1, and we know what activated Arf1 does. But how and why are Gea1, Gea2, and Sec7 localized to different Golgi compartments? How is the timing of their activation of Arf1 controlled? Answering these questions will help us form a

complete model of the trafficking events that must happen at the early, medial, and late Golgi, and how Gea1, Gea2, and Sec7 are regulated to coordinate their roles.

- Appendices -

Appendix I. Materials and Methods

Antibodies and immunoprecipitations

The anti-Gea2 rabbit polyclonal antibody was generated using purified Gea2 GEF domain (Covance) and used at a 1:500 dilution. This antibody cross-reacts to some extent with purified recombinant Gea1 but fails to detect Gea1 in yeast extracts. The anti-G6PDH rabbit polyclonal antibody was purchased from Sigma and used at a 1:30,000 dilution. The anti-His_6 mouse monoclonal antibody used to verify cleavage of His tags was purchased from Covance and used at a 1:500 dilution.

The GFP nanobody resin used for immunoprecipitation experiments was made using purified GFP nanobody and NHS-activated Sepharose Fast Flow (GE Healthcare) (Kirchhofer *et al.*, 2009). 25 ODs of cells were suspended in lysis buffer (50 mM Tris-HCl pH 7.5, 0.2% NP40 substitute, 150 mM NaCl, 1 mM EDTA, 1X complete protease inhibitor cocktail [Roche] and 1 mM PMSF) before lysis by mechanical disruption. After incubation, resin was washed three times with lysis buffer and proteins were eluted in SDS sample buffer.

Yeast growth assays

Yeast shuffling assays were used to assess *in vivo* sufficiency of Gea1 and Gea2 mutants (Gea2ΔC is residues 1-766). Double deletion strains (*gea1Δgea2Δ* and *gea1Δgea2Δarf1Δ*) were

maintained by a copy of GEA2 on a URA3, ARS-CEN plasmid. LEU2, ARS-CEN plasmids carrying the mutant constructs were introduced, and cells were cultured overnight in -Leu media. Cells were plated at 3-fold dilutions onto synthetic complete media or media with 5-FOA and incubated at 30°C for two days before imaging.

To test for sensitivity to the drug Congo Red, shuffled cells were plated at 3-fold dilutions onto synthetic complete media containing either 50 ng/μl or 100 ng/μl Congo Red (Sigma) and incubated at 30°C for two days before imaging.

Protein purification

Gea constructs were expressed with an N-terminal His_6 tag in Rosetta2 *E. coli* cells, with expression induced overnight with 250 μM IPTG at 15°C. Pelleted cultures were resuspended in 25 ml/L of culture of lysis buffer (40 mM Tris pH 8.0, 300 mM NaCl, 10% glycerol, 10 mM imidazole, 0.25X Roche complete protease inhibitor, 1 mM PMSF, 10 mM β-ME) before lysis by sonication. After the lysate was clarified by centrifugation, protein constructs were purified via nickel affinity (Ni-NTA resin, Qiagen) in batch, followed by anion exchange (MonoQ, GE Healthcare), overnight cleavage of the His_6 tag by TEV protease at 4°C, and gel filtration (Superdex 200, GE Healthcare), with a final buffer containing 20 mM Tris pH 8, 150 mM NaCl, and 1 mM DTT. The Gea2GEF construct was expressed and purified similarly through the nickel affinity step, then incubated at room temperature overnight with TEV, before an additional round nickel binding and elution to remove any uncleaved protein.

Purification of Arf and Rab GTPases has previously been described in detail (Ha *et al.*, 2005; Mcdonold and Fromme, 2014; Richardson and Fromme, 2015; Thomas and Fromme, 2016).

Liposome preparation

Lipid composition of PC, PC-Ni^{2+}, TGN, and TGN-Ni^{2+} liposomes is described in Appendix II. Liposomes were prepared in HK buffer (20 mM HEPES pH 7.5, 150 mM KOAc) as described previously (Paczkowski and Fromme, 2016), with 100 nm filters used to extrude liposomes used for GEF activity assays and 400 nm filters used to extrude liposomes used for membrane pelleting assays.

GEF activity assays

GEF activity was measured as described previously (Richardson and Fromme, 2015). All assays were carried out in HKM buffer (HK plus 2 mM $MgCl_2$) at 30°C. Arf1 exchange was measured after sequentially adding 200 μM GTP and 100 nM GEF to HKM with 333 μM liposomes (or 166 μM liposomes, for Figure 6, E and F). After equilibration for 5 minutes, Arf1 was added and native tryptophan fluorescence was measured for 12 minutes. For assays testing the effect of preloaded GTPases, 500 nM Arf1, Arl1, Ypt1-His_7, or Ypt6-His_7 or 400 nM prenylated Ypt1 was added to HKM with liposomes, followed by 200 μM GTP and 2 mM EDTA. After incubation for 12 minutes, 4 mM $MgCl_2$ was added, followed by 100 nM GEF. After 5 minutes of equilibration, 500 nM Arf1 was added and monitored for an additional 12 minutes. Each assay was carried out in triplicate for statistical analysis.

Liposome pelleting assays

Liposome pelleting assays were carried out as previously described (Paczkowski and Fromme, 2016). 500 μM liposomes were mixed with HKM buffer. To test intrinsic membrane binding of GEF constructs, 4 μg of each construct was incubated with liposomes for 10 minutes at room temperature before ultracentrifugation, separation of supernatant from pellet, and PAGE analysis. For recruiting assays, 2 μg of each GTPase was activated by 15 minutes of EDTA-mediated GTP exchange at 30°C before the addition of extra $MgCl_2$ and finally 4 μg of GEF. Parallel reactions lacking liposomes were run with all sets of binding reactions to account for background pelleting of GEF constructs.

PAGE gels were stained with Bio-Safe Coomassie (Bio-Rad) and imaged using a LI-COR Odyssey system. Band intensities were quantified in ImageJ. Percent GEF in pellet was calculated after subtraction of background pelleting for each construct. Each set of reactions was performed in at least triplicate for statistical analysis.

Microscopy

Cells were cultured in either synthetic complete media or synthetic dropout media at 30°C and imaged in log phase. Note that Gea2ΔC in Figure 2.6 corresponds to residues 1-766.

Images for Figures 2.1, 2.6, 4.3, 4.4 B, and 5.5 were captured using a CSU-X spinning disc confocal microscope system (Intelligent Imaging Innovations, Inc.) using a DMI600B microscope (Leica Biosystems), 100×/1.46 NA objective, and a QuantEM EMC CD camera

(Photometrics). Images were acquired, leveled, and analyzed using Slidebook 5.0 software (Intelligent Imaging Innovations, Inc.). Single confocal sections are shown. After background subtraction to limit analysis to Golgi puncta and selection of individual cells, Pearson's analysis was performed in Slidebook 5.0 to quantify colocalization of fluorescently tagged proteins.

Images for Figure 4.4 C were captured using an Andor Revolution spinning disk confocal microscope with dual cameras for simultaneous red/green channel acquisition. Images were leveled and analyzed using ImageJ. Single confocal planes are shown.

Images described in the Tables 4.2 and 5.1 and in the text were captured using a DeltaVision RT wide-field microscope (Applied Precision) followed by deconvolution in softWoRx. Images were leveled and analyzed using ImageJ.

Conservation analysis and mutant design

Conservation analysis was carried out using ClustalW and visualized using WebLogo, secondary structure was predicted using PSIPRED, and surface analysis on the Gea2 molecular replacement model was visualized in PyMOL.

SILAC mass spectrometry

For mass spectrometry experiments, cells were grown in (-)Arg (-)Lys drop-out medium ('light' version complemented with standard arginine and lysine; 'heavy' version complemented with lysine $^{13}C_6$, $^{15}N_2$ and arginine $^{13}C_6$, $^{15}N_4$). In this case, light and heavy media were used with

cells containing either wild type Gea2 or Gea2-HA. Cells were harvested by centrifugation and incubated for 10 minutes with 0.375% formaldehyde before neutralization with glycine. After mechanical disruption, lysates were incubated with anti-HA resin (Sigma). Resin was washed with lysis buffer before bound proteins were eluted and eluates from light and heavy medium were mixed together, reduced, alkylated and precipitated. After resuspension and digestion with trypsin, samples were dried in a SpeedVac evaporator, reconstituted and analysed by LC-MS/MS using a 125 μM ID capillary C18 column and an Orbitrap XL mass spectrometer coupled with an Eksigent nanoflow system. Database searching was performed using the SORCERER system (Sage-N Research) running the program SEQUEST. After searching a target-decoy budding yeast database, results were filtered either based on probability score to achieve a 1% false positive rate or manual inspection. Quantification of heavy/light peptide isotope ratios was performed using the Xpress program.

Multi-angle light scattering (MALS)

Proteins purified to homogeneity were exchanged into fresh buffer by serial concentration and redilution to a final concentration of 5 mg/ml, and separated in a Wyatt WTC-050S5 gel filtration column coupled to DAWN HELEOS-II light scattering and Optilab T-rEX refractive index detectors (Wyatt Technology) at room temperature. Data were analyzed via ASTRA 6 software to obtain the molecular weight of the sample.

Statistical tests

Significance for Figure 1, Figure 2, Figure 6, E and F, and Figure 7 was determined using an unpaired *t* test with a Welch's correction. Significance for all other figures was determined by a one-way ANOVA with a Tukey post-test. Error bars represent 95% confidence intervals.

Appendix II. Composition of liposomes used in this study

	PC	PC-Ni^{2+}	TGN	TGN-Ni^{2+}
Lipid	*Amount (Molar %)*			
DOPC	99	94	24	24
POPC			6	6
DOPE			7	7
POPE			3	3
DOPS			1	1
POPS			2	2
DOPA			1	1
POPA			2	2
PI			29	24
PI(4)P			1	1
CDP-DAG			2	2
PO-DAG			4	4
DO-DAG			2	2
Ceramide (C18)			5	5
Nickel-DOGS		5		5
Cholesterol			10	10
DiR	1	1	1	1

Appendix III. Yeast expression plasmids used in this study and developed for future use

Name	Description	Vector	Source
pCF1248	*GEA2* driven by P_{GEA2} (*URA3* maintenance plasmid for shuffling strains)	pRS416	This study
pCF1301	*GEA1-GFP* driven by P_{GEA2}	pRS415	This study
pCF1302	*GEA2-GFP* driven by P_{GEA1}	pRS415	This study
pCF1312	*gea1ΔC* (1-761)-*GFP* driven by P_{GEA1}	pRS415	This study
pCF1313	*gea2ΔC* (1-766)-*GFP* driven by P_{GEA2}	pRS415	This study
pCM09	*gea1ΔHDS3* (1-1225)-*GFP* driven by P_{GEA1}	pRS415	This study
pCM10	*GEA1 FL* (1-1408)-*GFP* driven by P_{GEA1}	pRS415	This study
pMG001	*GEA2 FL* (1-1459)-*GFP* driven by P_{GEA2}	pRS415	This study
pMG002	*gea2ΔHDS3* (1-1196)-*GFP* driven by P_{GEA2}	pRS415	This study
pMG033	*gea1* (1-1408) Y991C-*GFP*	pRS415	This study
YIplac211-iGFP-VRG4	Integrating plasmid for *GFP-VRG4* by two-step gene	YIplac211	Gift from B. Glick

Appendix IV. Bacterial expression plasmids used in this study and developed for future use

Name	Description	Vector	Source
pARF1	*ARF1*	pET3	Weiss 1989
pBCR314	*SEC7* (203-2009) with a cleavable His_6 tag	pFastBacHT	Richardson 2012
pCF1053	*arf1ΔN17*	pET28	Richardson 2012
pCF1163	*GEA1 FL* (1-1408) with a cleavable His_6 tag	pET28	Richardson 2012
pCF1184	*ARL1*	pET23	McDonold 2014
pCF1299	*GEA2ΔC* (1-782) with a cleavable His_6 tag	pET28	Richardson 2016
pCM14	*YPT6* with C-terminal His_7 tag and cleavable N-terminal *GST* tag	pGEX-6P	McDonold 2014
pLT35	*MRS6* with cleavable N-terminal His_6 tag	pET28	Thomas 2016
pLT40	*GDI1* with cleavable N-terminal GST tag	pGEX-6P	Thomas 2016
pLT41	*BET2* with cleavable N-terminal His_6 tag and Bet4	pCDF-Duet-1	Thomas 2016
pLT50	Full-length *YPT1* with cleavable N-terminal GST tag	pGEX-6P	Thomas 2016
pMG005	*GEA2 FL* (1-1459) with a cleavable His_6 tag	pET28	Richardson 2016
pMG006	*C. glabrata GEA* with a cleavable His_6 tag	pET28	This study
pMG007	*K. lactis GEA* with a cleavable His_6 tag	pET28	This study
pMG008	*K. thermotolerans GEA* with a cleavable His_6 tag	pET28	This study
pMG009	*Z. rouxii GEA* with a cleavable His_6 tag	pET28	This study
pMG010	*GEA2* (1-1459) with a cleavable His_6 tag	pFastBacHT	This study
pMG012	*GEA1* (1-1408) with a cleavable His_6 tag	pFastBacHT	This study
pMG013	*C. thermophilum GEA* with a cleavable His_6 tag	pFastBacHT	This study
pMG014	*M. thermophila GEA* with a cleavable His_6 tag	pFastBacHT	This study
pMG015	*S. stipitis GEA* with a cleavable His_6 tag	pFastBacHT	This study
pMG016	*C. thermophilum GEA* with a cleavable His_6 tag	pET28	This study
pMG017	*gea1ΔHDS3* (1-1225) with a cleavable His_6 tag	pET28	This study
pMG020	*gea2ΔHDS3* (1-1196) with a cleavable His_6 tag	pET28	Richardson 2016
pMG023	*M. thermophila GEA* with a cleavable His_6 tag	pET28	This study
pMG024	*gea1ΔN14* (15-1408) with a cleavable His_6 tag	pET28	This study
pMG025	*gea1* (1-1408) K127A with a cleavable His_6 tag	pET28	This study
pMG026	*gea1* (1-1408) D166A with a cleavable His_6 tag	pET28	This study
pMG027	*gea1* (1-1408) D467A with a cleavable His_6 tag	pET28	This study
pMG028	*gea2* (1-1459) K124A with a cleavable His_6 tag	pET28	This study
pMG029	*gea2* (1-1459) D163A with a cleavable His_6 tag	pET28	This study
pMG030	*gea2* (1-1459) D485A with a cleavable His_6 tag	pET28	This study
pMG031	*gea1* (1-1408) Y991C with a cleavable His_6 tag	pET28	This study
pMG032	*gea2* (1-1459) Y1001C with a cleavable His_6 tag	pET28	This study
pMG034	*gea2* (1-1459) with a cleavable His_6 tag on a long linker	pET28	This study
pMG035	*gea2ΔC* (1-782) with a cleavable His_6 tag on a long linker	pET28	This study

Appendix IV. (continued)

Name	Description	Vector	Source
pMG036	*gea2GEF* (558-782) with a cleavable His_6 tag	pET28	This study
pNMT1	*NMT1*	pCYC	Duronio 1990
pYC001	*gea2* (1-1459) E18A, C19A	pET28	This study
pYC002	*gea2* (1-1459) R27A, K28A, K31A	pET28	This study
pYC003	*gea2* (1-1459) K124A	pET28	This study
pYC004	*gea2* (1-1459) T150A, H151A, C152A	pET28	This study
pYC005	*gea2* (1-1459) R153A, F154A, E155A	pET28	This study
pYC006	*gea2* (1-1459) D162A, D163A	pET28	This study
pYC007	*gea2* (1-1459) N187A, S188A	pET28	This study
pYC008	*gea2* (1-1459) Y191A, D192A	pET28	This study
pYC009	*gea2* (1-1459) C202A, N203A	pET28	This study
pYC010	*gea2* (1-1459) R205A, R206A, S207A, E208A	pET28	This study
pYC011	*gea2* (1-1459) R211A, N212A, Q215A	pET28	This study
Ypt1-His_7	*YPT1* with C-terminal His_7 tag and cleavable N-terminal *GST* tag	pGEX-6P	Gift from T. Bretscher

Appendix V. Yeast strains used in this study

Name	Description	Source
SEY6210	*MATα suc2-Δ9 ura3-52 his3-Δ200 leu2-3,112 lys2-801 trp1-Δ901*	Robinson et al., 1988
SEY6210.1	*MATa suc2-Δ9 ura3-52 his3-Δ200 leu2-3,112 lys2-801 trp1-Δ901*	Robinson et al., 1988
BY4741α	*MATα ura3-Δ0 his3-Δ1 leu2-Δ0 lys2-Δ0*	Brachmann et al., 1998
CFY2376	SEY6210 *SEC7-Mars::TRP1 GEA1-mNeonGreen::HIS3*	This study
CFY2378	SEY6210 *SEC7-Mars::TRP1 GEA2-mNeonGreen::HIS3*	This study
CFY2490	SEY6210.1 *GEA1-3xMars::TRP1 GFP-VRG4*	This study
CFY2503	SEY6210.1 *GEA2-3xMars::TRP1 GFP-VRG4*	This study
CFY2872	*BY4741α GEA1Δ::KANMX GEA2Δ::HIS3 +pCF1248*	This study
CFY2873	*BY4741α GEA1Δ::NatMX GEA2Δ::HIS3 arf1Δ::KANMX +pCF1248*	This study
CFY1391	SEY6210.1 *GEA1-GFP::HIS3 KEX2-Mars::TRP1*	This study
CFY1348	SEY6210.1 *GEA2-GFP::HIS3 KEX2-Mars::TRP1*	This study
CFY1450	SEY6210.1 *GEA1-MARS::TRP1 SVP26-GFP::HIS3*	This study
CFY1536	SEY6210.1 *GEA2-MARS::TRP1 SEC7-iRFP::KANMX SVP26-GFP::HIS3*	This study
CFY2401	SEY6210.1 *GEA2-3xMars::TRP1*	This study
CFY2447	SEY6210.1 *GEA1-3xMars::TRP1 leu2::GFP-GOS1::LEU2*	This study
CFY2463	SEY6210.1 *GEA2-3xMars::TRP1 leu2::GFP-GOS1::LEU2*	This study
CFY2668	SEY6210.1 *GEA1-3xMars::TRP1 leu2::GFP-BOS1::LEU2*	This study
CFY2670	SEY6210.1 *GEA2-3xMars::TRP1 leu2::GFP-BOS1::LEU2*	This study
CFY2458	SEY6210.1 *GEA2-HA::HIS3 leu2::GFP-GOS1::LEU2*	This study

- REFERENCES -

Achstetter, Tilman, Alex Franzusoff, Charles Field, and Randy Schekman. 1988. "SEC7 Encodes an Unusual, High Molecular Weight Protein Required for Membrane Traffic from the Yeast Golgi Apparatus." *Journal of Biological Chemistry* 263 (24): 11711–17.

Aizel, Kaheina, Valérie Biou, Jorge Navaza, Lionel V. Duarte, Valérie Campanacci, Jacqueline Cherfils, and Mahel Zeghouf. 2013. "Integrated Conformational and Lipid-Sensing Regulation of Endosomal ArfGEF BRAG2." Edited by Frederick Hughson. *PLoS Biology* 11 (9). Public Library of Science: e1001652. doi:10.1371/journal.pbio.1001652.

Alberts, Bruce, Alexander Johnson, Julian Lewis, Martin Raff, Keith Roberts, and Peter Walter. 2007. *Molecular Biology of the Cell*. Garland Science.

Alexandrov, Kirill, Hisanori Horiuchi, Olivia Steele-Mortimer, Miguel C. Seabra, and Marino Zerial. 1994. "Rab Escort Protein-1 Is a Multifunctional Protein That Accompanies Newly Prenylated Rab Proteins to Their Target Membranes." *The EMBO Journal* 13 (22): 5262–73. https://www.ncbi.nlm.nih.gov/pmc/articles/PMC395482/pdf/emboj00070-0020.pdf.

Anders, N., and G. Jürgens. 2008. "Large ARF Guanine Nucleotide Exchange Factors in Membrane Trafficking." *Cellular and Molecular Life Sciences® : CMLS* 65 (21): 3433–45.

Antonny, Bruno, Sophie Beraud-Dufour, Pierre Chardin, and Marc Chabre. 1997. "N-Terminal Hydrophobic Residues of the G-Protein ADP-Ribosylation Factor-1 Insert into Membrane Phospholipids upon GDP to GTP Exchange." *Biochemistry* 36 (15): 4675–84.

Antonny, Bruno, Irit Huber, Sonia Paris, Marc Chabre, and Dan Cassel. 1997. "Activation of ADP-Ribosylation Factor 1 GTPase-Activating Protein by Phosphatidylcholine-Derived Diacylglycerols." *The Journal of Biological Chemistry* 272 (49): 30848–51. doi:10.1074/jbc.272.49.30848.

Arst Jr., Herbert N., Miguel Hernandez-Gonzalez, Miguel A. Peñalva, and Areti Pantazopoulou. 2014. "GBF/Gea Mutant with a Single Substitution Sustains Fungal Growth in the Absence of BIG/Sec7." *FEBS Letters* 588 (24). Federation of European Biochemical Societies: 4799–4806. doi:10.1016/j.febslet.2014.11.014.

Bacon, Rebecca A, Antti Salminen, Hannele Ruohola, Peter Novick, and Susan Ferro-novick. 1989. "The GTP-Binding Protein Yptl Is Required for Transport In Vitro®: The Golgi Apparatus Is Defective in Yptl Mutants." *Journal of Cell Biology* 109 (September): 1015–22. http://jcb.rupress.org.proxy.library.cornell.edu/content/jcb/109/3/1015.full.pdf.

Baker, Richard W., and Frederick M. Hughson. 2016. "Chaperoning SNARE Assembly and Disassembly." *Nature Reviews. Molecular Cell Biology* 17 (8): 465–79.

doi:10.1038/nrm.2016.65.

Balch, William E., Benjamin S. Glick, and James E. Rothman. 1984. "Sequential Intermediates in the Pathway of Intercompartmental Transport in a Cell-Free System." *Cell* 39 (3 PART 2): 525–36. doi:10.1016/0092-8674(84)90459-8.

Balch, William E, William G Dunphy, William A Braell, and James E Rothman. 1984. "Reconstitution of the Transport of Protein between Successive Compartments of the Golgi Measured by the Coupled Incorporation of N-Acetylglucosamine." *Cell* 39867484. http://www.cell.com/cell/pdf/0092-8674(84)90019-9.pdf?_returnURL=http%3A%2F%2Flinkinghub.elsevier.com%2Fretrieve%2Fpii%2F0092867484900199%3Fshowall%3Dtrue.

Bard, Frédéric, and Vivek Malhotra. 2006. "The Formation of TGN- to-Plasma-Membrane Transport Carriers TGN: Trans-Golgi Network." *Annu. Rev. Cell Dev. Biol* 22 (1): 439–55. doi:10.1146/annurev.cellbio.21.012704.133126.

Barfield, Robyn M., J. Christopher Fromme, and Randy Schekman. 2009. "The Exomer Coat Complex Transports Fus1p to the Plasma Membrane via a Novel Plasma Membrane Sorting Signal in Yeast." *Mol Biol Cell* 20 (23). American Society for Cell Biology: 4985–96. doi:10.1091/mbc.E09-04-0324.

Barlowe, Charles, Lelio Orci, Tom Yeung, Midori Hosobuchi, Susan Hamamoto, Nina Salama, Michael F Rexach, et al. 1994. "COPII: A Membrane Coat Formed by Sec Proteins That Drive Vesicle Budding from the Endoplasmic Reticulum." *Cell* 77 (6): 895–907. doi:10.1016/0092-8674(94)90138-4.

Barlowe, Charles, and Randy Schekman. 1993. "SEC12 Encodes a Guanine-Nucleotide-Exchange Factor Essential for Transport Vesicle Budding from the ER." *Nature* 365 (6444): 347–49.

Barr, Francis A. 2009. "Rab GTPase Function in Golgi Trafficking." *Seminars in Cell & Developmental Biology* 20 (7): 780–83. doi:10.1016/j.semcdb.2009.03.007.

Benli, Mustafa, Frank Döring, David G. Robinson, Xiaoping Yang, and Dieter Gallwitz. 1996. "Two GTPase Isoforms, Ypt31p and Ypt32p, Are Essential for Golgi Function in Yeast." *The EMBO Journal* 15 (23): 6460–75. https://www.ncbi.nlm.nih.gov/pmc/articles/PMC452471/pdf/emboj00023-0102.pdf.

Bensen, Eric S., Bonny G. Yeung, and Gregory S. Payne. 2001. "Ric1p and the Ypt6p GTPase Function in a Common Pathway Required for Localization of Trans-Golgi Network Membrane Proteins." *Mol Biol Cell* 12 (1). American Society for Cell Biology: 13–26. doi:10.1091/mbc.12.1.13.

Bhamidipati, Arunashree, Sally A. Lewis, and Nicholas J. Cowan. 2000. "ADP Ribosylation Factor-like Protein 2 (Arl2) Regulates the Interaction of Tubulin-Folding Cofactor D with

Native Tubulin." *Journal of Cell Biology* 149 (5): 1087–96. doi:10.1083/jcb.149.5.1087.

Bhatt, Jay M., Ekaterina G. Viktorova, Theodore Busby, Paulina Wyrozumska, Laura E. Newman, Helen Lin, Eunjoo Lee, et al. 2016. "Oligomerization of the Sec7 Domain Arf Guanine Nucleotide Exchange Factor GBF1 Is Dispensable for Golgi Localization and Function but Regulates Degradation." *American Journal of Physiology - Cell Physiology* 310 (6): C456–69. http://ajpcell.physiology.org/content/310/6/C456.

Bi, Xiping, Richard A. Corpina, and Jonathan Goldberg. 2002. "Structure of the Sec23/24-Sar1 Pre-Budding Complex of the COPII Vesicle Coat." *Nature* 419 (6904): 271–77. doi:10.1038/nature01040.

Bigay, Joëlle, and Bruno Antonny. 2012. "Curvature, Lipid Packing, and Electrostatics of Membrane Organelles: Defining Cellular Territories in Determining Specificity." *Developmental Cell* 23 (5): 886–95. doi:10.1016/j.devcel.2012.10.009.

Bonifacino, Juan S. 2004. "The GGA Proteins: Adaptors on the Move." *Nat Rev Mol Cell Biol* 5 (1): 23–32. doi:10.1038/nrm1279.

Bonifacino, Juan S. 2014. "Vesicular Transport Earns a Nobel." *Trends in Cell Biology*. Elsevier. doi:10.1016/j.tcb.2013.11.001.

Bonifacino, Juan S., and Jennifer Lippincott-Schwartz. 2003. "Coat Proteins: Shaping Membrane Transport." *Nature Reviews. Molecular Cell Biology* 4 (May): 409–14. doi:10.1038/nrm1099.

Bouvet, Samuel, Marie-Pierre Golinelli-Cohen, Vincent Contremoulins, and Catherine L. Jackson. 2013. "Targeting of the Arf-GEF GBF1 to Lipid Droplets and Golgi Membranes." *Journal of Cell Science* 126 (20): 4794–4805.

Brachmann, Carrie Baker, Adrian Davies, Gregory J. Cost, Emerita Caputo, Joachim Li, Philip Hieter, and Jef D. Boeke. 1998. "Designer Deletion Strains Derived from *Saccharomyces Cerevisiae* S288C: A Useful Set of Strains and Plasmids for PCR-Mediated Gene Disruption and Other Applications." *Yeast* 14 (2). John Wiley & Sons, Ltd.: 115–32. doi:10.1002/(SICI)1097-0061(19980130)14:2<115::AID-YEA204>3.0.CO;2-2.

Brown, H. Alex, Stephen Gutowski, Carolyn R. Moomaw, Clive Slaughter, and Paul C. Sternwels. 1993. "ADP-Ribosylation Factor, a Small GTP-Dependent Regulatory Protein, Stimulates Phospholipase D Activity." *Cell* 75 (6): 1137–44. doi:10.1016/0092-8674(93)90323-I.

Bui, Quynh Trang, Marie-Pierre Golinelli-Cohen, and Catherine L. Jackson. 2009. "Large Arf1 Guanine Nucleotide Exchange Factors: Evolution, Domain Structure, and Roles in Membrane Trafficking and Human Disease." *Molecular Genetics and Genomics : MGG* 282 (4): 329–50. doi:10.1007/s00438-009-0473-3.

Cai, Huaqing, Karin Reinisch, and Susan Ferro-Novick. 2007. "Coats, Tethers, Rabs, and

SNAREs Work Together to Mediate the Intracellular Destination of a Transport Vesicle." *Developmental Cell* 12 (5). Elsevier: 671–82. doi:10.1016/j.devcel.2007.04.005.

Casanova, James E. 2007. "Regulation of Arf Activation: The Sec7 Family of Guanine Nucleotide Exchange Factors." *Traffic* 8 (11): 1476–85.

Chantalat, Sophie, Regis Courbeyrette, Francesca Senic-Matuglia, Catherine L. Jackson, Bruno Goud, and Anne Peyroche. 2003. "A Novel Golgi Membrane Protein Is a Partner of the ARF Exchange Factors Gea1p and Gea2p." *Molecular Biology of the Cell* 14 (June): 2357–71. doi:10.1091/mbc.E02.

Chantalat, Sophie, Sei-Kyoung Park, Zhaolin Hua, Ke Liu, Renée Gobin, Anne Peyroche, Alain Rambourg, Todd Graham, and Catherine L. Jackson. 2004. "The Arf Activator Gea2p and the P-Type ATPase Drs2p Interact at the Golgi in *Saccharomyces Cerevisiae*." *Journal of Cell Science* 117 (Pt 5): 711–22.

Chen, Kuan-Yu, Pei-Chin Tsai, Jia-Wei Hsu, Hsin-Chia Hsu, Chiung-Ying Fang, Lin-Chun Chang, Yueh-Tso Tsai, Chia-Jung Yu, and Fang-Jen Lee. 2010. "Syt1p Promotes Activation of Arl1p at the Late Golgi to Recruit Imh1p." *Journal of Cell Science* 123 (Pt 20): 3478–89.

Chen, Yu A., and Richard H. Scheller. 2001. "SNARE-Mediated Membrane Fusion." *Nature Reviews. Molecular Cell Biology* 2 (2): 98–106. doi:10.1038/35052017.

Cherfils, Jacqueline, and Mahel Zeghouf. 2011. "Chronicles of the GTPase Switch." *Nature Chemical Biology* 7 (8): 493–95. doi:10.1038/nchembio.608.

———. 2013. "Regulation of Small GTPases by GEFs, GAPs, and GDIs." *Physiological Reviews* 93 (1): 269–309. doi:10.1152/physrev.00003.2012.

Christis, Chantal, and Sean Munro. 2012. "The Small G Protein Arl1 Directs the Trans-Golgi-Specific Targeting of the Arf1 Exchange Factors BIG1 and BIG2." *The Journal of Cell Biology* 196 (3): 327–35. doi:10.1083/jcb.201107115.

Cocucci, Emanuele, Franç Ois Aguet, Steeve Boulant, and Tom Kirchhausen. 2012. "The First Five Seconds in the Life of a Clathrin-Coated Pit." doi:10.1016/j.cell.2012.05.047.

Cremona, Ottavio, Gilbert Di Paolo, Markus R. Wenk, Anita Lüthi, Warren T. Kim, Kohji Takei, Laurie Daniell, et al. 1999. "Essential Role of Phosphoinositide Metabolism in Synaptic Vesicle Recycling." *Cell* 99 (2). MIT Press, Cambridge, MA: 179–88. doi:10.1016/S0092-8674(00)81649-9.

D'Souza-Schorey, Crislyn, and Philippe Chavrier. 2006. "ARF Proteins: Roles in Membrane Traffic and Beyond." *Nature Reviews. Molecular Cell Biology* 7 (5): 347–58. doi:10.1038/nrm1910.

de Figueiredo, Paul, Daniel Drecktrah, John A. Katzenellenbogen, Marian Strang, and William J.

Brown. 1998. “Evidence That Phospholipase A2 Activity Is Required for Golgi Complex and Trans Golgi Network Membrane Tubulation.” *Proceedings of the National Academy of Sciences of the United States of America* 95 (15): 8642–47. doi:10.1073/pnas.95.15.8642.

De Matteis, Maria Antonietta, and Anna Godi. 2004. “Protein–lipid Interactions in Membrane Trafficking at the Golgi Complex.” *Biochimica et Biophysica Acta (BBA) - Biomembranes* 1666 (1–2): 264–74. doi:10.1016/j.bbamem.2004.07.002.

De Matteis, Maria Antonietta, and Alberto Luini. 2008. “Exiting the Golgi Complex.” *Nature Reviews. Molecular Cell Biology* 9 (4). Nature Publishing Group: 273–84. doi:10.1038/nrm2378.

De Wit, M. C. Y., I. F. M. De Coo, D. J. J. Halley, M. H. Lequin, and G. M. S. Mancini. 2009. “Movement Disorder and Neuronal Migration Disorder due to ARFGEF2 Mutation.” *Neurogenetics* 10 (4): 333–36. doi:10.1007/s10048-009-0192-2.

Dell’Angelica, Esteban C., Rosa Puertollano, Chris Mullins, Ruben C. Aguilar, Jose D. Vargas, Lisa M. Hartnell, and Juan S. Bonifacino. 2000. “GGAs: A Family of ADP Ribosylation Factor-Binding Proteins Related to Adaptors and Associated with the Golgi Complex.” *The Journal of Cell Biology* 149 (1): 81–94. http://www.pubmedcentral.nih.gov/articlerender.fcgi?artid=2175099&tool=pmcentrez&rendertype=abstract.

Deng, Yi, Marie-Pierre Golinelli-Cohen, Elena Smirnova, and Catherine L. Jackson. 2009. “A COPI Coat Subunit Interacts Directly with an Early-Golgi Localized Arf Exchange Factor.” *EMBO Reports* 10 (1): 58–64. doi:10.1038/embor.2008.221.

Donaldson, Julie G., and Akira Honda. 2005. “Localization and Function of Arf Family GTPases.” *Biochemical Society Transactions* 33 (Pt 4): 639–42.

Donaldson, Julie G., and Catherine L. Jackson. 2011. “ARF Family G Proteins and Their Regulators: Roles in Membrane Transport, Development and Disease.” *Nature Reviews Molecular Cell Biology* 12 (6): 362–75.

Du, Li-Lin, and Peter Novick. 2001. “Yeast Rab GTPase-Activating Protein Gyp1p Localizes to the Golgi Apparatus and Is a Negative Regulator of Ypt1p.” *Molecular Biology of the Cell* 12 (5). American Society for Cell Biology: 1215–26. doi:10.1091/mbc.12.5.1215.

Duronio, Robert J., Emily Jackson-Machelski, Robert O. Heuckeroth, Peter O. Olins, Catherine S. Devine, Wes Yonemoto, Lee W. Slice, Susan S. Taylor, and Jeffrey I. Gordon. 1990. “Protein N-Myristoylation in *Escherichia Coli*: Reconstitution of a Eukaryotic Protein Modification in Bacteria.” *Proceedings of the National Academy of Sciences of the United States of America* 87 (4): 1506–10. doi:10.1073/pnas.87.4.1506.

Fasshauer, Dirk, R. Bryan Sutton, Axel T. Brunger, and Reinhard Jahn. 1998. “Conserved Structural Features of the Synaptic Fusion Complex: SNARE Proteins Reclassified as Q-

and R-SNAREs." *Proceedings of the National Academy of Sciences* 95 (26). National Academy of Sciences: 15781–86. doi:10.1073/pnas.95.26.15781.

Folsch, Heike. 2008. "Regulation of Membrane Trafficking in Polarized Epithelial Cells." *Current Opinion in Cell Biology* 20 (2): 208–13. doi:10.1126/scisignal.2001449.Engineering.

Franzusoff, Alex, Kevin Redding, Jeff Crosby, Robert S. Fuller, and Randy Schekman. 1991. "Localization of Components Involved in Protein Transport and Processing through the Yeast Golgi Apparatus." *Journal of Cell Biology* 112 (1): 27–37. doi:10.1083/jcb.112.1.27.

Ghaemmaghami, Sina, Won-Ki Huh, Kiowa Bower, Russell W. Howson, Archana Belle, Noah Dephoure, Erin K. O'Shea, and Jonathan S. Weissman. 2003. "Global Analysis of Protein Expression in Yeast." *Nature* 425 (6959): 737–41. doi:10.1038/nature02046.

Gillingham, Alison K., and Sean Munro. 2007a. "Identification of a Guanine Nucleotide Exchange Factor for Arf3, the Yeast Orthologue of Mammalian Arf6." *PLoS ONE* 2 (9): e842.

———. 2007b. "The Small G Proteins of the Arf Family and Their Regulators." *Annual Review of Cell and Developmental Biology* 23 (1): 579–611.

Goldberg, Jonathan. 1998. "Structural Basis for Activation of ARF GTPase: Mechanisms of Guanine Nucleotide Exchange and GTP-Myristoyl Switching." *Cell* 95 (2): 237–48.

Gomez-Navarro, Natalia, and Elizabeth Miller. 2016. "Protein Sorting at the ER-Golgi Interface." *Journal of Cell Biology* 215 (6): 769–78. doi:10.1083/jcb.201610031.

Goud, Bruno, and Paul A. Gleeson. 2010. "TGN Golgins, Rabs and Cytoskeleton: Regulating the Golgi Trafficking Highways." *Trends in Cell Biology* 20 (6): 329–36.

Grebe, Markus, José Gadea, Thomas Steinmann, Marika Kientz, Jens-Ulrich Rahfeld, Klaus Salchert, Csaba Koncz, and Gerd Jürgens. 2000. "A Conserved Domain of the Arabidopsis GNOM Protein Mediates Subunit Interaction and Cyclophilin 5 Binding." *The Plant Cell* 12 (3). American Society of Plant Biologists: 343–56. doi:10.1105/TPC.12.3.343.

Ha, Vi, Geraint Thomas, Stacey Stauffer, and Paul Randazzo. 2005. "Preparation of Myristoylated Arf1 and Arf6." *Methods in Enzymology* 404 (January): 164–74.

Hardwick, Kevin G., and Hugh R. B. Pelham. 1992. "SED5 Encodes a 39-kD Integral Membrane Protein Required for Vesicular Transport between the ER and the Golgi Complex." *Journal of Cell Biology* 119 (3): 513–21. doi:10.1083/jcb.119.3.513.

Heffernan, Linda F, and Jeremy C Simpson. 2014. "The Trials and Tubule-Ations of Rab6 Involvement in Golgi-to-ER Retrograde Transport" 1: 1453–59. doi:10.1042/BST20140178.

Hierro, Aitor, Adriana L Rojas, Raul Rojas, Namita Murthy, Grégory Effantin, Andrey V Kajava, Alasdair C Steven, Juan S Bonifacino, and James H Hurley. 2007. "Function Architecture of

the Retromer Cargo-Recognition Complex." *Nature* 449 (7165): 1063–67. doi:10.1038/nature06216.

Higashijima, Tsutomu, Kenneth Ferguson, Paul Sternweis, Elliott Ross, Murray Smigel, and Alfred Gilman. 1987. "The Effect of Activating Ligands on the Intrinsic Fluorescence of Guanine Nucleotide-Binding Regulatory Proteins." *Journal of Biological Chemistry* 262 (2): 752–56. http://www.jbc.org/content/262/2/752.short.

Hirst, Jennifer, Carol Irving, and Georg H H Borner. 2013. "Adaptor Protein Complexes AP-4 and AP-5: New Players in Endosomal Trafficking and Progressive Spastic Paraplegia." *Traffic*. John Wiley & Sons A/S. doi:10.1111/tra.12028.

Howell, Gareth J., Zoe G. Holloway, Christian Cobbold, Anthony P. Monaco, and Sreenivasan Ponnambalam. 2006. "Cell Biology of Membrane Trafficking in Human Disease." *International Review of Cytology* 252: 1–69. doi:10.1016/S0074-7696(06)52005-4.

Jackson, Catherine L., and James E. Casanova. 2000. "Turning on ARF: The Sec7 Family of Guanine-Nucleotide-Exchange Factors." *Trends in Cell Biology* 10: 60–67. http://www.sciencedirect.com/science/article/pii/S0962892499016992.

Jackson, Lauren P., Michael Lewis, Helen M. Kent, Melissa A. Edeling, Philip R. Evans, Rainer Duden, and David J. Owen. 2012. "Molecular Basis for Recognition of Dilysine Trafficking Motifs by COPI." *Developmental Cell* 23 (6): 1255–62. doi:10.1016/j.devcel.2012.10.017.

Jedd, Gregory, Celeste Richardson, Robert Litt, and Nava Segev. 1995. "The Ypt1 GTPase Is Essential for the First Two Steps of the Yeast Secretory Pathway." *Journal of Cell Biology* 131 (3): 583–90. doi:10.1083/jcb.131.3.583.

Kahn, Richard A., Elspeth Bruford, Hiroki Inoue, John M. Logsdon, Zhongzhen Nie, Richard T. Premont, Paul A. Randazzo, et al. 2008. "Consensus Nomenclature for the Human ArfGAP Domain-Containing Proteins." *Journal of Cell Biology* 182 (6): 1039–44. doi:10.1083/jcb.200806041.

Kelly, Bernard T., Stephen C. Graham, Nicole Liska, Philip N. Dannhauser, Stefan Honig, Ernst J. Ungewickell, and David J. Owen. 2014. "AP2 Controls Clathrin Polymerization with a Membrane-Activated Switch." *Science* 345 (6195): 459–63. doi:10.1126/science.1254836.

Kelly, Eoin E., Conor P. Horgan, Bruno Goud, and Mary W. McCaffrey. 2012. "The Rab Family of Proteins: 25 Years On." *Biochemical Society Transactions* 40 (6): 1337–47. doi:10.1042/BST20120203.

Kim, Jane J., Zhanna Lipatova, Uddalak Majumdar, and Nava Segev. 2016. "Regulation of Golgi Cisternal Progression by Ypt/Rab GTPases." *Developmental Cell* 36 (4): 440–52. doi:10.1016/j.devcel.2016.01.016.

Kirchhausen, T. 2000. "Three Ways to Make a Vesicle." *Nature Reviews. Molecular Cell Biology* 1

(3): 187–98. doi:10.1038/35043117.

Kirchhofer, Axel, Jonas Helma, Katrin Schmidthals, Carina Frauer, Sheng Cui, Annette Karcher, Mireille Pellis, et al. 2009. "Modulation of Protein Properties in Living Cells Using Nanobodies." *Nature Structural & Molecular Biology* 17. doi:10.1038/nsmb.1727.

Klemm, Robin, Christer Ejsing, Michal Surma, Hermann-Josef Kaiser, Mathias Gerl, Julio Sampaio, Quentin Robillard, et al. 2009. "Segregation of Sphingolipids and Sterols during Formation of Secretory Vesicles at the Trans-Golgi Network." *The Journal of Cell Biology* 185 (4): 601–12.

Köhler, Alwin, and Ed Hurt. 2007. "Exporting RNA from the Nucleus to the Cytoplasm." *Nature Reviews Molecular Cell Biology* 8 (10): 761–73. doi:10.1038/nrm2255.

Kosodo, Yoichi, Yoichi Noda, Hiroyuki Adachi, and Koji Yoda. 2002. "Binding of Sly1 to Sed5 Enhances Formation of the Yeast Early Golgi SNARE Complex." *Journal of Cell Science* 115 (18). http://jcs.biologists.org/content/115/18/3683.long.

Krauss, Michael, Jun Yong Jia, Aurélien Roux, Rainer Beck, Felix T. Wieland, Pietro De Camilli, and Volker Haucke. 2008. "Arf1-GTP-Induced Tubule Formation Suggests a Function of Arf Family Proteins in Curvature Acquisition at Sites of Vesicle Budding." *Journal of Biological Chemistry* 283 (41): 27717–23. doi:10.1074/jbc.M804528200.

Kyoung, Minjoung, and Erin D. Sheets. 2008. "Vesicle Diffusion close to a Membrane: Intermembrane Interactions Measured with Fluorescence Correlation Spectroscopy." *Biophysical Journal* 95 (12). CRC Press, Boca Raton, FL: 5789–97. doi:10.1529/biophysj.108.128934.

Lee, Stella Y., and Bill Pohajdak. 2000. "N-Terminal Targeting of Guanine Nucleotide Exchange Factors (GEF) for ADP Ribosylation Factors (ARF) to the Golgi." *Journal of Cell Science* 113 (Pt 1 (June): 1883–89.

Leventis, Peter A., and Sergio Grinstein. 2010. "The Distribution and Function of Phosphatidylserine in Cellular Membranes." *Annual Review of Biophysics* 39 (1): 407–27. doi:10.1146/annurev.biophys.093008.131234.

Lewis, Stephen M., Pak Phi Poon, Richard A. Singer, Gerald C. Johnston, and Anne Spang. 2004. "The ArfGAP Glo3 Is Required for the Generation of COPI Vesicles." *Molecular Biology of the Cell* 15 (9): 4064–72. doi:10.1091/mbc.E04-04-0316.

Lippincott-Schwartz, Jennifer, Lydia Yuan, Christopher Tipper, Myléne Amherdt, Lelio Orci, and Richard D. Klausner. 1991. "Brefeldin A's Effects on Endosomes, Lysosomes, and the TGN Suggest a General Mechanism for Regulating Organelle Structure and Membrane Traffic." *Cell* 67 (3): 601–16. doi:10.1016/0092-8674(91)90534-6.

Liu, Ya-Wen, Chun-Fang Huang, Kai-Bin Huang, and Fang-Jen S Lee. 2005. "Role for Gcs1p in

Regulation of Arl1p at Trans-Golgi Compartments □ D." *Molecular Biology of the Cell* 16: 4024–33. doi:10.1091/mbc.E05.

Losev, Eugene, Catherine A. Reinke, Jennifer Jellen, Daniel E. Strongin, Brooke J. Bevis, and Benjamin S. Glick. 2006. "Golgi Maturation Visualized in Living Yeast." *Nature* 441 (7096). Nature Publishing Group: 1002–6. doi:10.1038/nature04717.

Lowery, Jason, Tomasz Szul, Melanie Styers, Zoe Holloway, Viola Oorschot, Judith Klumperman, and Elizabeth Sztul. 2013. "The Sec7 Guanine Nucleotide Exchange Factor GBF1 Regulates Membrane Recruitment of BIG1 and BIG2 Guanine Nucleotide Exchange Factors to the Trans-Golgi Network (TGN)." *The Journal of Biological Chemistry* 288 (16): 11532–45.

Lundmark, Richard, Gary J. Doherty, Yvonne Vallis, Brian J. Peter, and Harvey T. Mcmahon. 2008. "Arf Family GTP Loading Is Activated By, and Generates, Positive Membrane Curvature." *Biochem. J* 414: 189–94. doi:10.1042/BJ20081237.

Luo, Ruibai, Bijan Ahvazi, Diana Amariei, Deborah Shroder, Beatriz Burrola, Wolfgang Losert, and Paul A. Randazzo. 2007. "Kinetic Analysis of GTP Hydrolysis Catalysed by the Arf1-GTP-ASAP1 Complex." *The Biochemical Journal* 402 (3): 439–47. doi:10.1042/BJ20061217.

Lynch-Day, Molly A., Deepali Bhandari, Shekar Menon, Ju Huang, Huaqing Cai, Clinton R. Bartholomew, John H. Brumell, Susan Ferro-Novick, and Daniel J. Klionsky. 2010. "Trs85 Directs a Ypt1 GEF, TRAPPIII, to the Phagophore to Promote Autophagy." *Proceedings of the National Academy of Sciences of the United States of America* 107 (17): 7811–16. doi:10.1073/pnas.1000063107.

Malsam, Jörg, and Thomas H. Söllner. 2011. "Organization of SNAREs within the Golgi Stack." *Cold Spring Harbor Perspectives in Biology* 3 (10). Cold Spring Harbor Laboratory Press: 1–17. doi:10.1101/cshperspect.a005249.

Martínez-Menárguez, José A. 2013. "Intra-Golgi Transport: Roles for Vesicles, Tubules, and Cisternae." *ISRN Cell Biology* 2013 (February). Hindawi: 1–15. doi:10.1155/2013/126731.

Matsuura-Tokita, Kumi, Masaki Takeuchi, Akira Ichihara, Kenta Mikuriya, and Akihiko Nakano. 2006. "Live Imaging of Yeast Golgi Cisternal Maturation." *Nature* 441 (7096). Nature Publishing Group: 1007–10. doi:10.1038/nature04737.

McDonold, Caitlin M., and J. Christopher Fromme. 2014. "Four GTPases Differentially Regulate the Sec7 Arf-GEF to Direct Traffic at the Trans-Golgi Network." *Developmental Cell* 30 (6). Elsevier Inc.: 759–67. doi:10.1016/j.devcel.2014.07.016.

McNew, James A., John G.S. Coe, Morten Søgaard, Boris V. Zemelman, Christian Wimmer, Wanjin Hong, and Thomas H. Söllner. 1998. "Gos1p, a *Saccharomyces Cerevisiae* SNARE Protein Involved in Golgi Transport." *FEBS Letters* 435 (1): 89–95. doi:10.1016/S0014-5793(98)01044-8.

McNew, James A., Francesco Parlati, Ryouichi Fukuda, Robert J. Johnston, Keren Paz, Fabienne Paumet, Thomas H. Sollner, and James E. Rothman. 2000. "Compartmental Specificity of Cellular Membrane Fusion Encoded in SNARE Proteins." *Nature* 407 (6801): 153–59. doi:10.1038/35025000.

Mellman, Ira, and W. James Nelson. 2008. "Coordinated Protein Sorting, Targeting and Distribution in Polarized Cells." *Nat Rev Mol Cell Biol* 9 (11): 833–45. doi:10.1038/nrm2525.Coordinated.

Mizuno-Yamasaki, Emi, Felix Rivera-Molina, and Peter Novick. 2012. "GTPase Networks in Membrane Traffic." *Annual Review of Biochemistry* 81: 637–59. doi:10.1146/annurev-biochem-052810-093700.

Monetta, Pablo, Ileana Slavin, Nahuel Romero, and Cecilia Alvarez. 2007. "Rab1b Interacts with GBF1 and Modulates Both ARF1 Dynamics and COPI Association." *Molecular Biology of the Cell* 18 (7): 2400–2410.

Morriswood, Brooke, and Graham Warren. 2013. "Cell Biology. Stalemate in the Golgi Battle." *Science (New York, N.Y.)* 341 (6153): 1465–66. doi:10.1126/science.1245656.

Mouratou, Barbara, Valerie Biou, Alexandra Joubert, Jean Cohen, David Shields, Niko Geldner, Gerd Jürgens, Paul Melançon, and Jacqueline Cherfils. 2005. "The Domain Architecture of Large Guanine Nucleotide Exchange Factors for the Small GTP-Binding Protein Arf." *BMC Genomics* 6 (January): 20.

Natarajan, Paramasivam, Jiyi Wang, Zhaolin Hua, and Todd R. Graham. 2004. "Drs2p-Coupled Aminophospholipid Translocase Activity in Yeast Golgi Membranes and Relationship to in Vivo Function." *Proceedings of the National Academy of Sciences of the United States of America* 101 (29). National Academy of Sciences: 10614–19. doi:10.1073/pnas.0404146101.

Novick, Peter. 2016. "Regulation of Membrane Traffic by Rab GEF and GAP Cascades." *Small GTPases* 7 (4): 252–56. doi:10.1080/21541248.2016.1213781.

Novick, Peter, Susan Ferro, and Randy Schekman. 1981. "Order of Events in the Yeast Secretory Pathway." *Cell* 25: 461–69. http://www.cell.com.proxy.library.cornell.edu/cell/pdf/0092-8674(81)90064-7.pdf?_returnURL=http%3A%2F%2Flinkinghub.elsevier.com%2Fretrieve%2Fpii%2F0092867481900647%3Fshowall%3Dtrue.

Novick, Peter, Charles Field, and Randy Schekman. 1980. "Identification of 23 Complementation Groups Required for Post-Translational Events in the Yeast Secretory Pathway." *Cell Copyright* 21 (0): 205–15. http://www.cell.com/cell/pdf/0092-8674(80)90128-2.pdf?_returnURL=http%3A%2F%2Flinkinghub.elsevier.com%2Fretrieve%2Fpii%2F0092867480901282%3Fshowall%3Dtrue.

Novick, Peter J., and Randy Schekman. 1979. "Secretion and Cell-Surface Growth Are Blocked

in a Temperature-Sensitive Mutant of *Saccharomyces Cerevisiae*." *Proceedings of the National Academy of Sciences of the United States of America* 76 (4): 1858–62. doi:10.1073/pnas.76.4.1858.

Nyathi, Yvonne, Barrie M. Wilkinson, and Martin R. Pool. 2013. "Co-Translational Targeting and Translocation of Proteins to the Endoplasmic Reticulum." *Biochimica et Biophysica Acta - Molecular Cell Research* 1833 (11): 2392–2402. doi:10.1016/j.bbamcr.2013.02.021.

Ortiz, Darinel, Martina Medkova, Christiane Walch-Solimena, and Peter Novick. 2002. "Ypt32 Recruits the Sec4p Guanine Nucleotide Exchange Factor, Sec2p, to Secretory Vesicles; Evidence for a Rab Cascade in Yeast." *The Journal of Cell Biology* 611 (6). The Rockefeller University Press: 21–9525. doi:10.1083/jcb.

Paczkowski, Jon E., and J. Christopher Fromme. 2016. "Analysis of Arf1 GTPase-Dependent Membrane Binding and Remodeling Using the Exomer Secretory Vesicle Cargo Adaptor." In *The Golgi Complex: Methods and Protocols*, edited by William J Brown, 41–53. New York, NY: Springer New York. doi:10.1007/978-1-4939-6463-5_4.

Paczkowski, Jon E., Brian C. Richardson, and J. Christopher Fromme. 2015. "Cargo Adaptors: Structures Illuminate Mechanisms Regulating Vesicle Biogenesis." *Trends in Cell Biology*. Elsevier Ltd. doi:10.1016/j.tcb.2015.02.005.

Paczkowski, Jon E., Brian C. Richardson, Amanda M. Strassner, and J. Christopher Fromme. 2012. "The Exomer Cargo Adaptor Structure Reveals a Novel GTPase-Binding Domain." *The EMBO Journal* 31 (21). Nature Publishing Group: 4191–4203. doi:10.1038/emboj.2012.268.

Palade, George. 1975. "Intracellular Aspects of the Process of Protein Synthesis." *Science* 189 (4206): 347–58. doi:10.1126/science.189.4206.867-b.

Panic, Bojana, James R. C. Whyte, and Sean Munro. 2003. "The ARF-like GTPases Arl1p and Arl3p Act in a Pathway That Interacts with Vesicle-Tethering Factors at the Golgi Apparatus." *Current Biology* 13 (5). Elsevier: 405–10. doi:10.1016/S0960-9822(03)00091-5.

Park, Sang Yoon, and Xiaoli Guo. 2014. "Adaptor Protein Complexes and Intracellular Transport." *Bioscience Reports* 34 (4): e00123. doi:10.1042/BSR20140069.

Park, Sei-Kyoung, Lisa Hartnell, and Catherine L. Jackson. 2005. "Mutations in a Highly Conserved Region of the Arf1p Activator GEA2 Block Anterograde Golgi Transport but Not COPI Recruitment to Membranes." *Molecular Biology of the Cell* 16 (8): 3786–99.

Payne, G S, and R Schekman. 1985. "A Test of Clathrin Function in Protein Secretion and Cell Growth." *Science* 230 (4729): 1009–14. http://science.sciencemag.org.proxy.library.cornell.edu/content/230/4729/1009/tab-pdf.

Peden, Andrew A., Rachel E. Rudge, Winnie W. Y. Lui, and Margaret S. Robinson. 2002. "Assembly and Function of AP-3 Complexes in Cells Expressing Mutant Subunits." *Journal*

of Cell Biology 156 (2). The Rockefeller University Press: 327–36. doi:10.1083/jcb.200107140.

Pelham, Hugh R. B. 2001. "SNAREs and the Specificity of Membrane Fusion." *Trends in Cell Biology* 11 (3): 99–101. doi:10.1016/S0962-8924(01)01929-8.

Peyroche, Anne, Bruno Antonny, Sylviane Robineau, Joel Acker, Jacqueline Cherfils, and Catherine L. Jackson. 1999. "Brefeldin A Acts to Stabilize an Abortive ARF-GDP-Sec7 Domain Protein Complex: Involvement of Specific Residues of the Sec7 Domain." *Molecular Cell* 3 (3): 275–85.

Peyroche, Anne, Sonia Paris, and Catherine L. Jackson. 1996. "Nucleotide Exchange on ARF Mediated by Yeast Gea1 Protein." *Localization of Components Involved in Protein Transport and Processing through the Yeast Golgi Apparatus.* 384 (6608): 479–81.

Pfeffer, Suzanne R. 2012. "Rab GTPase Localization and Rab Cascades in Golgi Transport." *Biochemical Society Transactions* 40 (6): 1373–77. doi:10.1042/BST20120168.

Poon, Pak Phi, Dan Cassel, Anne Spang, Miriam Rotman, Elah Pick, Richard A. Singer, and Gerald C. Johnston. 1999. "Retrograde Transport from the Yeast Golgi Is Mediated by Two ARF GAP Proteins with Overlapping Function." *EMBO Journal* 18 (3): 555–64. doi:10.1093/emboj/18.3.555.

Poon, Pak Phi, Steven F. Nothwehr, Richard A. Singer, and Gerald C. Johnston. 2001. "The Gcs1 and Age2 ArfGAP Proteins Provide Overlapping Essential Function for Transport from the Yeast Trans-Golgi Network." *Journal of Cell Biology* 155 (7). The Rockefeller University Press: 1239–50. doi:10.1083/jcb.200108075.

Poon, Pak Phi, Xiangmin Wangt, Miriam Rotmant, Irit Hubert, Edna Cukiermant, Dan Casselt, Richard A Singert, and Gerald C Johnston. 1996. "*Saccharomyces Cerevisiae* Gcsl Is an ADP-Ribosylation Factor GTPase-Activating Protein." *Biochemistry* 93: 10074–77. http://www.pnas.org/content/93/19/10074.long.

Preuss, Daphne, Jon Mulholland, Alex Franzusoff, Nava Segev, and David Botsteint. 1992. "Characterization of the Saccharomyces Golgi Complex through the Cell Cycle by Immunoelectron Microscopy." *Molecular Biology of the Cell* 3 (7): 789–803. doi:10.1016/0962-8924(92)90179-Q.

Puertollano, Rosa, Nicole N. van der Wel, Lois E. Greene, Evan Eisenberg, Peter J. Peters, and Juan S. Bonifacino. 2003. "Morphology and Dynamics of clathrin/GGA1-Coated Carriers Budding from the Trans-Golgi Network." *Mol Biol Cell* 14 (4): 1545–57. doi:10.1091/mbc.02-07-0109.

Qiu, Biao, Kai Zhang, Shengliu Wang, and Fei Sun. 2014. "C-Terminal Motif within Sec7 Domain Regulates Guanine Nucleotide Exchange Activity via Tuning Protein Conformation." *Biochemical and Biophysical Research Communications*. Vol. 446. doi:10.1016/j.bbrc.2014.02.125.

Ramaen, Odile, Alexandra Joubert, Philip Simister, Naïma Belgareh-Touzé, Maria Conception Olivares-Sanchez, Jean-Christophe Zeeh, Sophie Chantalat, et al. 2007. "Interactions between Conserved Domains within Homodimers in the BIG1, BIG2, and GBF1 Arf Guanine Nucleotide Exchange Factors." *Journal of Biological Chemistry* 282 (39): 28834–42. doi:10.1074/jbc.M705525200.

Renault, Louis, Petya Christova, Bernard Guibert, Sebastiano Pasqualato, and Jacqueline Cherfils. 2002. "Mechanism of Domain Closure of Sec7 Domains and Role in BFA Sensitivity." *Biochemistry* 41 (11): 3605–12.

Richardson, Brian C., and J. Christopher Fromme. 2015. "Biochemical Methods for Studying Kinetic Regulation of Arf1 Activation by Sec7." In *Methods in Cell Biology*, 130:101–26.

Richardson, Brian C., Steve L. Halaby, Margaret A. Gustafson, and J. Christopher Fromme. 2016. "The Sec7 N-Terminal Regulatory Domains Facilitate Membrane-Proximal Activation of the Arf1 GTPase." *eLife* 5 (JANUARY2016): 1–20. doi:10.7554/eLife.12411.001.

Richardson, Brian C., Caitlin M. McDonold, and J. Christopher Fromme. 2012. "The Sec7 Arf-GEF Is Recruited to the Trans-Golgi Network by Positive Feedback." *Developmental Cell* 22 (4). Elsevier Inc.: 799–810. doi:10.1016/j.devcel.2012.02.006.

Rivera-Molina, Félix E., and Peter J. Novick. 2009. "A Rab GAP Cascade Defines the Boundary between Two Rab GTPases on the Secretory Pathway." *Proceedings of the National Academy of Sciences of the United States of America* 106 (34): 14408–13. doi:10.1073/pnas.0906536106.

Robinson, Jane S., Daniel J. Klionsky, Lois M. Banta, and Scott D. Emr. 1988. "Protein Sorting in *Saccharomyces Cerevisiae*: Isolation of Mutants Defective in the Delivery and Processing of Multiple Vacuolar Hydrolases." *Molecular and Cellular Biology* 8 (11). American Society for Microbiology: 4936–48. doi:10.1128/MCB.8.11.4936.

Rojas, Ana Maria, Gloria Fuentes, Antonio Rausell, and Alfonso Valencia. 2012. "The Ras Protein Superfamily: Evolutionary Tree and Role of Conserved Amino Acids." *Journal of Cell Biology*. doi:10.1083/jcb.201103008.

Rothman, James E. 1994. "Mechanism of Intracellular Protein-Transport." *Nature* 372: 55–63. doi:10.1038/372055a0.

Santiago-Tirado, Felipe H., and Anthony Bretscher. 2011. "Membrane-Trafficking Sorting Hubs: Cooperation between PI4P and Small GTPases at the Trans-Golgi Network." *Trends in Cell Biology*. doi:10.1016/j.tcb.2011.05.005.

Sata, Makoto, Julie G. Donaldson, Joel Moss, and Martha Vaughan. 1998. "Brefeldin A-Inhibited Guanine Nucleotide-Exchange Activity of Sec7 Domain from Yeast Sec7 with Yeast and Mammalian ADP Ribosylation Factors." *Proceedings of the National Academy of Sciences of the United States of America* 95 (8): 4204–8. http://www.pubmedcentral.nih.gov/articlerender.fcgi?artid=22466&tool=pmcentrez&rende

rtype=abstract.

Sato, Ken, and Akihiko Nakano. 2007. "Mechanisms of COPII Vesicle Formation and Protein Sorting." *FEBS Letters* 581 (11): 2076–82. doi:10.1016/j.febslet.2007.01.091.

Schlacht, Alexander, Emily K. Herman, Mary J. Klute, Mark C. Field, and Joel B. Dacks. 2014. "Missing Pieces of an Ancient Puzzle: Evolution of the Eukaryotic Membrane-Trafficking System." *Cold Spring Harbor Perspectives in Biology* 6 (10). Cold Spring Harbor Laboratory Press: a016048. doi:10.1101/cshperspect.a016048.

Sciorra, Vicki A., Anjon Audhya, Ainslie B. Parsons, Nava Segev, Charles Boone, and Scott D. Emr. 2005. "Synthetic Genetic Array Analysis of the PtdIns 4-Kinase Pik1p Identifies Components in a Golgi-Specific Ypt31/rab-GTPase Signaling Pathway □ D." *Molecular Biology of the Cell* 16: 776–93. doi:10.1091/mbc.

Sclafani, Anthony, Shuliang Chen, Felix Rivera-Molina, Karin Reinisch, Peter Novick, and Susan Ferro-Novick. 2010. "Establishing a Role for the GTPase Ypt1p at the Late Golgi." *Traffic* 11 (4). Blackwell Publishing Ltd: 520–32. doi:10.1111/j.1600-0854.2010.01031.x.

Seaman, Matthew N. J. 2005. "Recycle Your Receptors with Retromer." *Trends in Cell Biology*. doi:10.1016/j.tcb.2004.12.004.

Segev, Nava, Jon Mulholland, and David Botstein. 1988. "The Yeast GTP-Binding YPT1 Protein and a Mammalian Counterpart Are Associated with the Secretion Machinery." *Cell* 52 (6). Cell Press: 915–24. doi:10.1016/0092-8674(88)90433-3.

Setty, Subba Rao Gangi, Marcus E. Shin, Atsuko Yoshino, Michael S. Marks, and Christopher G. Burd. 2003. "Golgi Recruitment of GRIP Domain Proteins by Arf-like GTPase 1 Is Regulated by Arf-like GTPase 3." *Current Biology* 13 (5): 401–4. doi:10.1016/S0960-9822(03)00089-7.

Sheen, Volney L., Vijay S. Ganesh, Meral Topcu, Guillaume Sebire, Adria Bodell, R. Sean Hill, P. Ellen Grant, et al. 2004. "Mutations in ARFGEF2 Implicate Vesicle Trafficking in Neural Progenitor Proliferation and Migration in the Human Cerebral Cortex." *Nat Genet* 36 (1): 69–76. doi:10.1038/ng1276.

Siniossoglou, S., and Hugh R. B. Pelham. 2001. "An Effector of Ypt6p Binds the SNARE Tlg1p and Mediates Selective Fusion of Vesicles with Late Golgi Membranes." *EMBO Journal* 20 (21): 5991–98. doi:10.1093/emboj/20.21.5991.

Siniossoglou, Symeon, Sew Y. Peak-Chew, and Hugh R. B. Pelham. 2000. "Ric1p and Rgp1p Form a Complex That Catalyses Nucleotide Exchange on Ypt6p." *The European Molecular Biology Organization Journal* 19 (18): 4885–94. doi:10.1093/emboj/19.18.4885.

Smaczynska-de Rooij, Iwona I., Rosaria Costa, and Kathryn R. Ayscough. 2008. "Yeast Arf3p Modulates Plasma Membrane PtdIns(4,5)P2 Levels to Facilitate Endocytosis." *Traffic* 9 (4).

Blackwell Publishing Ltd: 559–73. doi:10.1111/j.1600-0854.2008.00708.x.

Smith, Richard D, and Vladimir V Lupashin. 2008. "Role of the Conserved Oligomeric Golgi (COG) Complex in Protein Glycosylation." *Carbohydrate Research* 343 (12): 2024–31. doi:10.1016/j.carres.2008.01.034.

Smulan, Lorissa J., Wei Ding, Elizaveta Freinkman, Sharvari Gujja, Yvonne J.K. Edwards, and Amy K. Walker. 2016. "Cholesterol-Independent SREBP-1 Maturation Is Linked to ARF1 Inactivation." *CellReports* 16: 9–18. doi:10.1016/j.celrep.2016.05.086.

Spang, Anne, Johannes M. Herrmann, Susan Hamamoto, and Randy Schekman. 2001. "The ADP Ribosylation Factor-Nucleotide Exchange Factors Gea1p and Gea2p Have Overlapping, but Not Redundant Functions in Retrograde Transport from the Golgi to the Endoplasmic Reticulum." *Molecular Biology of the Cell* 12 (4): 1035–45.

Stalder, Danièle, and Bruno Antonny. 2013. "Arf GTPase Regulation through Cascade Mechanisms and Positive Feedback Loops." *FEBS Letters*. doi:10.1016/j.febslet.2013.05.015.

Stearns, Tim, Richard A. Kahn, David Botstein, and M. Andrew Hoyt. 1990. "ADP Ribosylation Factor Is an Essential Protein in *Saccharomyces Cerevisiae* and Is Encoded by Two Genes." *Molecular and Cellular Biology* 10 (12): 6690–99.

Strahl, Thomas, Hiroko Hama, Daryll B. DeWald, and Jeremy Thorner. 2005. "Yeast Phosphatidylinositol 4-Kinase, Pik1, Has Essential Roles at the Golgi and in the Nucleus." *The Journal of Cell Biology* 171 (6): 967–79. doi:10.1083/jcb.200504104.

Suda, Yasuyuki, Kazuo Kurokawa, Ryogo Hirata, and Akihiko Nakano. 2013. "Rab GAP Cascade Regulates Dynamics of Ypt6 in the Golgi Traffic." *Proceedings of the National Academy of Sciences of the United States of America* 110 (47): 18976–81. doi:10.1073/pnas.1308627110.

Takatsu, Hiroyuki, Yohei Katoh, Yoko Shiba, and Kazuhisa Nakayama. 2001. "Golgi-Localizing, γ-Adaptin Ear Homology Domain, ADP-Ribosylation Factor-Binding (GGA) Proteins Interact with Acidic Dileucine Sequences within the Cytoplasmic Domains of Sorting Receptors through Their Vps27p/Hrs/STAM (VHS) Domains." *Journal of Biological Chemistry* 276 (30). American Society for Biochemistry and Molecular Biology: 28541–45. doi:10.1074/jbc.C100218200.

Tanigawa, Gary, Lelio Orci, Mylene Amherdt, Mariella Ravazzola, J. Bernd Helms, and James E. Rothman. 1993. "Hydrolysis of Bound GTP by ARF Protein Triggers Uncoating of Golgi-Derived COP-Coated Vesicles." *Journal of Cell Biology* 123 (6 PART 1): 1365–71. doi:10.1083/jcb.123.6.1365.

Thomas, Laura L., and J. Christopher Fromme. 2016. "GTPase Cross Talk Regulates TRAPPII Activation of Rab11 Homologues during Vesicle Biogenesis." *The Journal of Cell Biology* 215 (4): 499–513. doi:10.1083/jcb.201608123.

Tomás, Mónica, Emma Martínez-Alonso, José Ballesta, and José A. Martínez-Menárguez. 2010. "Regulation of ER-Golgi Intermediate Compartment Tubulation and Mobility by COPI Coats, Motor Proteins and Microtubules." *Traffic* 11 (5). Blackwell Publishing Ltd: 616–25. doi:10.1111/j.1600-0854.2010.01047.x.

Trahey, Meg, and Jesse C. Hay. 2010. "Transport Vesicle Uncoating: It's Later than You Think." *F1000 Biology Reports* 2: 47. doi:10.3410/B2-47.

Tsai, Pei-Chin, Jia-Wei Hsu, Ya-Wen Liu, Kuan-Yu Chen, and Fang-Jen S. Lee. 2013. "Arl1p Regulates Spatial Membrane Organization at the Trans-Golgi Network through Interaction with Arf-GEF Gea2p and Flippase Drs2p." *Proceedings of the National Academy of Sciences of the United States of America* 110 (8): E668-77. doi:10.1073/pnas.1221484110.

Ullrich, Oliver, Sigrid Reinsch, Sylvie Urb, Marino Zerial, and Robert G. Parton. 1996. "Rab11 Regulates Recycling through the Pericentriolar Recycling Endosome." *The Journal of Cell Biology* 135 (4): 913–24. http://jcb.rupress.org/content/jcb/135/4/913.full.pdf.

van Meer, Gerrit, Dennis R. Voelker, and Gerald W. Feigenson. 2008. "Membrane Lipids: Where They Are and How They Behave." *Nature Reviews Molecular Cell Biology* 9 (2): 112–24. doi:10.1038/nrm2330.

Volchuk, A., Mariella Ravazzola, Alain Perrelet, William S. Eng, Maurizio Di Liberto, Oleg Varlamov, Masayoshi Fukasawa, et al. 2004. "Countercurrent Distribution of Two Distinct SNARE Complexes Mediating Transport within the Golgi Stack." *Mol Biol Cell* 15 (4). American Society for Cell Biology: 1506–18. doi:10.1091/mbc.E03-08-0625\rE03-08-0625 [pii].

Wai, Timothy, and Thomas Langer. 2016. "Mitochondrial Dynamics and Metabolic Regulation." *Trends in Endocrinology & Metabolism* 27 (2): 105–17. doi:10.1016/j.tem.2015.12.001.

Walch-Solimena, Christiane, and Peter Novick. 1999. "The Yeast Phosphatidylinositol-4-OH Kinase Pik1 Regulates Secretion at the Golgi." *Nature Cell Biology* 1 (8). Nature Publishing Group: 523–25. doi:10.1038/70319.

Wang, Chao-Wen, Susan Hamamoto, Lelio Orci, and Randy Schekman. 2006. "Exomer: A Coat Complex for Transport of Select Membrane Proteins from the Trans-Golgi Network to the Plasma Membrane in Yeast." *The Journal of Cell Biology* 174 (7): 973–83. doi:10.1083/jcb.200605106.

Waters, M. Gerard, Tito Serafini, and James E. Rothman. 1991. "'Coatomer': a Cytosolic Protein Complex Containing Subunits of Non-Clathrin-Coated Golgi Transport Vesicles." *Nature* 349 (6306): 248–51. doi:10.1038/349248a0.

Weiss, Ofra, Janet Holden, Cherrie Rulka, and Richard A. Kahn. 1989. "Nucleotide Binding and Cofactor Activities of Purified Bovine Brain and Bacterially Expressed ADP-Ribosylation Factor." *THE JOURNAL OF BIOLOGICAL CHEMISTRY* 264 (35): 21066–72.

http://www.jbc.org/content/264/35/21066.full.pdf.

Wennerberg, Krister, Kent L. Rossman, and Channing J. Der. 2005. "The Ras Superfamily at a Glance." *Journal of Cell Science* 118 (Pt 5): 843–46. doi:10.1242/jcs.01660.

Whiteside, Simon T., and Stephen Goodbourn. 1993. "Signal Transduction and Nuclear Targeting: Regulation of Transcription Factor Activity by Subcellular Localisation." *Journal of Cell Science* 104 (Pt 4): 949–55. http://jcs.biologists.org/content/joces/104/4/949.full.pdf.

Whyte, James R. C., and Sean Munro. 2002. "Vesicle Tethering Complexes in Membrane Traffic." *Journal of Cell Science* 115 (Pt 13): 2627–37. http://jcs.biologists.org.proxy.library.cornell.edu/content/115/13/2627.

Wood, Salli A., John E. Park, and William J. Brown. 1991. "Brefeldin A Causes a Microtubule-Mediated Fusion of the Trans-Golgi Network and Early Endosomes." *Cell* 67 (3): 591–600. doi:10.1016/0092-8674(91)90533-5.

Wooding, Steven, and Hugh R. B. Pelham. 1998. "The Dynamics of Golgi Protein Traffic Visualized in Living Yeast Cells." *Molecular Biology of the Cell* 9 (9). American Society for Cell Biology: 2667–80. doi:10.1091/MBC.9.9.2667.

Yu, I-Mei, and Frederick M. Hughson. 2010. "Tethering Factors as Organizers of Intracellular Vesicular Traffic." *Annual Review of Cell and Developmental Biology* 26 (1). Annual Reviews: 137–56. doi:10.1146/annurev.cellbio.042308.113327.

Zhang, Chun Jiang, J. Bradford Bowzard, Aimee Anido, and Richard A. Kahn. 2003. "Four ARF GAPs in *Saccharomyces Cerevisiae* Have Both Overlapping and Distinct Functions." *Yeast* 20 (4). John Wiley & Sons, Ltd.: 315–30. doi:10.1002/yea.966.